Georgia Water Resources Institute
Annual Technical Report
FY 2014

Introduction

Mission Statement:

GWRI strives to improve the science and practice of water resources planning and management in ways that balance quality of life, environmental sustainability, and economic growth. GWRI pursues this mission through its education, research, information dissemination, and technology/knowledge transfer programs at the state, national, and international levels.

Organizational Structure: The GWRI organizational structure includes a Director, Associate Director, Assistant Director, Advisory Board, and technical support staff. The technical support staff comprises several Ph.D. graduate students who work on GWRI projects while carrying out doctoral research, and information technology support staff. The Advisory Board includes representatives from major state and federal water agencies as well as environmental and citizen groups. At Georgia Tech, GWRI reports to the Senior Vice-Provost for Research under the Office of the Provost.

Research Program Sponsorship and Administration: GWRI activities are sponsored by (i) the Department of the Interior/USGS as part of the state and national research programs, and (ii) other national and international funding agencies and organizations supporting research in water related areas. Through its annual state and national competitive programs, GWRI provides research awards to Georgia Universities. The award process includes submission of technical proposals, technical peer reviews, and reviews for relevance to Georgia needs by the State Environmental Protection Division (Georgia EPD).

Other External Funding: In addition to the 104B and 104G programs, GWRI generates additional funding through participation in competitive national and international research programs. Recent funding has been provided by the Georgia Environmental Protection Division, the California Energy Commission, NOAA, and the ACF Stakeholders. GWRI involvement in national and international research activities is crucial to maintaining the expert capacity and funding portfolio necessary to provide quality services to the state of Georgia and all other sponsors.

FY2014 RESEARCH PROJECTS THROUGH 104B PROGRAM

(1) Validation of Oysters as Biomonitors of Pharmaceutical Pollution in Georgia; M. Black; University of Georgia.

(2) The effect of salt marsh hydrodynamics on estuarine flow; Improvement and Uncertainty Assessment; K. Haas and D. Webster; Georgia Institute of Technology.

(3) Implications of eutrophication and climate change in promoting toxic cyanobacterial blooms in agricultural ponds across Georgia; S. Wilde and D. Mishra; University of Georgia.

(4) Baseline Conservation Analysis for Agricultural Irrigation in Priority Watersheds of the Lower Flint River Basin; M. Masters; Albany State University.

EXTENDED FY2013 RESEARCH PROJECTS THROUGH 104B PROGRAM

(1) Unimpaired Flows for the ACF River Basin: Improvement and Uncertainty Assessment, A. Georgakakos and M. Kistenmacher, sponsored by USGS under grant #1266663 (Project# 2013GA333B).

(2) Tracking the impact of on-site wastewater treatment systems on stream water quality in the Metro-Atlanta area, M. Habteselassie and D. Radcliffe, sponsored by USGS under grant #1266663 (Project# 2013GA330B).

OTHER RESEARCH PROJECTS AND ACCOMPLISHMENTS

(1) Technical Support for the Development of a Sustainable Water Management Plan for the Apalachicola-Chattahoochee-Flint (ACF) River Basin, Aris Georgakakos PI, Georgia Institute of Technology, sponsored by the ACF Stakeholders.

RECENT PUBLICATIONS

Kistenmacher, M., and A.P. Georgakakos, "Ensemble Forecasting of Water Resources Systems, Water Resources Research, doi: 10.1002/2014WR016564, 2015.

Sharif, H.E., J. Wang, and A. P. Georgakakos, "Modeling regional crop yield and irrigation demand using SMAP type of soil moisture data", Journal of Hydrometeorology, 16(2), doi: 10.1175/JHM-D-14-0034.1, 2015.

Georgakakos, A.P., P. Fleming, M. Dettinger, C. Peters-Lidard, T.C. Richmond, K. Reckhow, K. White, and D. Yates: Water Resources Chapter, 2014 National Climate Assessment Draft, http://ncadac.globalchange.gov, 2014.

Georgakakos, A.P., H. Yao, and K.P. Georgakakos, "Ensemble streamflow prediction adjustment for upstream water use and regulation", Journal of Hydrology, doi: 10.1016/j.jhydrol.2014.06.044, 2014.

Kim, D.H., and A.P. Georgakakos, "Hydrologic River Routing using Nonlinear Cascaded Reservoirs," Water Resources Research, doi: 10.1002/2014WR015662, 2014.

Chen, C-J., and A.P. Georgakakos, "Seasonal Prediction of East African Rainfall," International Journal of Climatology, doi: 10.1002/joc.4165, 2014.

Climate of the Southeast United States: Variability, Change, Impacts, and Vulnerability, co-author of Chapter 10, "Impacts of Climate Change and Variability on Water Resources in the Southeast USA," Island Press, Washington DC, 341p, 2013.

Chen, C-J., and A.P. Georgakakos, "Hydro-Climatic Forecasting Using Sea Surface Temperatures—Methodology and Application for the Southeast U.S.," Journal of Climate Dynamics, doi: 10.1007/s00382-013-1908-4, 2013.

Research Program Introduction

Four research projects were funded through the 104B Program (each at $18,000) in FY2014:

(1) Validation of Oysters as Biomonitors of Pharmaceutical Pollution in Georgia; M. Black; University of Georgia.

(2) The effect of salt marsh hydrodynamics on estuarine flow; Improvement and Uncertainty Assessment; K. Haas and D. Webster; Georgia Institute of Technology.

(3) Implications of eutrophication and climate change in promoting toxic cyanobacterial blooms in agricultural ponds across Georgia; S. Wilde and D. Mishra; University of Georgia.

(4) Baseline Conservation Analysis for Agricultural Irrigation in Priority Watersheds of the Lower Flint River Basin; M. Masters; Albany State University.

However, projects (1) and (4) were granted no-cost extensions into Fiscal Year 2015. As such, their associated projects reports are formally considered to be a part of the next fiscal year and will be contained in the FY2015 Annual Report.

Tracking the impact of on-site wastewater treatment systems on stream water quality in the Metro-Atlanta area

Basic Information

Title:	Tracking the impact of on-site wastewater treatment systems on stream water quality in the Metro-Atlanta area
Project Number:	2013GA330B
Start Date:	3/1/2013
End Date:	9/30/2014
Funding Source:	104B
Congressional District:	GA-10
Research Category:	Water Quality
Focus Category:	Wastewater, Water Quality, Treatment
Descriptors:	None
Principal Investigators:	Mussie Ykeallo Habteselassie, David Radcliffe

Publications

There are no publications.

Tracking the impact of on-site wastewater treatment systems on stream water quality in the Metro-Atlanta area

Grant Report

By Robert Sowah* and Mussie Habteselassie

September, 2014

Department of Crop and Soil Sciences
University of Georgia
Griffin Campus

*Graduate student who worked under this project

Table of Contents

Summary

Onsite wastewater treatment systems (OWTS), also known as septic systems, are widely used throughout the southeast. In Metropolitan Atlanta, it is estimated that 26% of all residential units are served by OWTS. As widely as OWTS are used, their impact on water quality remains enigmatic. Although a great deal is known about the impact of individual septic units, there is still little information on the combined effect of these systems on water quality at the watershed level. Both failing and properly functioning septic systems have the potential to contribute to surface water pollution under the right conditions. In this study, we tracked the influence of OWTS on water quality at the watershed level using pollution monitoring strategies and microbial source tracking techniques. Twenty four watersheds of varying septic system density were monitored for fecal indicator bacteria and host-specific *Bacteroidales* over 8 sampling seasons. The watersheds were classified into two groups; high density watersheds (HD) were those watersheds with greater than 77 septic systems per km^2 whilst low density watersheds (LD) were the watersheds with less than 38 septic systems per km^2. OWTS density ranged from 8 to 373 units km^{-2}.

Our results point to ongoing fecal pollution of streams of urbanizing watersheds in the metro-Atlanta area. These pollution issues vary in temporal and spatial scales and can be attributed to watershed level factors including the density of septic systems in the watersheds. This is evidenced by the higher levels of the human marker in HD watersheds and the positive correlation between OWTS density and human marker yield. There appears to be a strong seasonal influence on OWTS density – water quality interaction, with spring showing the strongest OWTS impact. The outcome of this study provides the tools that can be used at the watershed level to isolate the influence of OWTS on water quality. Evidently the combination of baseflow sampling, pollution monitoring and microbial source tracking is a promising approach for identifying the contributions of septic systems as well as other non-point sources of fecal pollution at the watershed level.

Introduction

Onsite wastewater treatment systems (OWTS), also known as septic systems, are widely used throughout the southeast. It is estimated that more than 30% of homes in Georgia are on OWTS (U.S. EPA, 2002), which is higher than the national average (25%). A 2005 estimate puts the number of OWTS in Metropolitan Atlanta at 526,000 (Metropolitan North Georgia Water Planning District, 2006). These systems are not evenly distributed. The percentage of housing units on OWTS in counties in and around the Metropolitan Atlanta ranges from 6% (Clayton County) to 100% (Paulding County). In the coastal region, the use may be as high as 90% (P. Flournoy, research supervisor, UGA Marine Extension Service, personal correspondence). One can only expect the number of OWTS to grow as population growth continues in the region.

The issue of OWTS's impact on water quality remains enigmatic, with anecdotal evidence suggesting that these systems can contribute to fecal pollution of surface waters. Although a great deal is known about the impact of individual septic units, there is still little information on the combined effect of these systems on water quality at the watershed level. It has long been known that improperly functioning or poorly maintained systems are sources of pollution. However, recent work (Habteselassie et al., 2011; Arnade, 1999) has indicated that properly maintained and functioning OWTS can make significant contributions of contaminants to surface waters, especially after high precipitation events. The principal contaminants are microbial pathogens and nutrients.

Recently, widespread fecal pollution incidents have put the spotlight on OWTS and non-point sources of fecal pollution in general. This is in the light of stringent controls over point sources in the last three decades. In Georgia, over 600 stream segments are listed as impaired by fecal pollutants (fecal coliforms) and not surprisingly OWTS are cited as potential sources of the fecal coliforms (GDNR, 2011). A study by Fong et al. (2005) in the lower Altamaha River basin of Georgia found that human viruses were prevalent in the Altamaha Sound and other sampling sites in areas that support shellfish harvesting activities. Human enteroviruses or adenoviruses were found in 67% of the surface water samples. The Altamaha River basin has been a subject of

several studies because of water quality impairment along its tributaries. OWTS were identified as one of the non-point sources of fecal contaminants (GDNR, 2002). Similar studies in the Florida Keys and coastal regions have demonstrated a high risk of fecal pollution of surface water resources close to areas of high septic density compared to areas of low septic density.

Identifying the sources of fecal pollution at the watershed level is an important element in current water quality management strategies such as the total maximum daily load (TMDL) (Ahmed et al., 2012; Habteselassie et al., 2011). Moreover, tracking the sources fecal pollutants at the watershed level is a vital component in any management effort to protect public water supplies, especially in areas where surface water bodies are the primary source of public water supply. In the Metro Atlanta area where surface waters supply more than 98% of public water (Landers and Ankcorn, 2008) and fecal pollution continues to present challenges to the water supply system, source tracking holds the key to unlock appropriate management strategies needed to protect water resources.

As widely as OWTS are used in the Metropolitan Atlanta area for wastewater treatment, questions still remain about their aggregate impact on water quality at the watershed level. Although the tendency among watershed managers and stakeholders is to blame OWTS for poor water quality, the evidence against OWTS is at best circumstantial, prompting this study which aims among others to differentiate the sources of fecal pollution in urbanizing watersheds. The overall goal of this study is to better define the role of OWTS on water quality in watersheds that are found in the metro-Atlanta area. These watersheds are of varying OWTS density from high to low density. In this study, microbial source tracking techniques are combined with pollution monitoring strategies to investigate the impact of OWTS on water quality in streams in watersheds within the water district. Moreover, the seasonality of such impact will be explored to determine patterns in OWTS – water quality interactions.

Methods

Site characterization

The study area is in Gwinnett County, northeast of Atlanta, GA and has a mean annual precipitation of about 1245 mm (National Weather Service; http://www.nws.noaa.gov/climate/xmacis.php?wfo=ffc). The study area consists of 24 watersheds which range in size from 0.18 to 8.81 km^2. A map of the study area and watershed boundaries, modified from Landers and Ankcorn (2008), is presented in Figure 1. The selected watersheds are in the Ocmulgee and Oconee River basins, which drain to the Altamaha River and ultimately into the Atlantic Ocean. The selected watersheds are typical of urbanizing watersheds along the Interstate 85 corridor in the southeastern Piedmont region of the U.S. This region, which has seen rapid population growth over the past two decades, depends largely on surface water for more than 65% of public water supply. The watersheds represent a gradient of land use conditions from low to high density of septic systems, as well as developed to undeveloped uses. Watersheds 1 – 11 and 15 are characterized as having low density of septic systems (LD) with the remaining twelve characterized as having high density of septic system (HD). An arbitrary threshold of less than 38 septic systems per km^2 was set for LD watersheds and greater than 77 septic systems per km^2 for HD watersheds (Table 1). These threshold values make sense when one considers the U.S. EPA's designation of areas with greater than 15 units per km as regions of potential groundwater contamination (U.S. EPA, 1977). Considering the improvements in septic system technology and regulation, it was reasonable to raise the threshold values in this study.

Watershed characteristics were determined from spatial datasets processed in geographic information systems. Watershed characteristics described by Landers and Ankcorn (2008) and land uses determined using the StreamStats interactive map of Georgia (http://water.usgs.gov/osw/streamstats/georgia.html) are shown in Table 1. The average septic density (units km^{-2}), percent impervious coverage and percent agricultural land use are 22, 6.7 and 32.5 respectively for LD, and 216, 18.3 and 4.2 respectively for HD watersheds. Other watershed selection criteria in addition to septic density included similar geological setting,

precipitation, climate, accurate base-flow measurement locations and available spatial datasets of natural, infrastructure and water-use characteristics. Weather data for the area was collected from the Georgia Automated Environmental Monitoring Network (http://www.georgiaweather.net/). Additional information on site characteristics can be found in Landers and Ankcorn (2008)

Sample collection

Surface water samples from streams in the 24 watersheds were collected during baseflow on 7 sampling events spanning November, 2011 to November, 2013, creating a data set with two spring samples, two summer samples and three winter samples. Baseflow conditions were determined using long-term discharge measurements at two USGS stream gages (http://waterdata.usgs.gov/ga/nwis/uv/?site_no=02205522; http://waterdata.usgs.gov/ga/nwis/uv/?site_no=02207385) near the study site. Also, baseflow sampling coincided with periods of zero precipitation 72 hours prior to the sampling event. Baseflow sampling coincided with the spring (n = 72; March 2012, April 2013 and March 2014), summer (n = 48; July 2012 and 2013) and winter (n = 72; November 2011, 2012 and 2013) seasons. At each monitoring station, samples were collected in duplicate in 1 liter sterile high-density polypropylene, screw-capped bottles. Samples were kept on ice and transported to the laboratory for analysis (usually within 6 hours of sample collection). Sample collection and analysis followed guidelines of the National Field Manual for the Collection of Water-Quality Data (USGS, variously dated). Baseflow discharge (m^3 sec^{-1}) was measured at each monitoring point during sampling events by our project partners at the United States Geological Survey (USGS) Georgia Water Science Center in Atlanta. The velocity-area method (Rantz, 1982) was used for discharge measurements.

Fecal indicator bacteria analysis

Water samples were analyzed for the FIB *E. coli* and enterococci using the Colilert-18 and Enterolert kits (IDEXX Laboratories Inc., Westbrook, ME). The Colilert-18 and Enterolert kits are defined substrate methods for *E. coli* and enterococci respectively and are U.S. Environmental Protection Agency (U.S. EPA) approved and are included in Standard Methods for Examination of Water and Wastewater. Each sample was diluted (10–fold dilution based on previous analysis of samples from the monitored streams) to 100 ml volume using sterile deionized water. The Colilert-18 and Enterolert substrates were then added to the 100 ml dilution to dissolve. The samples were then poured into a 97 well tray, sealed and incubated for 18 hours

and 24 hours for *E. coli* and enterococci respectively. The number of positive wells, based on UV fluorescence, was used to estimate the MPN of *E. coli* and enterococci using manufacturer supplied MPN tables. All samples were run with negative controls (100 ml of diluent used to dilute samples) and followed manufacturer recommended quality control procedures.

Nucleic acid extraction

Nucleic acid (DNA) were extracted from water samples for quantitative polymerase chain reaction (qPCR) by first filtering 100 ml of water samples through 47 mm diameter 0.40 μm pore size polycarbonate filters (GE Whatman, Pittsburgh, PA). This serves to concentrate bacterial DNA for downstream qPCR applications. Following sample filtration, the filters were placed in microcentrifuge tubes and stored at -20^{o}C prior to DNA extraction. The filters were later processed for bacterial DNA using the PowerFecal DNA Isolation Kit (MoBio Laboratories, Inc., Carlsbad, CA) according to the manufacturer's instructions. At the end of the extraction protocol, bacterial DNA was eluted to a final volume of 50 ul and stored at -20^{o}C for downstream molecular applications.

Microbial source tracking

The sources of fecal pollutants impacting streams in the monitored watersheds were investigated using microbial source tracking techniques. In this process, quantitative polymerase chain reaction (qPCR) was used to identify and quantify the contributions of different sources of fecal pollutants to the streams. Human and ruminant sources of fecal pollution were the focus of attention as our research and site survey indicated that these were the most likely contributors to total fecal pollution in streams. For tracking human sources of fecal pollution, the BacHum marker (Kildare et al., 2007) was used whilst the BacR marker (Reischer et al., 2006) was used to track ruminant sources in the waterrsheds. These genetic markers were developed in previous studies from 16S rRNA genes of host specific bacteria of the order Bacteroidales. Moreover, a generic Bacteroidales marker (AllBac) devoped by Layton et al. (2006) was used to quantify total fecal pollution in the watersheds. To achieve quantitation by qPCR, a standard curve was generated by first amplifying the AllBac, BacR and BacH targets in bacterial DNA samples using conventional PCR. The conventional PCR assay (Bio-Rad MyCycler Thermal Cycler, Hercules, CA) was run at a final volume of 25 ul with a reaction mixture containing 2x GoTaq Colorless Master Mix, 0.2 uM of forward and reverse primers and 2 ul of sample DNA. The PCR

products were cloned into pGEM-T Easy Vectors (Promega, Madison, WI) and transformed into competent *E. coli* cells (JM109 High Efficiency Competent Cells, Promega). Extracted plasmid DNA (PureYield Plasmid Midiprep System, Promega) was quantified and serially diluted 10-fold to generate reaction standards.

The standards were amplified during each qPCR assay to generate a standard curve used to estimate the copies of target gene markers in water samples. The copies of genetic marker in samples were estimated using the formula below

$$C_n = C_0(1+E)^n$$

where (C_n) is the amount of PCR products from input target molecules (C_0) after (n) cycles and (E) is the amplification efficiency.

Standard curves, which were calculated as simple linear regressions, were used to calculate amplification efficiencies (which ranged from 90 to 100% in this study) at each instrument run. Amplification efficiencies were calculated according to the formula

$$E = 10^{\frac{1}{-s}} - 1$$

In theory 100% efficiency implies that the amount of PCR product doubles with each cycle and (s) is the slope of the standard curve

$$s = -\frac{1}{\log(1+E)}$$

The StepOnePlus Real-Time PCR System (Life Technologies, Grand Island, NY) was used for all reactions. Each qPCR reaction was made up 20 ul reaction volume with 2x SYBR Select Master Mix (Lifetechnologies), optimized concentration of 150 nM for both forward and reverse primers, with 2 ul of sample DNA. A meltcurve was generated with each instrument run to confirm the specificity of amplified PCR products. Reaction conditions for both conventional and qPCR assays are provided in Table 2.

Data analysis

FIB levels in streams were expressed as stream yield (MPN sec^{-1} km^{-2}) by multiplying FIB count (MPN 100 ml^{-1}) by the stream discharge (m^3 sec^{-1}) to obtain the stream load. The load was then divided by the watershed area to give the stream yield. Similarly, Bacteroidales marker copies were expressed as stream yield (Copies sec^{-1} km^{-2}). Both bacterial count and stream yield

were reviewed for normality and log-transformed to achieve normality prior to data analysis. The relative abundance of human and ruminant genetic markers as a fraction of total fecal pollution (generic marker) was estimated. However, caution should be exercised in the interpretation of the relative amounts as concerns over differential persistence, abundance, mobility of markers and most importantly variations in the distribution of gene copies of target markers among individuals affects the prediction of relative amounts of fecal host pollution (Wuertz et al., 2011). One-way analysis of variance (ANOVA) was used to test differences in bacterial counts and yield between high and low density watershed groups. All data analysis was performed in SAS 9.3 (SAS Institute, Cary, NC) and statistical significance estimated at the 95% confidence level.

Results and discussion

Indicator bacteria quantification

Microbial water quality was assessed by enumerating *E. coli* and enterococci levels in stream water samples. Table 3 and Figures 2 and 3 summarize *E. coli* and enterococci counts and stream yields across watershed groups and over seasons. The ranges of FIB counts were consistently wider in LD watersheds than HD watersheds. The data also suggests widespread fecal pollution across both LD and HD watersheds (Figure 2). In LD watersheds, approximately 49% of all samples exceeded the one-time single sample *E. coli* action value for recreational water use of 235 MPN 100 ml^{-1}. The percentage of samples that exceeded the *E. coli* threshold in HD watersheds was 45% (Figure 2a). Enterococci counts exceeded the single sample action value of 70 MPN 100 ml^{-1} in 90% and 92% of all samples collected in LD and HD watersheds, respectively (Figure 2b). The recommended action values are provided in the revised recreational water quality criteria (U.S. EPA, 2012). According to the EPA, an action value is the single-sample "do not exceed" value for recreational water use.

Identification and quantification of host-specific markers

General and host-specific *Bacteroidales* markers in water samples were quantified with qPCR to identify the sources of fecal pollutions in the watersheds. The dynamic range of quantification for the general Bacteroidales marker was six orders of magnitude; from 15 to 15 x 10^5 copies per µl of template DNA. The linear range for the BacHum and BacR markers was also six orders of

magnitude between 2 to 15 x 10^4 copies per µl. Figures 4, 5 and 6 chart the variations in general and host-specific marker copies according to OWTS density and seasons. In terms of generic marker density, low density OWTS impacted areas showed higher marker copy numbers compared to high density areas (Figure 4a). A similar scenario was observed for fecal indicator bacteria counts (Figure 2) which confirms that low density areas present higher risk of fecal pollution in comparison to areas of high OWTS density. Low density areas, with greater agricultural activities and larger areas of forest and hence wildlife, are likely impacted by several fecal pollution sources, which shows in the wide variations in both general Bacteroidales copies numbers and indicator bacteria counts.

A look at marker density for ruminants (Figure 5a) highlights the variations in fecal pollution attributable to ruminant sources, particularly in LD watersheds. Ruminant marker density in HD watersheds on the other hand changed very little over time and by season (Figure 5a & b). The low level of agricultural activities and reduced influence of wildlife resulting from limited forest cover can explain the consistent ruminant marker density observed in HD watersheds.

The stream yield of general Bacteroidales in contrast indicates that both watershed groups do contribute similar levels of fecal pollutants to streams in the study watersheds (Figure 4c). This can be attributed to the contribution of OWTS to streamflow which has the effect of increasing fecal pollutants passing through the stream channel in the HD watersheds. Ruminant marker yield was, as expected, higher in LD watersheds than HD watersheds. A significant increase ($p = 0.04$) in human marker yield was observed in HD watersheds over LD watersheds for spring 2012 (Figure 6). The data for winter 2012 and spring 2014 did not show a significant difference between HD and LD watersheds. We did not report data for the rest of the sampling dates because only a few sites in each watershed group were positive for the human marker. Additionally, a frequency occurrence of 43% was calculated for the human marker in HD watersheds compared to 37% in LD watersheds. This once again confirms our suspicions that in HD watersheds inputs from septic systems may be contributing to fecal pollution of surface waters since our research indicates that there are no wastewater discharge permits (NPDES) in the study watersheds (Georgia GIS Clearing House, https://data.georgiaspatial. org/index.asp). Data from the study indicates a positive correlation between OWTS density and human specific

marker yield. This relationship was strongest in spring of 2012 with a correlation coefficient R = 0.67 (Figure 7a). Samples from winter 2012 (Figure 7b) and spring 2014 (data not shown) were also positively correlated with OWTS density, albeit with low R values.

Conclusion

The results of this study points to ongoing fecal pollution issues in streams of urbanizing watersheds in the metro-Atlanta area. These pollution issues vary in temporal and spatial scales and can be attributed to several factors including the density of septic systems in the watersheds. This is evidenced by the higher levels of the human marker in HD watersheds and the positive correlation between OWTS density and human marker yield. There appears to be a strong seasonal influence on OWTS density – water quality interaction, with spring showing the strongest OWTS impact.

References

Ahmed, W., Sidhu, J. P. S., and Toze, S. (2012) Evaluation of the nifH Gene Marker of Methanobrevibacter smithii for the Detection of Sewage Pollution in Environmental Waters in Southeast Queensland, Australia. *Environ Sci Technol* **46**, 543-550.

Arnade, L. J. (1999) Seasonal Correlation of Well Contamination and Septic Tank Distance. *Ground Water* **37**, 920-923.

Fong, T.-T., Griffin, D. W., and Lipp, E. K. (2005) Molecular assays for targeting human and bovine enteric viruses in coastal waters and their application for library-independent source tracking. *Appl Environ Microbiol*, 2070.

GDNR (Georgia Department of Natural Resources). 2011. Draft total maximum daily load evaluation for two segments of Lake Allatoona in the Coosa River Basin. Available online at http://www.gaepd.org/Documents/TMDL_page.html.

GDNR (Georgia Department of Natural Resources). 2002. Total maximum daily loads (TMDLs) for fecal coliform in 303(d) listed streams in the Altamaha River Basin. U.S. Environmental Protection Agency, Region 4. Georgia Department of Naural Resources, Atlanta, GA.

Habteselassie, M. Y., Kirs, M., Conn, K. E., Blackwood, A. D., Kelly, G., and Noble, R. T. (2011) Tracking microbial transport through four onsite wastewater treatment systems to receiving waters in eastern North Carolina. *J Appl Microbiol* **111**, 835-847.

Kildare, B. J., Leutenegger, C. M., McSwain, B. S., Bambic, D. G., Rajal, V. B., and Wuertz, S. (2007) 16S rRNA-based assays for quantitative detection of universal, human-, cow-, and dog-specific fecal< i> Bacteroidales</i>: A Bayesian approach. *Water Res* **41**, 3701-3715.

Landers, M. N., and Ankcorn, P. D. (2008). "Methods to Evaluate Influence of Onsite Septic Wastewater-Treatment Systems on Base Flow in Selected Watersheds in Gwinnett County, Georgia, October 2007." U. S. Geological Survey.

Layton, A., McKay, L., Williams, D., Garrett, V., Gentry, R., and Sayler, G. (2006) Development of Bacteroides 16S rRNA gene TaqMan-based real-time PCR assays for estimation of total, human, and bovine fecal pollution in water. *Appl Environ Microbiol* **72**, 4214-4224.

Metropolitan North Georgia Water Planning District, 2006. Septic Systems status and issues working paper: Atlanta, Georgia, 37p., accessed September 25, 2014 at http://documents.northgeorgiawater.org/District_Septic_Report_Mar2006.pdf.

Rantz, S.E., 1982, Measurement and computation of stream-flow—Volume 1, Measurement of stage and discharge: U.S. Geological Survey Water-Supply Paper 2175, 284 p.,also available online at http://pubs.usgs.gov/wsp/wsp2175/.

Reischer, G. H., Kasper, D. C., Steinborn, R., Mach, R. L., and Farnleitner, A. H. (2006) Quantitative PCR method for sensitive detection of ruminant fecal pollution in freshwater and evaluation of this method in alpine karstic regions. *Appl Environ Microbiol* **72**, 5610-5614.

US Environmental Protection Agency (2012) Recreational Water Quality Criteria, accessed September 19, 2014 at *http://water.epa.gov/scitech/swguidance/standards/criteria /health/recreation/upload/RWQC2012.pdf*.

U.S. Geological Survey (variously dated) National field manual for the collection of water-quality data: U.S. Geological Survey Techniques of Water-Resources Investigations, book 9, chaps. A1-A9,accessed August 30, 2014 at *http://pubs.water.usgs.gov/twri9A.*

U.S. Environmental Protection Agency (2002) Onsite waste-water-treatment systems manual: National Risk Management Research Laboratory Report EPA/625/R-00/008.

U.S. Environmental Protection Agency (1977) The Report to Congress - Waste Disposal Practices and Their Effects on Groundwater. U.S. Environmental Protection Agency, Washington, D.C..

Wuertz, S., Wang, D., Reischer, G. H., and Farnleitner, A. H. (2011) Library-Independent Bacterial Source Tracking Methods. *Microbial Source Tracking: Methods, Applications, and Case Studies*, 61-112.

Tables and Figures

Table 1. Septic system properties and land use characteristics in the study area

Watershed ID	Low density (LD) or high density (HD) of septic systems	Basin area (km^2)	Septic density (units/km^2)	Median distance of septic to stream (m)	% Forest cover	% Agriculture land use	% Developed area	% Impervious area	% Slope
1	LD	8.39	8	163	51.0	27.7	9.4	4.2	8.8
2	LD	1.55	10	126	44.5	25.8	13.8	3.3	10.6
3	LD	2.67	14	163	48.8	32.9	10.2	4.3	8.5
4	LD	0.62	36	172	46.4	23.9	22.0	11.6	7.3
5	LD	1.48	20	86	32.6	45.5	17.8	5.4	5.8
6	LD	5.28	15	108	30.2	49.2	14.4	4.1	6.5
7	LD	1.11	18	90	43.7	29.4	18.5	6.3	10.6
8	LD	1.27	17	94	34.2	48.9	14.3	3	9.2
9	LD	2.95	27	159	26.4	42.6	23.4	7.8	7.7
10	LD	4.4	34	119	43.1	17.2	36.1	7.3	8.3
11	LD	4.2	25	119	31.8	36.3	25.6	7.6	7.8
15	LD	1.68	37	140	14.7	10.3	70.6	15.2	4.6
12	HD	3.29	115	105	44.1	10.6	41.8	12.3	9.1
13	HD	8.81	88	117	33.8	6.6	54.5	13.2	8
14	HD	1.74	141	104	26.0	6.1	60.7	16.1	8.5
16	HD	2.59	187	99	19.6	0.1	77.6	26.4	5.7
17	HD	1.68	230	138	21.0	12.0	66.8	20.1	7.5
18	HD	0.98	308	151	31.3	1.5	66.6	18.4	7.4
19	HD	0.18	373	105	11.4	0.0	88.2	20.3	7.8
20	HD	0.54	290	83	24.8	0.0	75.5	18.3	6
21	HD	1.14	214	63	22.2	5.0	70.7	17.5	8.6
22	HD	1.94	157	63	21.7	4.5	71.7	18.9	7
23	HD	0.52	233	65	22.9	3.1	73.9	18.4	7.3
24	HD	0.67	253	55	19.4	1.6	77.7	20	7.6
Mean LD		**2.97**	**22**	**128**	**37.3**	**32.5**	**23.0**	**6.7**	**8**
Mean HD		**2.01**	**216**	**96**	**24.8**	**4.2**	**68.8**	**18.3**	**7.5**

Table 2. General and host-specific Bacteroidales marker conditions for qPCR reactions

Host	Marker name	Primers	Sequences (5' - 3')	Reaction condition	Source
General Bacteroidales	AllBac	AllBacF	GAGAGGAAGGTCCCCCAC	2 min at 50^{o}C, denaturation for 10 min at 95^{o}C; cycling: 30 sec at 95^{o}C, 45 sec at 60^{o}C	Layton et al. (2006)
		AllBacR	CGCTACTTGGCTGGTTCAG		
Human specific	BacHum	BacHum 160F	TGAGTTCACATGTCCGCATGA	2 min at 50^{o}C, denaturation for 10 min at 95^{o}C; cycling: 15 sec at 95^{o}C, 1 min at 60^{o}C	Kildare et al. (2007)
		BacHum 241R	CGTTACCCCGCCTACTATCTAATG		
Ruminant specific	BacR	BacR_f	GCGTATCCAACCTTCCCG	2 min at 50^{o}C, denaturation for 10 min at 95^{o}C; cycling: 15 sec at 95^{o}C, 1 min at 60^{o}C	Reischer et al. (2006)
		BacR_r	CATCCCCATCCGTTACCG		

Table 3. Mean and ranges of microbial water quality parameters (Data summarized by season and watershed group; LD or HD = watersheds with low or high density of septic systems, respectively)

	Spring						Summer					
	LD watersheds			HD watersheds			LD watersheds			HD watersheds		
Parameter	Mean	Low	High	Mean	Low	High	Mean	Low	High	Mean	Low	High
E. coli count (MPN 100 ml^{-1})	485	41	2,739	413	10	1,643	533	28	1,970	313	68	985
E. coli yield (MPN sec^{-1} km^{-2})	35,937	2,456	255,944	33,900	542	164,293	22,563	1,066	83,628	24,382	892	100,495
Enterococci count (MPN 100 ml^{-1})	285	56	1399	759	54	5,635	2,238	259	11401	879	92	5963
Enterococci yield (MPN sec^{-1} km^{-2})	22,720	3,294	130,682	58,919	3,961	305,189	127,832	4,539	538,160	72,146	2,199	524,120

	Winter						Pooled dataset					
	LD watersheds			HD watersheds			LD watersheds			HD watersheds		
Parameter	Mean	Low	High	Mean	Low	High	Mean	Low	High	Mean	Low	High
E. coli count (MPN 100 ml^{-1})	261	15	1,181	238	10	1,358	404	15	2,739	309	10	1,643
E. coli yield (MPN sec^{-1} km^{-2})	7,383	75	55,017	5,719	125	28,595	20,029	75	255,944	19,103	125	164,293
Enterococci count (MPN 100 ml^{-1})	251	20	1,173	301	31	1,351	829	20	11,401	597	31	5,963
Enterococci yield (MPN sec^{-1} km^{-2})	6,210	234	29,484	6,432	565	41,515	45,677	234	538,160	40,204	565	524,120

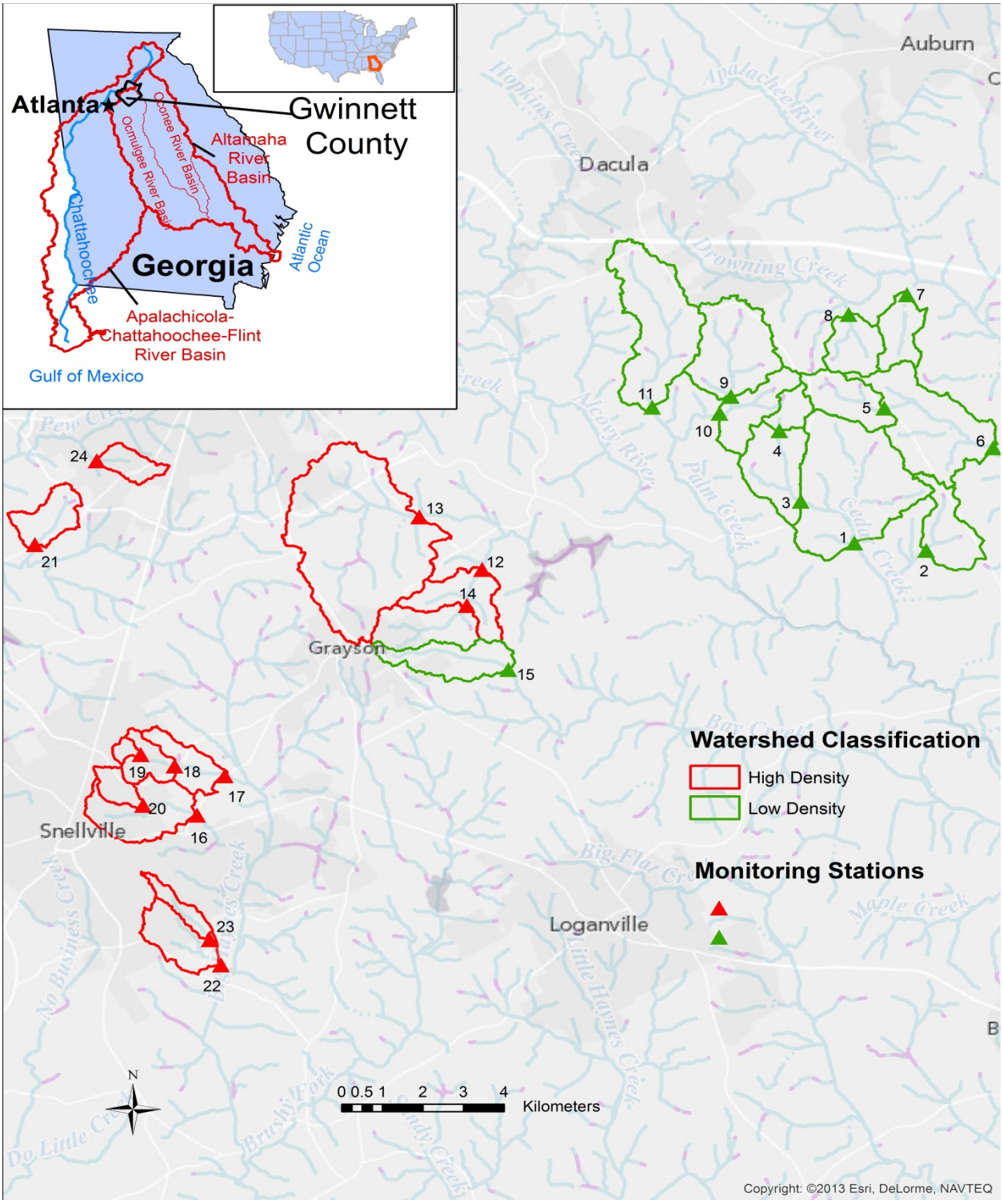

Figure 1. Location of the study site with boundaries for watersheds with low (LD) or high (HD) density of septic systems and monitoring stations in Gwinnett County, GA

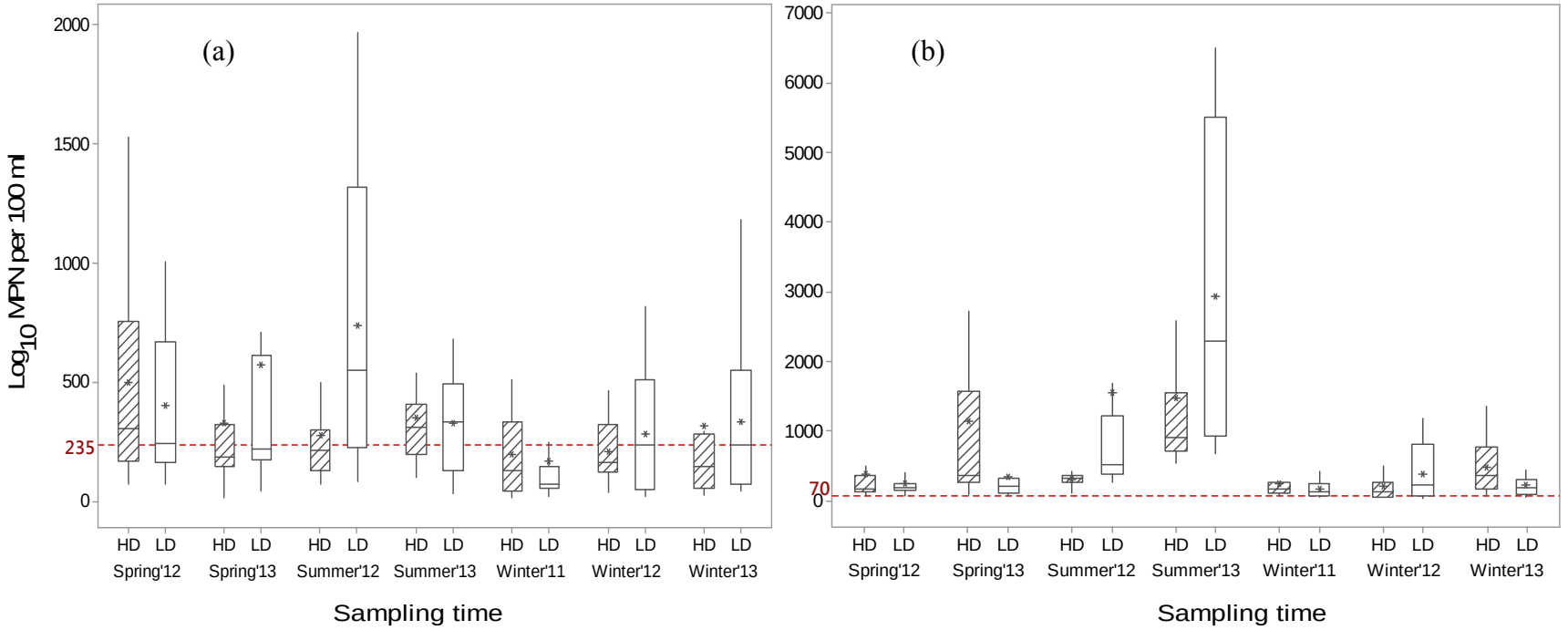

Figure 2. *E. coli* (a) and enterococci (b) counts in streams of watersheds with low (LD) or high (HD) density of septic systems over the sampling period. Broken line represents the single sample threshold value for *E. coli* and enterococci for recreational use. Mean bacterial count for each sampling event is represented by (x) on each boxplot.

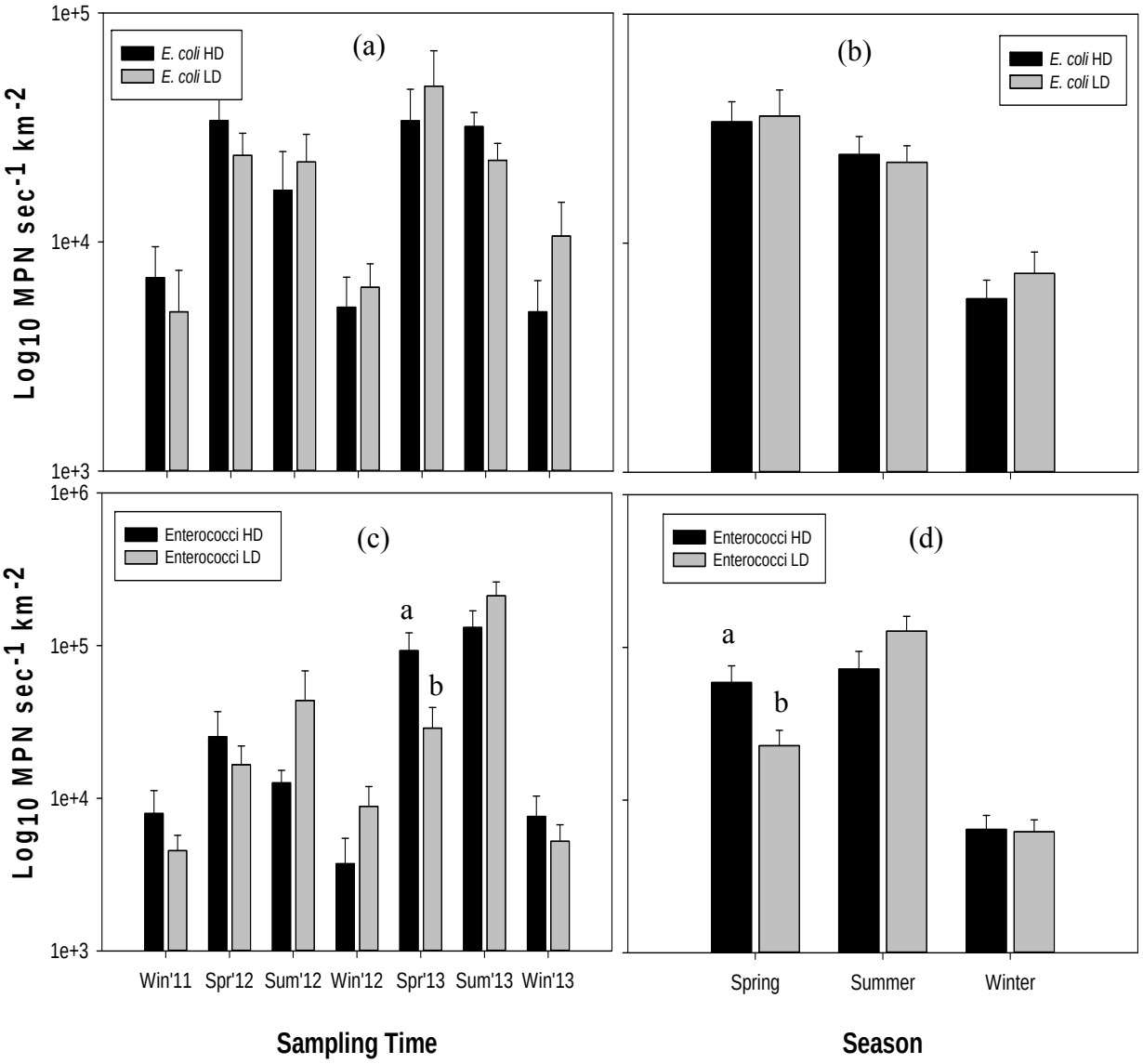

Figure 3. *E. coli* and enterococci stream yield grouped by sampling period and season in watersheds with high density or low density of septic systems; significant differences between high density and low density watersheds within season are represented by letter designations. Bars without letter designations are not statistically different between high and low density watersheds within season.

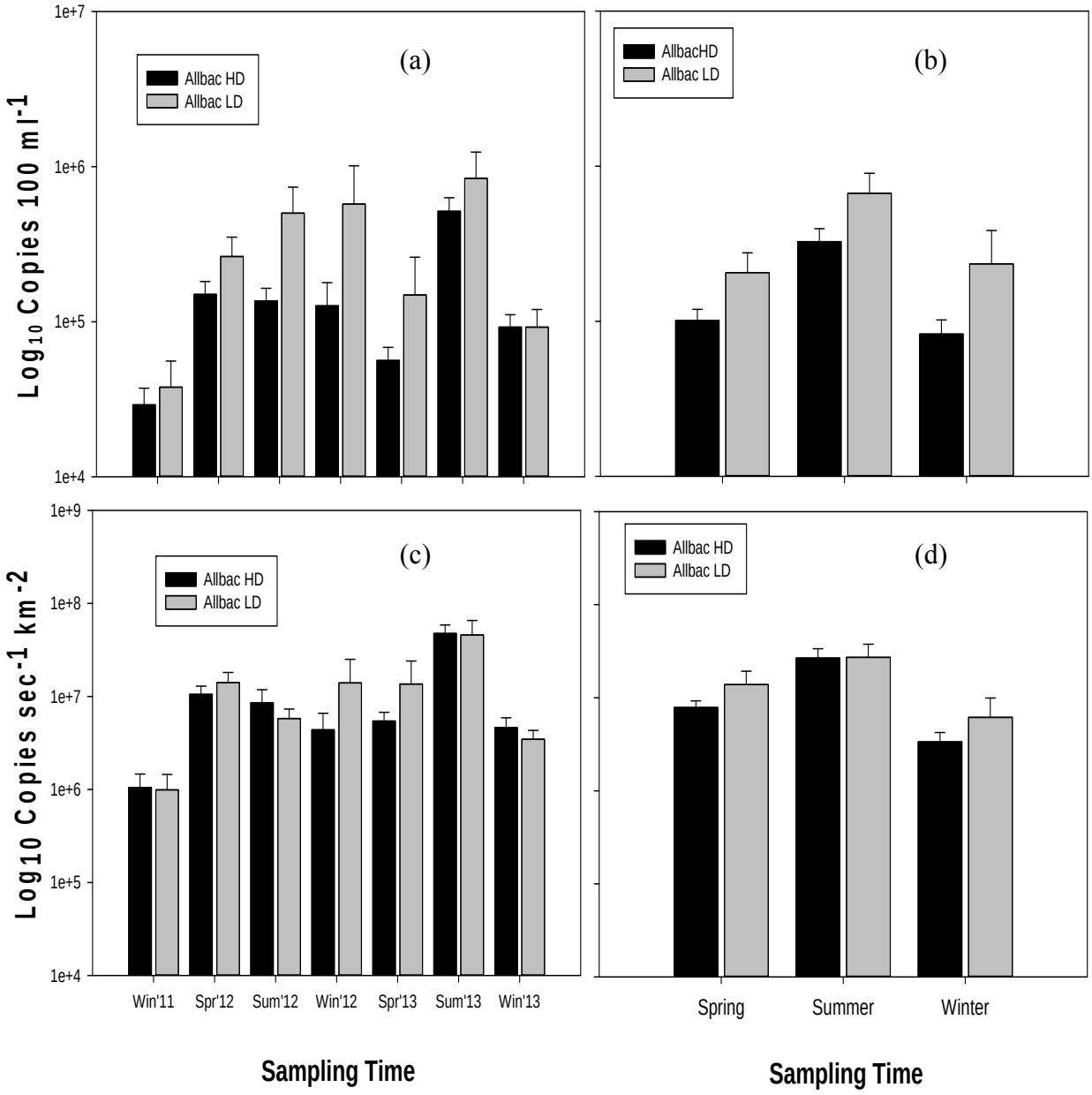

Figure 4. General Bacteroidales density (a and b) and stream yield (c and d) in high density (HD) and low density (LD) watersheds

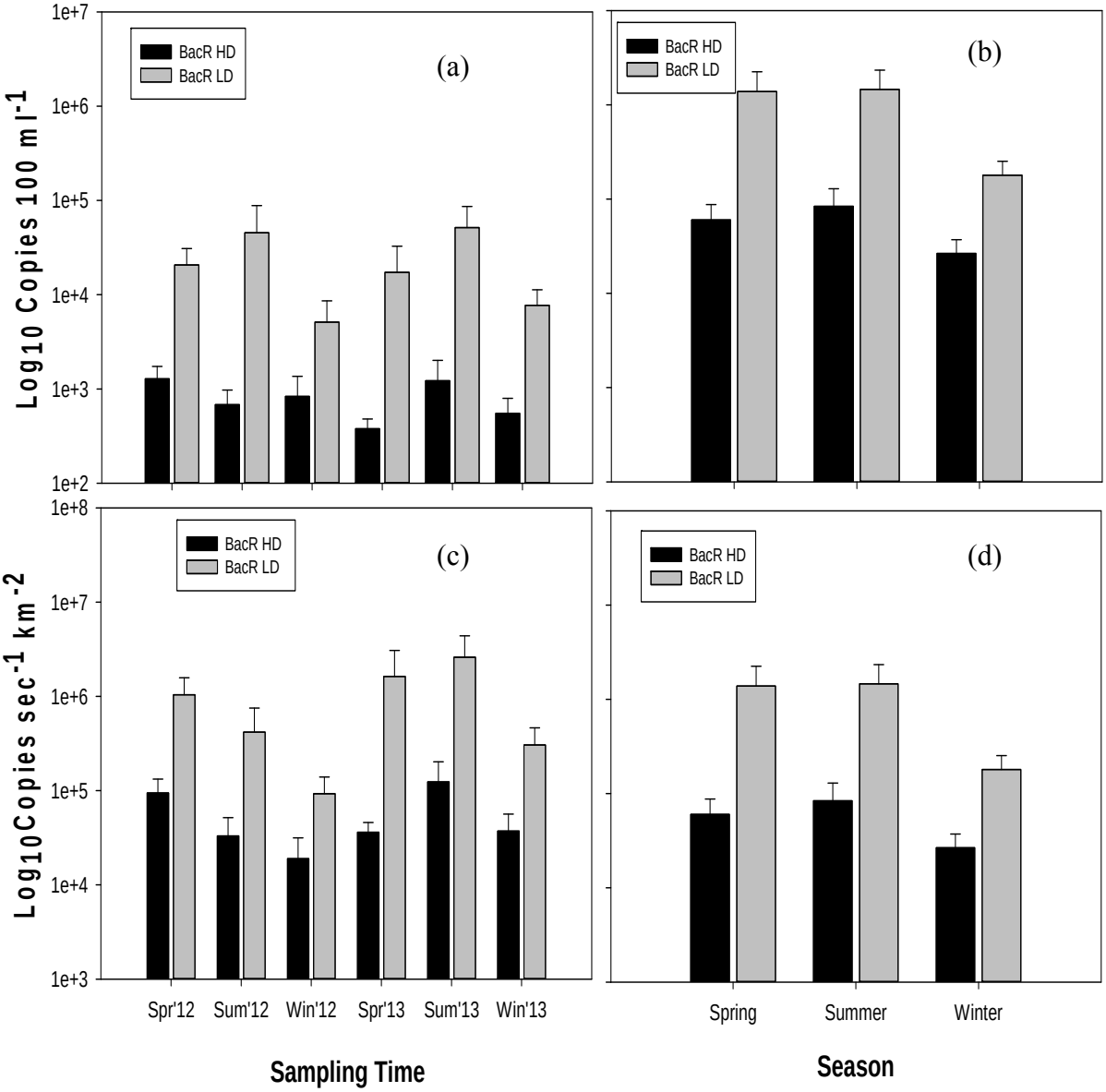

Figure 5. Ruminant marker density (a and b) and stream yield (c and d) in HD and LD watersheds according to sampling period and season

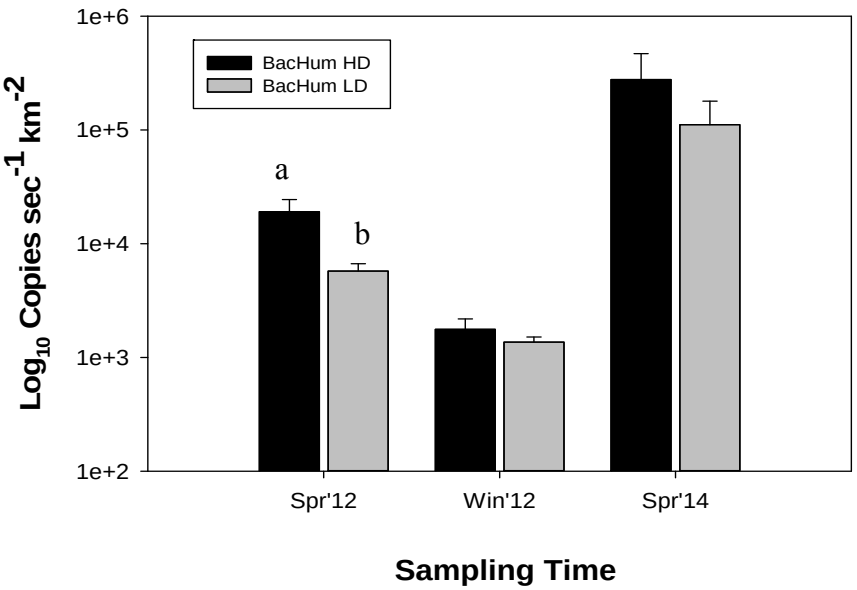

Figure 6. Comparison of human specific marker yield according to OWTS density over three sampling periods. Bars with letter designations are significantly different for HD and LD watersheds.

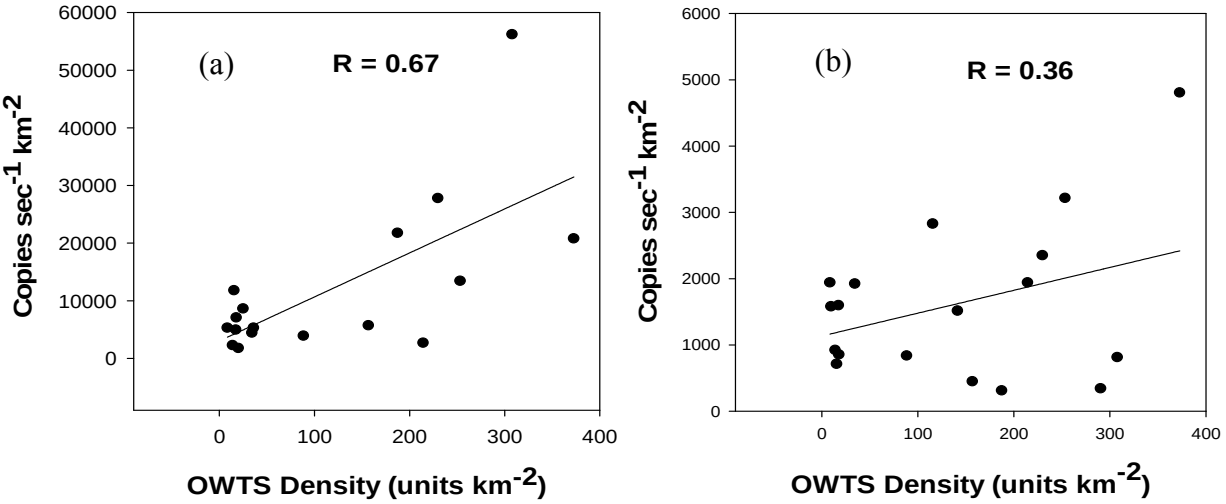

Figure 7. Relationship between OWTS density and human specific marker for samples collected in spring 2012 (a) and winter 2012 (b)

Unimpaired Flows for the ACF River Basin: Improvement and Uncertainty Assessment

Basic Information

Title:	Unimpaired Flows for the ACF River Basin: Improvement and Uncertainty Assessment
Project Number:	2013GA333B
Start Date:	3/1/2013
End Date:	11/30/2014
Funding Source:	104B
Congressional District:	Georgia
Research Category:	Climate and Hydrologic Processes
Focus Category:	Hydrology, Management and Planning, Water Quantity
Descriptors:	None
Principal Investigators:	Aris P. Georgakakos, Martin Kistenmacher

Publications

There are no publications.

Value of Drought Prediction for the Management of the ACF River Basin

Technical Report

Developed by

The Georgia Water Resources Institute/Georgia Tech

Developed under

State Water Resources Research Institute 104b Program

May 2015

Value of Drought Prediction for the Management of the ACF River Basin

Technical Report

Developed by

The Georgia Water Resources Institute/Georgia Tech

Authors

Aris P. Georgakakos and **Martin Kistenmacher**

Sponsored by

State Water Resources Research Institute 104b Program: Fiscal Year 2013/2014

ACF Stakeholders

May 2015

Acknowledgements

This study was funded in part by the ACF Stakeholders through a sub-contract with Black & Veatch Inc. Additional funds were provided by the Georgia Water Resources Institute (through the 104b program of the National Institute for Water Resources and USGS) and Georgia Tech.

We are grateful to the ACF Stakeholders for the opportunity to support their effort toward the development of a shared vision water management plan. It is our sincere hope that our work will facilitate the successful conclusion of this historic process with new and reliable technical information.

Report Citation

This report should be cited as follows:

Georgakakos, A.P., and M. Kistenmacher, 2015: Value of Drought Prediction for the Management for the ACF River Basin. Technical Report, Georgia Water Resources Institute, Georgia Institute of Technology, Atlanta, Georgia, 34p.

Executive Summary

This study demonstrates that (i) skillful, multi-lead flow forecasts can be generated for all ACF sub-basins throughout the year based on preceding unimpaired inflow and soil moisture predictor variables, and (ii) the use of forecast information in reservoir operations would accrue benefits to a variety of water uses including navigation, environmental flow support, hydropower generation, water use management, and recreation.

While forecast value was demonstrated in relation to droughts, reliable forecasts are also possible and useful for non-drought periods. Overall, the study finds that proactive, forecast-based operations can improve the management of ACF by anticipating future hydrologic conditions and water stresses, and leveraging management opportunities months in advance.

Contents

1. Introduction

From a water resources management standpoint, the most critical attributes of *meteorological* variables (e.g., rainfall, evapotranspiration, etc.) are their marked uncertainty and variability across a wide range of temporal scales, from minutes to decades. As a consequence, *hydrologic* variables including streamflow, soil moisture, and aquifer recharge are also markedly uncertain and variable, occasionally bringing about extreme events far above or below average conditions. Floods and droughts are such extreme events of keen water management concern and interest. This investigation focuses on seasonal droughts, but the results also apply to wet climatic periods.

The work presented in this report investigates (i) the feasibility and accuracy of multi-lead drought forecasts, and (ii) the value of using drought forecasts in reservoir and water resources management in the Apalachicola-Chattahoochee-Flint (ACF) river basin.

Section 2.1 of the report presents the motivation for this investigation. Section 2.2 first discusses general quantities that may serve as potential drought indicators, and subsequently describes a list of specific indicators for the ACF river basin. Section 2.3 outlines the technical process of generating, validating, and assessing flow forecasts. Section 2.4 provides four examples of seasonal flow forecasts, two of which pertain to the Lake Lanier watershed and two to the ACF watershed upstream of the Chattahoochee gage on the Apalachicola River. Section 2.5 explains how forecasts can be incorporated in the management process, especially the operation of reservoirs, and outlines the decision framework best suited to utilize forecasts. Section 2.6 presents a case study demonstrating that the use of flow forecasts in the operation of the ACF reservoirs can indeed improve basinwide management and performance. While this demonstration focuses on objectives related to environmental and navigation flows, it may be modified to benefit other water uses as well. The report concludes with Chapter 3 which summarizes the overall findings and conclusions of the investigation.

2. Drought Prediction and Management

2.1 Drought Management Purpose

A key component of a sustainable water management plan is a set of provisions for managing the system during droughts. Indeed, the ACF baseline operations currently used to operate the reservoir in the ACF basin (see Appendix A and B for further detail) include adjustments to some water uses during dry hydrologic conditions. Specifically, the hydropower generation hours are decreased as reservoir storage falls below certain thresholds. Additionally, the environmental flow requirements downstream of J. Woodruff become less stringent when the system composite storage and basin inflows decrease.

Both of these adjustments are largely reactive. Specifically, water management actions, such as changes in water use and flow targets, come into effect only *after* drought conditions have clearly impacted the basin. The purpose of the investigation described in this section is to explore the value and operational feasibility of *proactive* drought management rules, i.e., rules that use forecasts of future hydrologic conditions to adjust reservoir operations and water use levels in anticipation of these conditions. In particular, we focus on two questions: (a) Can drought and non-drought periods be reliably forecasted, and (b) can operations be adjusted to take advantage of these forecasts? With respect to the first question, a variety of different indicators are evaluated to determine their ability to forecast future hydrologic conditions. Particular attention is paid to how reliable these indicators are, and how far into the future hydrologic conditions can be forecasted. The second question involves using the forecasts to adjust reservoir operations and water use target levels to mitigate impacts that would have occurred in the absence of proactive drought management measures.

Forecast-based operation is not just important for mitigating impacts during droughts. Forecasts can also be used to anticipate wet conditions, during which reservoir operations can be adjusted to increase water uses and augment stakeholder benefits.

This investigation is not intended to develop the best possible drought management assessment, prediction, and management procedures, but rather to demonstrate the feasibility and value of developing and operationalizing such procedures (proof of concept).

2.2 Drought Indicators

Indicators are variables that serve to detect the arrival (or predict the onset) of different hydrological conditions. General indicator categories include, among others:

- Unimpaired flow (UIFs);
- Precipitation;
- Soil moisture storage;
- Reservoir storage;

- Groundwater storage;
- Salinity;
- Other indices.

For this study, the following specific indicators are considered:

- Local/Cumulative UIFs;
- Mean Areal Precipitation (MAP);
- Standard Precipitation Index (SPI);
- Palmer Drought Severity Index;
- Palmer Modified Drought Index;
- Palmer Z-Index;
- Palmer Hydrologic Drought Severity Index;
- Total Soil Moisture Storage computed by the GWRI Watershed Model;
- Lower Soil Moisture Storage computed by the GWRI Watershed Model;

Each of these indicators are computed for 10 different ACF sub-basins (**Figure 2-1**):

(i) Buford;
(ii) West Point;
(iii) W.F. George;
(iv) Montezuma;
(v) Albany;
(vi) Bainbridge;
(vii) Buford +West Point;
(viii) Buford +West Point + W.F. George;
(ix) Entire Flint + the sub-basin from W.F. George to J. Woodruff;
(x) ACF basin upstream of the Chattahoochee gage.

The unimpaired flow dataset has been developed by the U.S. Army Corps of Engineers [USACE, 1997 & 2004], Mean aerial precipitation is computed from the gridded CRU dataset [Harris et al., 2013], while the SPI and the various Palmer indices were derived from the National Climate Division Dataset developed by NOAA. Additionally, soil moisture storage variables are obtained from the GWRI rainfall-runoff model calibrated for each sub-basin.

Figure 2-1: ACF Sub-basins and Drought Index Locations

Hydrologic models generate streamflows from meteorological inputs, such as precipitation and potential evapotranspiration, by simulating the flow of water through the surface and sub-surface systems (**Figure 2-2**). The GWRI rainfall-runoff model uses two storage components (zones) to simulate the subsurface processes. The upper soil moisture zone controls *interflow* which represents the fast responding streamflow contribution. The lower soil moisture zone controls the slow responding *baseflow* which sustains streamflow during long dry periods. The model total soil moisture storage, and the storage of the lower zone are used as indicator variables.

For each dataset, historical measurements from 1939-2008 are used to develop and validate the drought assessment and forecasting schemes.

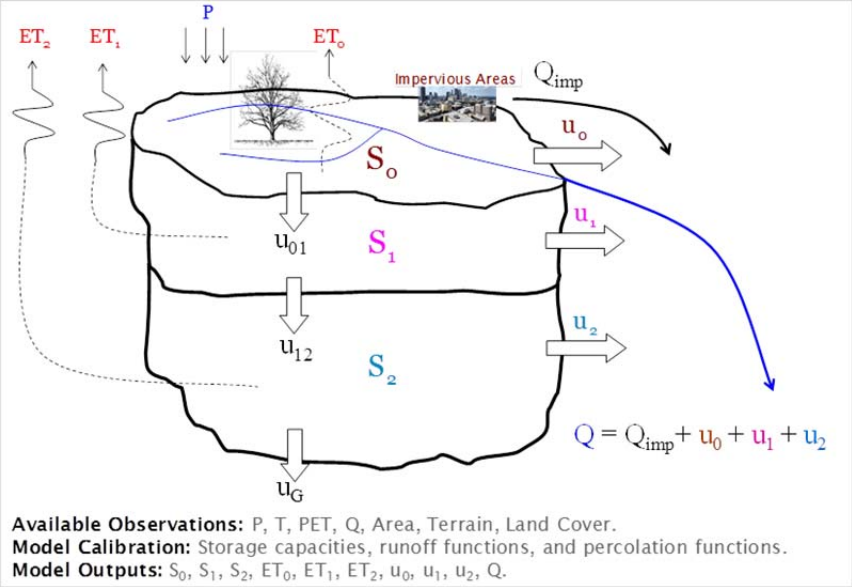

Figure 2-2: GWRI Rainfall-Runoff Model

2.3 Drought Forecasting Goal, Model Development and Validation Process

The **goal of the drought forecasting approach** is to predict the *cumulative* unimpaired flow volume expected to materialize out of a particular ACF sub-basin over a certain calendar period.

Considering that 9 indicator variables are computed for each of 10 ACF sub-basins, a total of 90 different indicators are generated and assessed. These indicators are used as predictor variables to develop models that forecast the unimpaired flow of each sub-basin.

The forecasting **model development and validation process** is outlined below:

1. *Specify forecast model attributes:* Select the time of the year when the forecast will be issued, the length of the forecasting horizon, and the predictor variables (i.e., the indicators to be used) to develop the forecasting model.

2. *Calibrate the forecasting model:* Use portion of the historically observed data to develop models that relate the predictor variables to the unimpaired flows.

3. *Assess model validity and accuracy:* Use a different (non-overlapping) data portion than the data portion used in Step 2 to assess the validity and accuracy of each forecasting model configuration.

The previous process is repeated for each of the 10 ACF sub-basins, forecast issue date, forecast horizon length, and combination of indicators to identify the best forecasting model for each sub-basin and time of the year.

Developing and evaluating drought forecasting models is a highly tedious process, requiring assessment of numerous predictor variable combinations for each sub-basin and time of the year. To facilitate these computations, GWRI has developed tools that automate this process and can quickly assess the forecasting value of various alternative model configurations.

2.4 Forecasting Model Examples

Forecasting models were developed for all 10 sub-basins and various calendar periods. This section discusses four model examples, two of which pertain to the Lake Lanier sub-basin and two to the ACF sub-basin upstream of the Chattahoochee gage on the Apalachicola River.

2.4.1 Forecasting Models for Lake Lanier

Figure 2-3 presents assessment results for two forecasting models developed for the Lake Lanier watershed.

The first forecasting model is developed to generate forecasts on April 1 of each year for the cumulative unimpaired flow of the following *two* months (April 1 to May 31). The second model is developed to issue forecasts on the same calendar date as the first (April 1) but aims to predict the cumulative unimpaired flow of the following *four* months (April 1 to July 31).

After evaluating various predictor variable combinations, the best performing models are identified to be those using the UIFs and the soil moisture storages of the previous two months (March and February) as predictor variables. Namely, both models use four predictor variables [i.e., UIF_{Lanier} (March), UIF_{Lanier} (February), SM_{Lanier} (March), SM_{Lanier} (February)] to predict the UIF volume for the upcoming two and four months respectively. (The PDSI index for March and February is also found to perform well in the second model.) The mathematical relationship between predictor and predicted variables is derived through regression analysis.

Forecast evaluation is carried out through retrospective assessments in which the models are used on April 1 of each historical year to predict the forthcoming UIF volume. The forecasts issued for all historical years are then evaluated against the UIF volumes actually observed. **Figure 2-3** presents the forecasted and observed quantities for 1939 to 2008 and shows that UIF forecasts exhibit good skill in both cases. This is confirmed by the correlation coefficient between observed and forecasted UIF volumes which is estimated to be 0.76 and 0.74 respectively for the first and second forecasting model.

Additional forecasting models were developed for Lake Lanier for other calendar dates and lead times. While each model uses different predictor variables, forecast assessments show that UIF forecast skill is overall good from January to April and from April to October.

2.4.2 Forecasting Models for the Chattahoochee Gage (Apalachicola)

Figure 2-4 presents assessment results for two forecasting models developed for the ACF sub-basin upstream of the Chattahoochee gage on the Apalachicola River.

The first forecasting model is developed to generate forecasts on May 1 of each year for the cumulative unimpaired flow of the following *six* months (May 1 to October 31). The second model is developed to issue forecasts on August 1 of each year for the following *three* months (August 1 to October 31).

For May 1 forecasts, the best performing model uses the UIF and soil moisture values of the previous two months (April and March) as predictor variables: UIF_{Chatt} (April), UIF_{Chatt} (March), $SM_{ACF\text{-}Chatt}$ (April), and $SM_{ACF\text{-}Chatt}$ (March). As noted earlier, the soil moisture index is the storage of the lower soil moisture zone of the GWRI rainfall-runoff model calibrated for the ACF sub-basin upstream of the Chattahoochee gage.

For August 1 forecasts, the best performing model uses the UIF and soil moisture values of the previous two months (July and June) as predictor variables: UIF_{Chatt} (July), UIF_{Chatt} (June), $SM_{ACF\text{-}Chatt}$ (July), and $SM_{ACF\text{-}Chatt}$ (June). Comparable forecast performance is also obtained by using the PDSI index for July and June instead of soil moisture.

Figure 2-4 presents the forecasted and observed quantities for 1939 to 2008 and shows that UIF forecasts exhibit good skill in both cases. The correlation coefficient between observed and forecasted UIF volumes is estimated to be 0.71 and 0.82 respectively for the first and second forecasting model.

Additional forecasting models developed for the Chattahoochee gage and other calendar dates and lead times indicate that forecast skill is good throughout the year.

Furthermore, models developed for other locations on the Chattahoochee and Flint Rivers yielded similar positive results and findings.

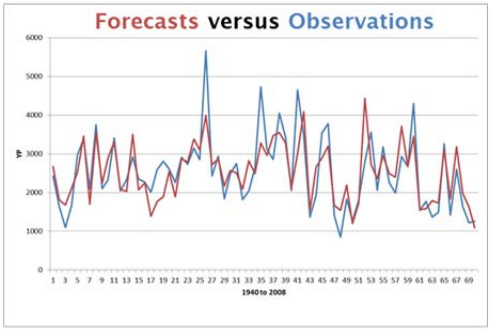

First Model:
Forecasted Quantity: UIF_{Lanier} : April 1 - May 31 (**2 m**)
Forecast Issue Date: April 1
Predictor Variables: UIF_{Lanier}(Mar, Feb); SM_{Lanier}(Mar, Feb)
Correlation (Observed vs. Predicted): **0.759**
Error St. Dev.: 564 cfs

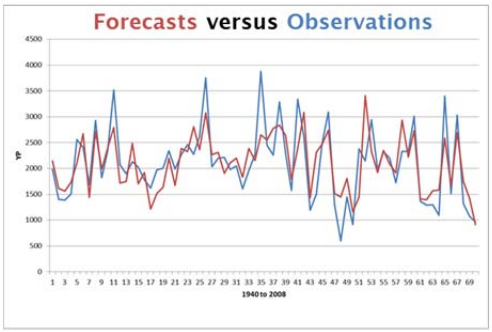

Second Model:
Forecasted Quantity: UIF_{Lanier} : April 1 - July 31 (**4 m**)
Forecast Issue Date : April 1
Predictor Variables: UIF_{Lanier}(Mar, Feb); SM_{Lanier}/PDSI(Mar, Feb)
Correlation (Observed vs. Predicted): **0.735**
Error St. Dev.: 439 cfs

Figure 2-3: Forecasting Model Examples for the Lake Lanier Watershed

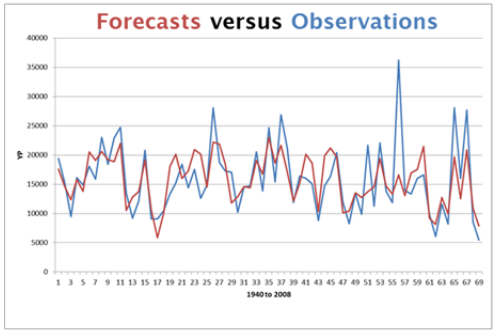

First Model:
Forecasted Quantity: UIF_{Chatt} : May 1 - Oct 31 (**6 m**)
Forecast Generation: May 1
Index Variables: UIF_{Chatt}(Apr, Mar); SS_{ACF}/PDSI(Apr, Mar)
Correlation (Observed vs. Predicted): **0.708**
Error St. Dev.: 4,087 cfs

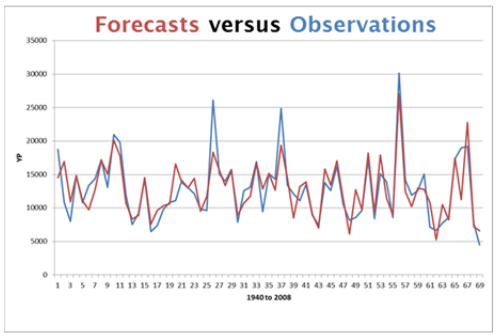

Second Model:
Forecasted Quantity: UIF_{Chatt} : Aug 1 - Oct 31 (**3 m**)
Forecast Generation: August 1
Index Variables: UIF_{Chatt}(Jul, Jun); SS_{ACF}/PDSI(Jul, Jun)
Correlation (Observed vs. Predicted): **0.82**
Error St. Dev.: 2,518 cfs

Figure 2-4: Forecasting Model Examples for the Chattahoochee Gage (Apalachicola)

2.5 Forecast Value in Reservoir Operations and Water Resources Management

The forecasting models described in the previous sections were used to answer the question "Can operations be adjusted to take advantage of these forecasts?" The ACF basin, however, has multiple purposes, and operations could be adjusted in several alternative ways to benefit different stakeholders and water uses. Thus, adjusted operations should therefore include new rules that use forecast information, but also rules that reflect the manner in which the basin stakeholders envision to share the benefits of forecast-based operations. However, a comprehensive study evaluating the merits and trade-offs of different forecast-based operating policies and benefit sharing schemes is beyond the scope of this report. Instead, the potential value of forecast-based operations will be shown through a case study that uses forecasts to vary the level of flow support at one location in the basin.

The case study builds on a water management alternative, denoted as AltPulse, derived from baseline operations. The baseline operations are described in detail in Appendix B and represent the current operations, physical characteristics, and water use conditions in the ACF basin. The AltPulse scenario is identical to the baseline operations, except for the following changes:

- The logic used to coordinate the major reservoirs has been slightly modified.
- More flexible hydropower generation rules have been added.
- Flow pulses out of J. Woodruff consisting of a minimum of 9,000 cfs for at least two consecutive weeks in May and July have been added.

Both the baseline operations and the AltPulse scenarios were assessed via river basin models that simulate the behavior of the river and characterize its ability to meet environmental and socio-economic objectives under different water management alternatives. Daily flow data from the historical period from 1939-2008 is used to drive all model simulations and assessments. The models then generate time series of results over the same historical period. Model outputs include various water related quantities such as reservoir storages and elevations; hydropower generation (primary and secondary); consumptive uses by sector; high, normal, and low river flows; environmental conditions; and other important variables. Systematic analysis and inter-comparisons of these results are then used to determine how well stakeholder interests are met by particular water management alternatives. Appendix A contains a detailed description of the river basin models and data used as part of this study.

Figure 2-5 compares the simulated ACF composite storage sequences under the baseline (red) and AltPulse (dark blue) scenarios. The AltPulse composite storage is often higher than the baseline storage (for example during high flow periods) and does not fall significantly lower than the baseline storage even during drought times. These results indicate that the AltPulse scenario is able to keep more water in the system, although some of the other water uses may be affected, as discussed in Georgakakos and Kistenmacher [2015]. The basin stakeholders will ultimately

have to decide on whether the AltPulse water management alternative is desirable. Nonetheless, the question we consider next is whether this water management alternative can be improved upon by forecast-based operations.

Figure 2-5 also depicts results for two additional water management alternatives. Both alternatives are based on the AltPulse scenario, but provide increased flow support downstream of J. Woodruff in May and July. Specifically, one alternative (light blue) maintains the same pulse magnitude (9,000 cfs) but increases the duration of the pulses from a minimum of two weeks in each month to four weeks in each month. The other alternative (gray) increases the pulse duration as well as the magnitude by requiring four weeks of 16,000 cfs in each month. The figure shows that these management alternatives may result in lower composite storages than the baseline and the AltPulse scenarios. This is particularly true during droughts (lower right figure excerpt), where the releases needed to provide increased flow support result in large decreases in composite storage, especially for the 16,000 cfs pulses. On the other hand, the increased flow requirements do not significantly stress the system during wet periods (lower left figure excerpt). In most years, composite storage would only be slightly lowered under these pulsed scenarios. And during the wettest years, even the largest flow support requirements (i.e., 4 weeks of 16,000 cfs in May and July) could be met naturally without having to make any extra reservoir releases.

These results illustrate that increased flow support can be provided comfortably during wet periods, while doing so during drier periods may deplete system storage and increase overall water stress. Motivated by these observations, the value of forecast-based operations is illustrated by deriving new operating policies that adjust the level of flow support based on forecasted hydrologic conditions. Specifically, operational policy adjustments are developed in the following sequential decision framework.

Sequential Decision Framework Incorporating Flow Forecasts:

(i) At a critical decision date (say March 1 or April 1 of each year), the UIF forecasting models are used to forecast the hydrologic conditions for the coming months.
(ii) Based on whether the forecasts anticipate wet, normal, or dry streamflow conditions, the operating policy is adjusted to provide different levels of flow support.
(iii) Next, the reservoir system is operated to provide the adjusted level of flow support for the coming months.
(iv) At the next critical decision time (say May 1 or June 1 of each year), new forecasts are issued (given the actually observed predictor variables in previous months), and the process is repeated sequentially as the system evolves.

This is an example of an adaptive operating rule that adjusts the level of flow support as hydrologic conditions are anticipated to change over time. Such adjustments can be made at several critical times during each year to best leverage the information of the forecasts.

The benefits associated with forecast-informed operating policies are two-fold. First, higher levels of flow support could be provided during certain years without causing significant adverse impacts on composite storage or other water uses. Second, individual water users would know ahead of time what level of flow support is to be provided in the coming months. This is particularly important for water uses like commercial navigation since moving goods through the river network requires prior planning. Committing the reservoir system to support navigable flows provides assurance that navigation activities will indeed be supported and can be planned for the following weeks or months.

Forecasts are equally valuable for other water uses such as hydropower. Unlike current operational procedures, forecast-based operations would provide the energy sector with critical information on the amount and duration of dependable hydropower capacity and primary energy that the ACF system can commit several months in advance. If used effectively, this information can reduce energy generation costs and improve power planning and scheduling.

2.6 Using Forecasts to Improve Reservoir Operations

The general strategy outlined in the previous section was fine-tuned to develop the operating policy shown in **Figure 2-6**. The quantities to be forecasted are cumulative unimpaired flows at the Chattahoochee gage just downstream of J. Woodruff and are issued during two separate times of the year. The first forecast is issued at the beginning of April and considers a six-month future horizon spanning until October. Based on the value of these forecasts, different levels of flow support are committed for the upcoming month of May. If the forecasts are relatively high, the decision is to provide the highest pulse level (4 weeks at 16,000 cfs). On the other hand, if the forecasts are very low, the decision is to provide the lowest pulse level (2 weeks at 9,000 cfs). Lastly, if the forecast is between these two levels, the decision is to support 4 weeks of 9,000 cfs.

In addition to making commitments for May flow support, estimates of July flow commitments are also made at the May 1 forecast time. However, these commitments are tentative and may be adjusted later in June, when updated forecasts are issued. This second set of forecasts is issued on June 1 and considers a four-month horizon spanning from June to October. Based on the value of these forecasts, different levels of flow support are committed for the upcoming month of July. Once again, the level of flow support varies with the forecasted inflow conditions. If the forecasts indicate drier conditions, flow support levels are decreased. Additionally, if the composite storage at the beginning of June is low ($\leq$ 3,000,000 acre-feet), the decision is to provide the lowest pulse level.

The ACF system is simulated using the previous operating policy and the resulting composite storage sequence is shown in **Figure 2-7**. Under the forecast-based operations, the ACF composite storage remains significantly above that of the baseline for most of the simulation

period and falls to the baseline level only during severe droughts. With respect to the AltPulse water management scenario, the forecast-based operations show slight drawdowns during wet periods, and no significant differences during drought periods. Thus, the forecast-based operations lead to an ACF composite storage sequence that is clearly better than that of the baseline and comparable to that of the AltPulse scenario. But, how do the operating policies compare with respect to flow support?

Figure 2-7 also lists the different levels of flow support that were committed during the simulation period. The AltPulse scenario only commits 9,000 cfs for 2 weeks in both May and July for every single year. On the other hand, the forecast-based operations can provide increased pulse commitments 80% of the time for May and 77% of the time for July. Additionally, commitments made in April for July only had to be adjusted downward in June 3% of the time. Namely, although tentative, the flow support commitments made in April for July are quite reliable.

3. Summary of Drought Prediction and Management for the ACF

The previous sections outline the development and assessment of flow forecasting models and forecast-based operating policies for the ACF River basin. Given a set of indicator variables, forecasts of hydrologic conditions are generated at critical times of the year. This information is then combined with reservoir management rules to develop operating policies that can anticipate and respond to future hydrologic conditions.

The study shows that skillful, multi-lead flow forecasts can be generated for all ACF sub-basins throughout the year. Best predictor variables include the unimpaired flows and soil moisture storages of the months preceding the date of the forecast. Soil moisture storage sequences are generated by the GWRI rainfall-runoff model calibrated for each ACF sub-basin. Retrospective assessments carried out for the 1939 – 2008 historical period show that flow forecast skill is high several months in advance.

Forecast accuracy and lead time could increase if rainfall forecasts were also available. Recently published research for the ACF shows that this is indeed possible [Chen and Georgakakos, 2014].

The study also shows that forecast-based operations are able to increase flow commitments downstream of J. Woodruff to provide benefits for environmental and navigation water uses. Increased flow commitments can be provided without causing impacts on upstream reservoir storages by using the forecasts to adjust the level of flow support depending on forecasted hydrologic conditions. While forecasts were only issued in April and June to make flow commitments for the following months of May and July, additional forecasts and release commitments could be also be applied in other months and seasons given that high quality flow

forecasts are available throughout the year. It should be stressed that while forecasts can be used to anticipate drought conditions, forecasts can also be of value during non-drought periods. For instance, if wet conditions are anticipated, then water uses could be met at higher than normal levels without significant system impacts.

Forecast-based operations could provide benefits for a variety of water uses other than flow support for navigation and the environment. For instance, forecasts of hydrologic conditions could be used to increase or decrease the hydropower generation commitments and/or water withdrawals from the system. Furthermore, forecasts can also be issued for sub-regions of the basins, such as forecasts for the Lanier and West Point watersheds, and used to fine-tune operations at those reservoirs. Additionally, forecasts in the Flint River basin may be able to support adaptive demand management to support increased low flow requirements.

It is also important to note that forecasts can provide value even if they are not explicitly included into the reservoir operating policies. In the case study, it was shown that higher pulse flows sometimes occur naturally without extra supporting releases. Knowledge that such flows are likely to occur would allow some stakeholders to benefit from these pulses even if the reservoirs do not adjust their releases. Similar concepts apply for other water users, such as the agricultural or hydropower sectors, that may be able to adjust their strategies based on forecasted hydrologic conditions.

Thus, the study shows that forecast-based operations can indeed be developed and used to improve the management of the ACF by anticipating future hydrologic conditions and stresses, and proactively adjusting reservoir operations and water sharing procedures.

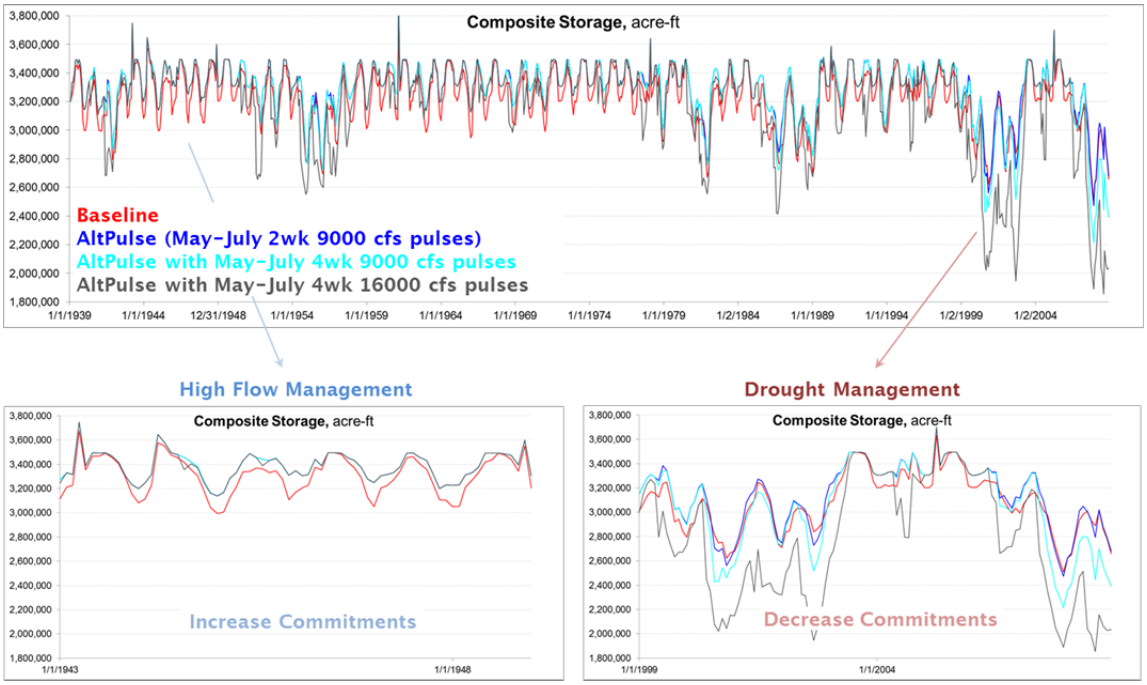

Figure 2-5: Simulated ACF Composite Storage for Different Levels of Flow Support

Figure 2-6: Forecast-based Operating Policy that Adjusts Pulse Magnitudes and Duration for Different Future Hydrologic Conditions

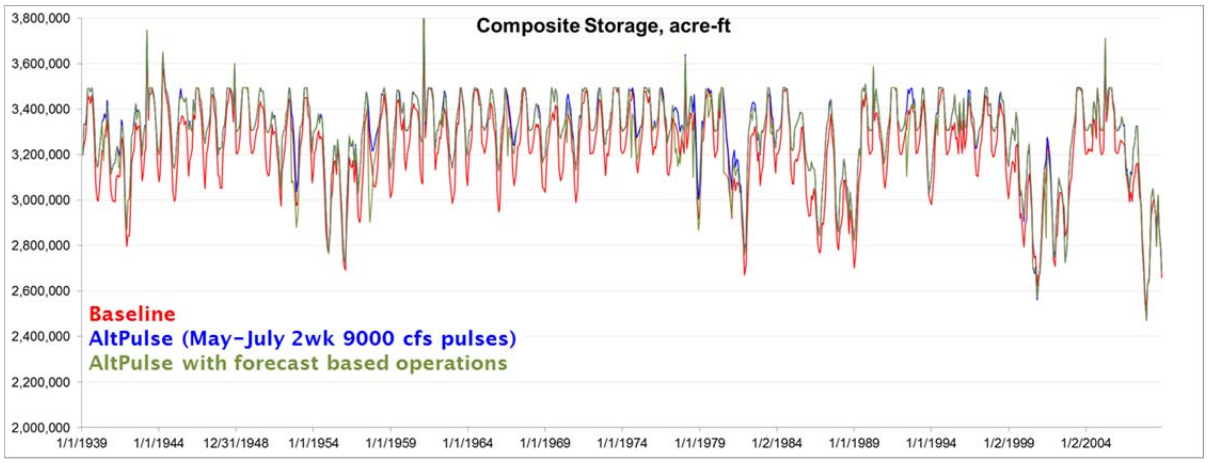

May Flows	AltPulse	AltPulse with forecast based operations
Committed for 9,000 2 Week (%)	100	20
Committed for 9,000 4 Weeks (%)	0	20
Committed for 16,000 4 Weeks (%)	0	60
July Flows: From MAY		
Committed for 9,000 2 Week (%)	100	20
Committed for 9,000 4 Weeks (%)	0	80
July Flows: From JUNE		
Committed for 9,000 2 Week (%)	100	22.9
Committed for 9,000 4 Weeks (%)	0	38.6
Committed for 16,000 4 Weeks (%)	0	38.6

Updated Commitments

Figure 2-7: Simulated ACF Composite Storage for Different Operating Policies with and without Forecast Information

References

Black & Veatch, 2012: Approach to Water Withdrawals and Returns Reporting Technical Memorandum.

Chen, C-J., and A. P. Georgakakos, "Hydro-Climatic Forecasting Using Sea Surface Temperatures—Methodology and Application for the Southeast U.S.," *Journal of Climate Dynamics*, 42, 2955-2982, 2014. DOI 10.1007/s00382-013-1908-4.

Georgakakos, A.P., and M. Kistenmacher, 2012: Unimpaired Flow Assessment for the Apalachicola-Chattahoochee-Flint River Basin. Technical Report, Georgia Water Resources Institute, Georgia Institute of Technology, Atlanta, Georgia, 211p.

Georgakakos, A.P., and M. Kistenmacher, 2015: Water Management Scenario Assessments for the ACF River Basin. Technical Report, Georgia Water Resources Institute, Georgia Institute of Technology, Atlanta, Georgia, 41p.

Harris, I., Jones, P.D., Osborn, T.J. and Lister, D.H. (2013), Updated high-resolution grids of monthly climatic observations – the CRU TS3.10 Dataset. Int. J. Climatol.. doi: 10.1002/joc.3711.

US Army Corps of Engineers, Mobile District, 1997: ACT/ACF Comprehensive Water Resources Study, Surface Water Availability, Volume I, Unimpaired Flow.

US Army Corps of Engineers, Mobile District, 2004: Extended Unimpaired Flow Report January 1994 – December 2001 for the Alabama-Coosa-Tallapoosa and Apalachicola Chattahoochee Flint (ACT/ACF) River Basins.

US Army Corps of Engineers, Mobile District. June 2012: Apalachicola-Chattahoochee-Flint (ACF) Remand Modeling Technical Report.

US Army Corps of Engineers, Mobile District, 2004: Extended Unimpaired Flow Report January 1994 – December 2001 for the Alabama-Coosa-Tallapoosa and Apalachicola Chattahoochee Flint (ACT/ACF) River Basins.

Appendix A: Model and Data

The following sections describe the ACF River Basin models used as part of this study. The purpose of river basin modeling is discussed first, and the specific modeling tools employed in this process are identified together with the required input data sets.

A.1 Modeling Purpose and Tools

The ACF River Basin is a complex system with a variety of water uses and water management facilities. The development of a sustainable water management plan requires careful analysis to identify water management alternatives that may be of interest to the ACF stakeholders. The complexity and size of the basin necessitates the development and use of modeling tools. River basin models are designed to simulate the behavior of the river and characterize its ability to meet its environmental and socio-economic objectives under different water management alternatives.

The modeling and assessment process typically includes several iterative and interactive phases. First, system characteristics, operating rules, and stakeholder interests and metrics are acquired through extensive stakeholder consultations. Second, suitable models of the basin and its environmental and socio-economic outputs are developed and validated. Third, water management alternatives are formulated and modelled in close consultation with the basin stakeholders. Fourth, detailed assessments of each management alternative are carried out to determine how the system responds over time. The results consist of time series of various water related quantities such as reservoir storages and elevations; hydropower generation (primary and secondary); consumptive uses by sector; high, normal, and low river flows; environmental conditions; and other important variables. These results are systematically analyzed and inter-compared to determine how well stakeholder interests are met by particular water management alternatives. Trade-offs between different water uses are explored and better management alternatives are identified. And fifth, the process is repeated until the basin stakeholders come to an agreement that the most satisfying management alternative(s) have been identified and the river meets their collective expectations.

Two river basin models were used to study water management alternatives in the ACF Basin. The first model, ACF-DSS, identifies desirable reservoir operating policies that can satisfy a variety of water use objectives. ACF-DSS achieves this goal by combining simulation and optimization methods. Promising ACF-DSS model runs were post-processed to identify operating rules to be further evaluated by HEC-ResSim. Unlike ACF-DSS, HEC-ResSim is a simulation model where the operating policies have to be specified a-priori. Namely, HEC-ResSim does not find optimal operating rules, but rather evaluates the system response to pre-defined rules. Additional HEC-ResSim simulations were performed to allow results and models to be easily passed on to the U.S. Army Corps of Engineers, who are most familiar with the HEC-ResSim software package. All of the modeled scenarios and results presented in the

remainder of this summary are based on HEC-ResSim model runs. The results of the ACF-DSS are voluminous and have been provided to ACFS.

A.2 Temporal Model Resolution

The natural availability of water varies throughout a year, as well as inter-annually, depending on whether the system is experiencing drought, normal, or wet conditions. A long inflow time series is a key model input to account for this natural variability and to ensure that water management alternatives are robust and perform well under a range of conditions. Specifically, daily flow data from the historical period from 1939-2008 is used to drive all model simulations and assessments. This flow data comprise the unimpaired flow (UIF) sequence and is discussed further below.

A.3 Spatial Model Resolution

The ACF River Basin model included 24 discrete locations in space, as shown in **Figure A-1** and **Table A-1**. The locations are sub-divided into two general categories: reservoirs and river nodes. Reservoirs represent impoundments in a river behind which water can be stored, while nodes represent locations on the rivers. Any flows of water entering or exiting the river basin (withdrawals, inflows, net evaporation, etc.) are modelled to occur at one of these 24 locations. At a particular location, these flows represent aggregate quantities occurring within the river reach and sub-watershed between that location and the next upstream location.

A.4 Unimpaired Flows and Net Evaporation Rates

Unimpaired flows (UIFs) are a major input to the river basin model. These flows represent historical streamflows that have been processed to remove the effects of as many human influences as possible so that new water management alternatives can be compared without inheriting the effects of human activity (consumptive uses, reservoir operations, and other interventions). The flows denote the amount of water that is entering the river system and can be managed to provide for a variety of water uses through the basin. The UIFs used in this study are based on a dataset developed by the U.S. Army Corps of Engineers [USACE, 1997 & 2004], consisting of 23 daily time series, one for each modelled location, spanning the period from 1939 to 2008. A slight modification to this dataset was made. The original reach between Griffin and Montezuma in the U.S. Army Corps of Engineers dataset was sub-divided to allow water planning and management metrics to be computed at an additional location along the Flint River. Specifically, a new node was added at Carsonville and used to create two smaller reaches: Carsonville (bounded by the upstream Griffin and downstream Carsonville nodes) and Montezuma (bounded by the upstream Carsonville and downstream Montezuma nodes).

Net evaporation rates represent the difference between evaporation and precipitation from the reservoir surface. Daily time series of net evaporation rates for the major reservoirs in the basin

were also taken from the unimpaired flow dataset developed by the U.S. Army Corps of Engineers.

GWRI has carried out a systematic assessment of the ACF UIFs [Georgakakos and Kistenmacher, 2012: Unimpaired Flow Assessment for the ACF River Basin].

A.5 Consumptive Use Targets

Consumptive uses represent the difference between water withdrawals and returns in a particular river reach, and are based on data described in a separate report by Black and Veatch [Black & Veatch, 2013];

Consumptive uses, consisting of twelve averages for each month of the year, were developed by compiling measured or estimated data corresponding to average water uses between 2002 and 2011. (For some water uses, this data was available for shorter time periods.) At each location, different water uses (e.g., municipal, industrial, thermal, and agricultural) were collected individually and then combined into aggregate consumptive use quantities. For modeling purposes, daily time series of consumptive uses were developed by assuming that (a) the monthly data repeats year after year from 1939 to 2008 and (b) each day within a particular month has the same use level.

A.6 Physical Reservoir Characteristics

The characteristics of the system facilities in their current state were obtained from the HEC-ResSim model described in USACE [2012]. Such data include storage-area-elevation curves, spillway gate and outlet capacities, tailwater curves, and hydropower generation capacities and efficiencies.

Table A-1: Modelled ACF River Basin Reservoirs and River Nodes

Location	River	Type
Buford	Chattahoochee	Reservoir
Norcross	Chattahoochee	River Node
Morgan Falls	Chattahoochee	Reservoir
Atlanta	Chattahoochee	River Node
Whitesburg	Chattahoochee	River Node
West Point Dam	Chattahoochee	Reservoir
West Point Gage	Chattahoochee	River Node
Bartletts Ferry	Chattahoochee	Reservoir
Goat Rock	Chattahoochee	Reservoir
Oliver	Chattahoochee	Reservoir
North Highlands	Chattahoochee	Reservoir
Columbus	Chattahoochee	River Node
W.F. George	Chattahoochee	Reservoir
George Andrews	Chattahoochee	Reservoir
Griffin	Flint	River Node
Carsonville	Flint	River Node
Montezuma	Flint	River Node
Albany	Flint	River Node
Newton	Flint	River Node
Bainbridge	Flint	River Node
J. Woodruff	Chattahoochee/Flint Confluence	Reservoir
Chattahoochee	Apalachicola	River Node
Blountstown	Apalachicola	River Node
Sumatra	Apalachicola	River Node

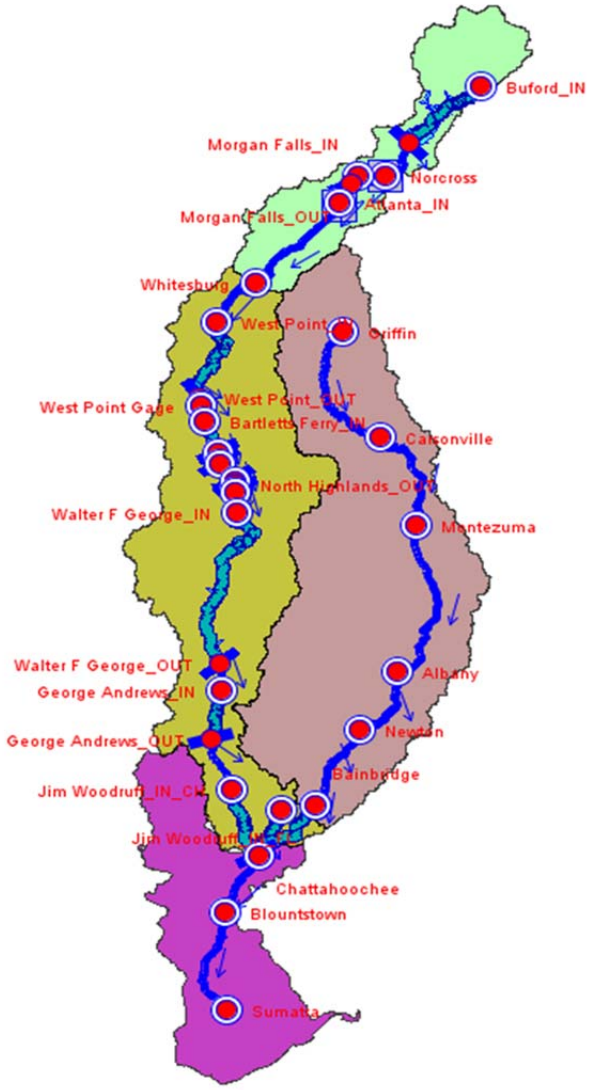

Figure A-1: A map of the ACF river basin.

Appendix B: Baseline Operations

The following sections present the existing ACF operating procedures and conditions. General concepts pertaining to the modeling of different water uses are discussed first. Next, operating rules pertaining to local basin objectives and projects are presented. Lastly, system-wide operations are covered. We note that, while the modelled operations are intended to mimic the actual operations as best as possible, they might differ slightly from the way in which the U.S. Army Corps of Engineers operates the system in real-life. Nonetheless, the current operations, physical characteristics, and current water use conditions serve as a baseline scenario against which changes in reservoir operations, system infrastructure, and water use levels are compared.

B.1 General Modeling Concepts

A multitude of water uses exist throughout the basin and are included in the model of the ACF River Basin. When natural conditions are favorable, some water uses can be met without any particular operating provisions. If this is not possible, special operating rules can be used to guide reservoirs to make releases that meet specific water uses. Operating rules are only defined at reservoirs, but they can also be designed to provide benefits at downstream river nodes. A hierarchy-based approach is used to model reservoirs with multiple operating rules. Priorities are assigned to each individual operating rule, and water uses associated with the highest priority rule are met first. After the highest priority rule has been considered, reservoir operations focus on meeting the next priority rule, and so on. However, lower priority rules can only be met if doing so does not negatively impact a water use associated with a higher priority rule. In the absence of any operating rules at a particular reservoir, a default operating rule attempts to keep the reservoir storage at the top of the conservation pool. If a reservoir does include other operating rules, then this default rule is also implemented as the lowest priority rule; i.e., the reservoir storage is targeted to be at the top of the conservation pool, but may deviate from this target if other rules require releases that increase or decrease reservoir storage. Meeting consumptive use targets throughout the basin has not been defined as part of operating rules at any ACF reservoir. However, consumptive uses are always withdrawn from the system if the simulated flows and storages are large enough to allow this to occur. Additionally, if a reservoir is operated to meet minimum flow targets at a downstream location, then losses due to consumptive uses between the reservoir and that location are also provided for in determining reservoir releases.

It is noted that other important water uses beyond those associated with the operating rules discussed in the following sections exist. For instance, some stakeholders may advocate for a certain flow regime along a stretch of the river even though supporting such a regime is currently not part of the U.S. Army Corps of Engineers operating rules. Such water uses were not considered in the following sections, not because they are unimportant, but because the focus here is to describe the operating rules encoded in the model. The extent to which system

operations meet stakeholder interests not explicitly encoded in the model can be evaluated by computing the associated performance metrics from model results, as described in Section 5.1.

B.2 Local Reservoir Operations

The following sections proceed from upstream to downstream and describe the operating rules used to meet various water use requirements.

B.2.1 Buford Dam to Whitesburg

The stretch from Buford Dam to Whitesburg includes two reservoirs (Buford Dam and Morgan Falls), and three nodes along the Chattahoochee River.

Buford Dam (Lake Lanier) is modelled as the most upstream location and reservoir on the Chattahoochee River. **Table B-1** lists the local operating rules at Buford. The rules are arranged in order of decreasing priority, with rules listed first having higher priority than the rules listed later. Operating rules include goals/constraints to be met at the dam (such as hydropower generation, minimum releases requirements, and keeping storage at the top of the conservation zone, among others), as well as goals/constraints to be met at downstream river nodes (such as keeping downstream flow rates above and below certain levels). Operating rules at Buford may vary with reservoir elevation. Action zones, shown in **Figure B-1**, represent ranges in the reservoir elevation where different operating rules may be applied.

Morgan Falls is modelled as a run-of-the-river reservoir and is not subject to explicit operating rules. Instead, the reservoir is operated such that outflows equal inflows.

B.2.2 West Point Dam to George Andrews

The stretch of the Chattahoochee River from West Point Dam to George Andrews includes seven reservoirs and two river nodes (West Point Gage and Columbus). Out of the seven reservoirs, only West Point Dam and W.F. George are subject to explicit operating rules, while the remaining reservoirs (Bartlett's Ferry, Goat Rock, Oliver, North Highlands, and George Andrews) are modelled as run-of-the-river facilities.

Tables B-2 and **B-3** list the local operating rules for West Point Dam and W.F. George, respectively. These rules are again arranged in order of decreasing priority. Operating rules at both reservoirs may also vary with reservoir elevation according to the action zones depicted in **Figures B-2** and **B-3**. It should be noted that the top of the West Point Dam conservation pool (Zone 1) is higher in the winter than the top of the conservation pool currently being used by the U.S. Army Corps of Engineers.

B.2.3 Flint River

The Flint River is represented by five river nodes: Griffin, Carsonville, Montezuma, Albany, Newton, and Bainbridge. There are no official operating rules for the Flint River since there are no reservoirs being modelled. Consumptive uses are still considered at each of these river nodes.

B.2.4 J. Woodruff Dam to Sumatra

The Chattahoochee and Flint Rivers merge into the reservoir behind J. Woodruff Dam. Continuing further downstream, three additional river nodes are used to represent the Apalachicola River: Chattahoochee Gage, Blountstown, and Sumatra.

The local operating rules for J. Woodruff are listed in **Table B-4** in order of decreasing priority and may vary with reservoir elevation according to the action zones depicted in **Figure B-4**. Note that there are some operating rules for maintaining certain flow regimes immediately downstream of J. Woodruff that are not listed in **Table B-4**. These rules are discussed in further detail in the Section 3.3.2 because they are a function of basin-wide conditions.

B.3 System-Wide Operations

Several operating rules are based on conditions throughout the ACF Basin. Specifically, the storages in the major federal reservoirs are kept in balance by coordinating operations across the system. Furthermore, some operating rules pertaining to the J. Woodruff outflows depend on storages and inflows further upstream.

B.3.1 Reservoir Coordination

The U.S. Army Corps of Engineers operates the major reservoirs (Buford, West Point, W.F. George, and J. Woodruff) in the ACF Basin as a system, by coordinating the operations between downstream and upstream reservoirs. The purpose of reservoir coordination is to keep the reservoir storages in the individual reservoirs balanced and avoid situations where one reservoir is empty and another one is full. Tandem operations are used to balance reservoir storages since all of the major reservoirs are located in series. Tandem operations compare the storages of an upstream reservoir and a downstream reservoir. If the downstream reservoir storage is lower than the storage in the upstream reservoir, additional releases are made from the upstream reservoir to increase the downstream storage. On the other hand, if the downstream reservoir storage is higher than that of the upstream reservoir, no additional releases are required from the upstream reservoir.

Coordination between upstream and downstream reservoirs is performed for each of the adjacent major reservoirs in the ACF Basin proceeding from upstream to downstream. Namely, Buford Dam balances with West Point Dam, West Point Dam balances with W.F. George, and W.F. George balances with J. Woodruff. Balancing operations between two adjacent reservoirs are performed by first using the information provided in **Table B-5** to determine which action zones

are supposed to be balanced. If the downstream reservoir is within an action zone that is higher than the action zone corresponding to the upstream reservoir, no extra releases from the upstream reservoir are required. Otherwise, the upstream reservoir is required to make additional releases.

The magnitude of the releases required to balance the reservoirs is determined by computing how full each action zone is via the following ratio for each reservoir:

(Actual storage - storage at bottom of action zone)/ (storage at top of action zone- storage at bottom of action zone).

For the baseline operations, releases are made from the upstream reservoir until its ratio equals the ratio of the downstream reservoir.

B.3.2 J. Woodruff Minimum Release Requirements

The Revised Interim Operations Plan (RIOP) used by the U.S. Army Corps of Engineers to operate the system includes two operating rules pertaining to the magnitude of releases out of J. Woodruff. Both rules are functions of variables that depend on water quantities further upstream of J. Woodruff. Specifically, the following two variables are used:

Composite Storage: The sum of the storages in the three largest upstream reservoirs (Buford, West Point, and W.F. George)

Basin Inflows: The sum of the unimpaired inflows entering ACF basin above and including J. Woodruff, minus consumptive uses and net evaporation losses. Basin inflows are computed both on each day (one-day basin inflow) and as a moving average over the seven previous days (seven-day basin inflows).

The first rule imposes minimum release requirements out of J. Woodruff, as shown in **Table B-6**. The requirements vary according to the amount of composite storage and seven-day basin inflows. For composite storage, several different zones are defined, as shown in **Figure B-5**. Zones with higher levels of composite storage require higher minimum releases than zones with lower composite storage. Drought operations are triggered when the composite storage is in Zone 4 or lower and, once triggered, remain in effect until the composite storage has recovered to Zone 3.

However, drought operations are not modelled in any of the water management scenarios presented in this report because they can introduce significant non-linear effects and non-comparable results. For instance, if a management scenario triggers drought operations, then its flow requirements would be reduced. On the other hand, a management scenario that does not trigger drought operations (or does so later), would be required to release more water and thereby reduce its storage. To avoid such complications, drought operations were disabled in all of the water management scenarios. This does not change the conclusions of the assessments and, if necessary, all management scenarios can be re-evaluated with drought operations in place.

Minimum release requirements usually increase with increasing seven-day basin inflows, though when composite storage falls into Zone 4 or the drought zone, they are no longer dependent on basin inflows and are reduced to 5,000 and 4,500 cfs, respectively. Requirements also vary throughout the year, being higher from March to May, lower from June to November, and constant at 5,000 cfs from December to February.

The second rule limits the fall-rates (i.e., the decrease of the water level elevation on consecutive days) downstream of J. Woodruff. Limits only apply to falling elevations and not to rising ones. In the model, fall-rate limits are enforced through constraints on the decrease in J. Woodruff releases by converting them to limits on the releases. **Figure B-6** shows the maximum allowed decrease of daily releases as a function of the flow rate out of J. Woodruff. When the system is in drought operations, the fall-rate limits do not apply. Instead, the drop in the one-day basin inflows on consecutive days is used to limit the decrease in releases out of J. Woodruff.

It should be noted that these two rules only place constraints on the minimum release requirements and maximum fall-rates, and do not specify the exact magnitude of the J. Woodruff releases. Depending on the state of the system, it is possible that releases in excess of the minimum release requirements and/or fall-rates lower than the maximum limit may occur.

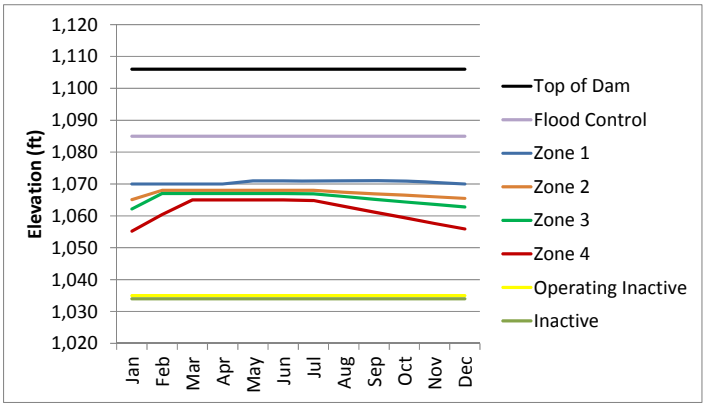

Figure B-1: Buford Action Zones: Baseline Operations

Table B-1: Buford Operating Rules: Baseline Operations

Top of Dam	None.
Flood Control	Release < 10,000 cfs.
	Flow at Norcross < 11,000 cfs.
	Flow at Atlanta < 13,200 cfs.
	Release > 600 cfs through small turbine.
	Flow at Atlanta > 800 cfs.
Zone 1 (Conservation)	Release < 10,000 cfs.
	Flow at Norcross < 11,000 cfs.
	Flow at Atlanta < 13,200 cfs.
	Release > 600 cfs through small turbine.
	Power Generation ≥ 3 hours at full capacity.
	Flow at Atlanta > 800 cfs.
	Tandem Operations with West Point Dam.
	During fish spawning (April-June), limit decreases in reservoir elevation.
Zone 2 Zone 3	Release < 10,000 cfs.
	Flow at Norcross < 11,000 cfs.
	Flow at Atlanta < 13,200 cfs.
	Release > 600 cfs through small turbine.
	Power Generation ≥ 2 hours at full capacity.
	Flow at Atlanta > 800 cfs.
	Tandem Operations with West Point Dam.
	During fish spawning (April-June), limit decreases in reservoir elevation.
Zone 4	Release < 10,000 cfs.
	Flow at Norcross < 11,000 cfs.
	Flow at Atlanta < 13,200 cfs.
	Release > 600 cfs through small turbine.
	Flow at Atlanta > 800 cfs.
	Tandem Operations with West Point Dam.
	During fish spawning (April-June), limit decreases in reservoir elevation.
Operating Inactive	Release net reservoir inflow up to 600 cfs during drought operations.
Inactive	None.

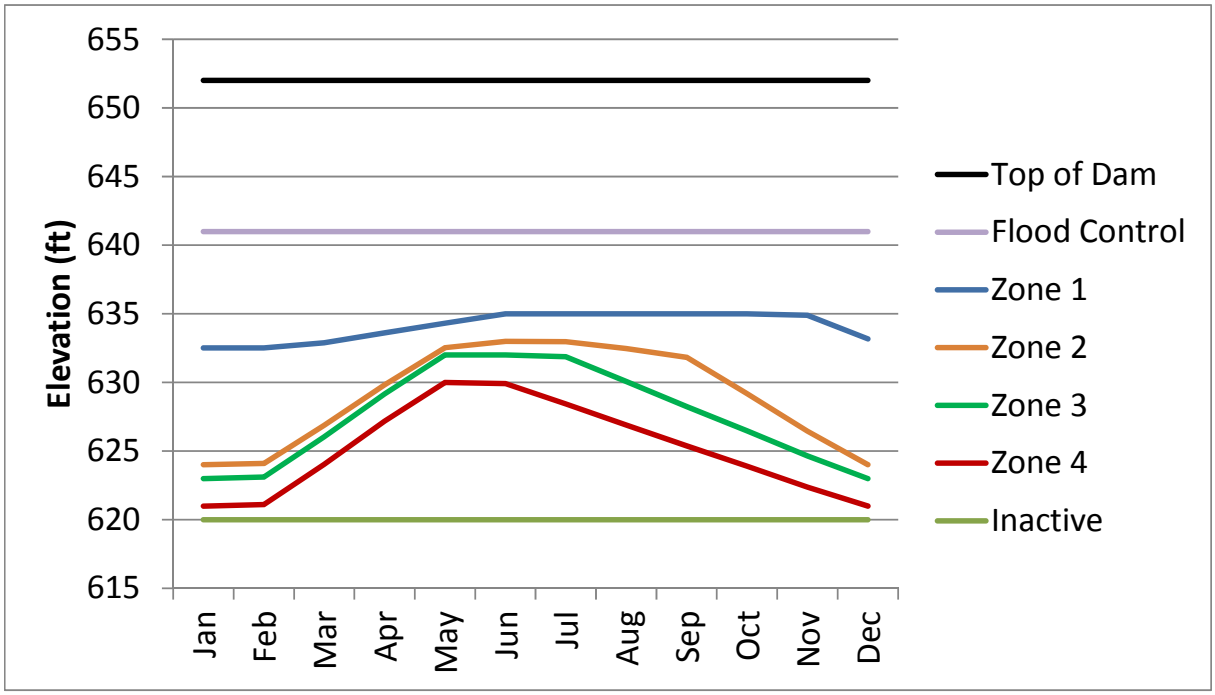

Figure B-2: West Point Dam Action Zones: Baseline Operations

Table B-2: West Point Dam Operating Rules: Baseline Operations

Zone	Rules
Top of Dam	None.
Flood Control	Induced surcharge operations.
	Release > 675 cfs through small turbine.
	Power Generation ≥ 4 hours at full capacity.
	Limit fall-rate of releases to 3,000 cfs/hr
	Release < 40,000 cfs.
Zone 1 (Conservation)	Release > 675 cfs through small turbine.
	Power Generation ≥ 4 hours at full capacity.
	Release < 40,000 cfs.
	Tandem Operations with W.F. George.
	During fish spawning (April-June), limit decreases in reservoir elevation.
Zone 2 Zone 3	Release > 675 cfs through small turbine.
	Power Generation ≥ 2 hours at full capacity.
	Release < 40,000 cfs.
	Tandem Operations with W.F. George.
	During fish spawning (April-June), limit decreases in reservoir elevation.
Zone 4	Release > 675 cfs through small turbine.
	Release < 40,000 cfs.
	Tandem Operations with W.F. George.
	During fish spawning (April-June), limit decreases in reservoir elevation.
Inactive	None.

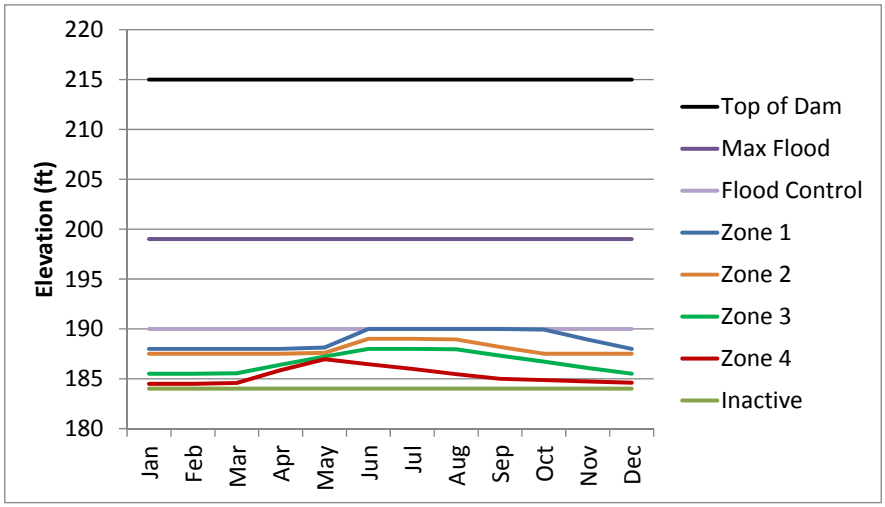

Figure B-3: W.F. George Action Zones: Baseline Operations

Table B-3: W.F. George Operating Rules: Baseline Operations

Zone	Rules
Top of Dam	None.
Max Flood	Induced surcharge operations.
	Release < 40,000 cfs.
Flood Control	Induced surcharge operations.
	Make minimum releases to keep the difference between reservoir and downstream tailwater elevations below certain thresholds.
	Power Generation ≥ 4 hours at full capacity.
	Release < 30,000 cfs if reservoir elevation <189; Release 40,000 cfs otherwise.
	Tandem Operations with J. Woodruff.
Zone 1 (Conservation)	Make minimum releases to keep the difference between reservoir and downstream tailwater elevations below certain thresholds.
	Release < 30,000 cfs if reservoir elevation < 189; Release 40,000 cfs otherwise.
	Power Generation ≥ 4 hours at full capacity.
	Tandem Operations with J. Woodruff.
	During fish spawning (April-June), limit decreases in reservoir elevation.
Zone 2 Zone 3	Make minimum releases to keep the difference between reservoir and downstream tailwater elevations below certain thresholds.
	Power Generation ≥ 2 hours at full capacity.
	Tandem Operations with J. Woodruff.
	During fish spawning (April-June), limit decreases in reservoir elevation.
Zone 4	Make minimum releases to keep the difference between reservoir and downstream tailwater elevations below certain thresholds.
	Tandem Operations with J. Woodruff.
	During fish spawning (April-June), limit decreases in reservoir elevation.
Inactive	None.

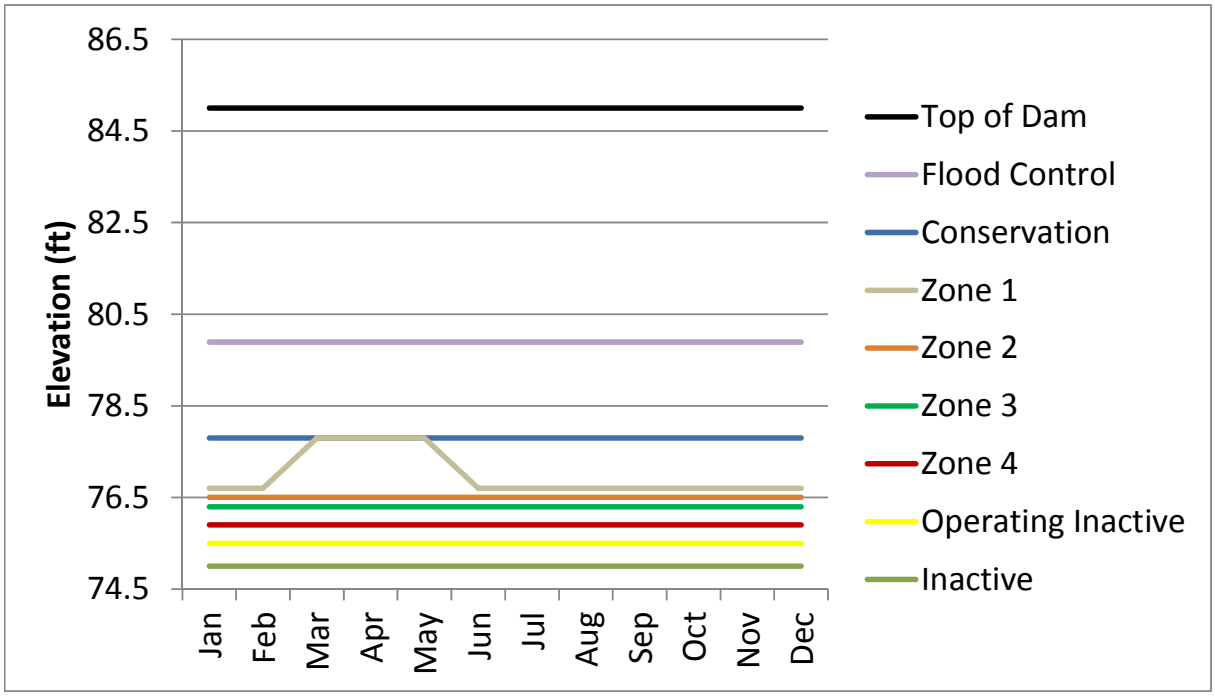

Figure B-4: J. Woodruff Action Zones: Baseline Operations

Table B-4: J. Woodruff Operating Rules: Baseline Operations

Zone	Rules
Top of Dam	None.
Flood Control	Make minimum releases to keep the difference between reservoir and downstream tailwater elevations below certain thresholds.
	Comply with Endangered Species Act: Limit fall-rate of river stage downstream of J. Woodruff as specified in Figure 3-6 and make minimum releases as specified in Table 3-6.
Conservation Zone 1 Zone 2 Zone 3 Zone 4	Comply with Endangered Species Act: Limit fall-rate of river stage downstream of J. Woodruff as specified in Figure 3-6 and make minimum releases as specified in Table 3-6.
	Make minimum releases as specified in Table 3-6.
	Sturgeon Spawning: From Mar-May, limit the drop in downstream river stage to be less than 8 feet over a 2 week moving window when flows are < 40,000 cfs.
	Fish Spawning: From April to May, limit the daily drop in downstream river stage to be 0.5 ft.
	During fish spawning (April-June), limit decreases in reservoir elevation.
	During fish spawning (April-June), limit decreases in reservoir elevation.
Operating Inactive	Release net reservoir inflow up to 4,550 cfs during drought operations, otherwise net reservoir inflow up to 5,050 cfs.

Table B-5: Reservoir Zones To Be Balanced for Reservoir Coordination: Baseline Operations.

Buford	**West Point**	**W.F. George**	**J. Woodruff**
Top of Dam	Top of Dam	Top of Dam	Top of Dam
Flood Control	Flood Control	Flood Control	Flood Control
Zone 1	Zone 1	Zone 1	Zone 1
Zone 2	Zone 2	Zone 2	Zone 2
Zone 3	Zone 3	Zone 3	Zone 3
Zone 4	Zone 4	Zone 4	Zone 4
Operating Inactive	Inactive	Inactive	Operating Inactive

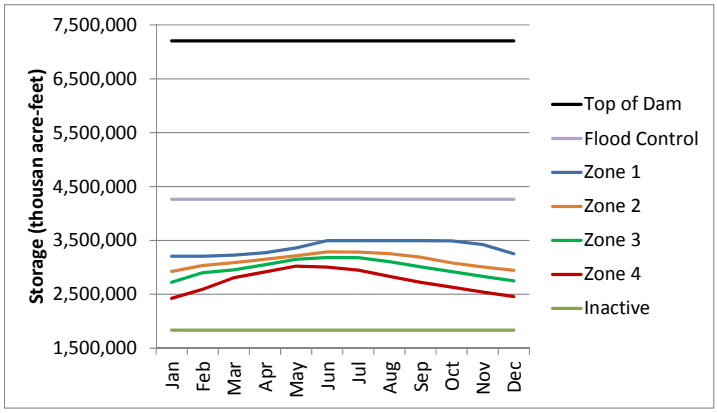

Figure B-5: RIOP Composite Storage Zones: Baseline Operations

Table B-6: RIOP Minimum Release Requirements out of J. Woodruff: Baseline Operations

March – May

Composite Storage Zone	Basin Inflows (cfs)	Minimum Releases (cfs)
Zone 1 and Zone 2	≥ 34,000	25,000
	≥ 16,000 and < 34,000	16,000 + 0.5*(Basin Inflows-16,000)
	≥ 5000 and < 16,000	Basin Inflows
	< 5,000	5000
Zone 3	≥ 39,000	25,000
	≥ 11,000 and < 39,000	11,000 + 0.5*(Basin Inflows-11,000)
	≥ 5,000 and < 11,000	Basin Inflows
	< 5,000	5,000

June- November

Composite Storage Zone	Basin Inflows (cfs)	Minimum Releases (cfs)
Zone 1, Zone 2, and Zone 3	≥ 24,000	16,000
	≥ 8,000 and < 24,000	8,000 + 0.5*(Basin Inflows-8,000)
	≥ 5000 and < 8,000	Basin Inflows
	< 5,000	5000

December - February

Composite Storage Zone	Basin Inflows (cfs)	Minimum Releases (cfs)
Zone 1, Zone 2, and Zone 3	Any	5,000

All Months

Composite Storage Zone	Basin Inflows (cfs)	Minimum Releases (cfs)
Zone 4	Any	5,000
Drought Zone	Any	4,500

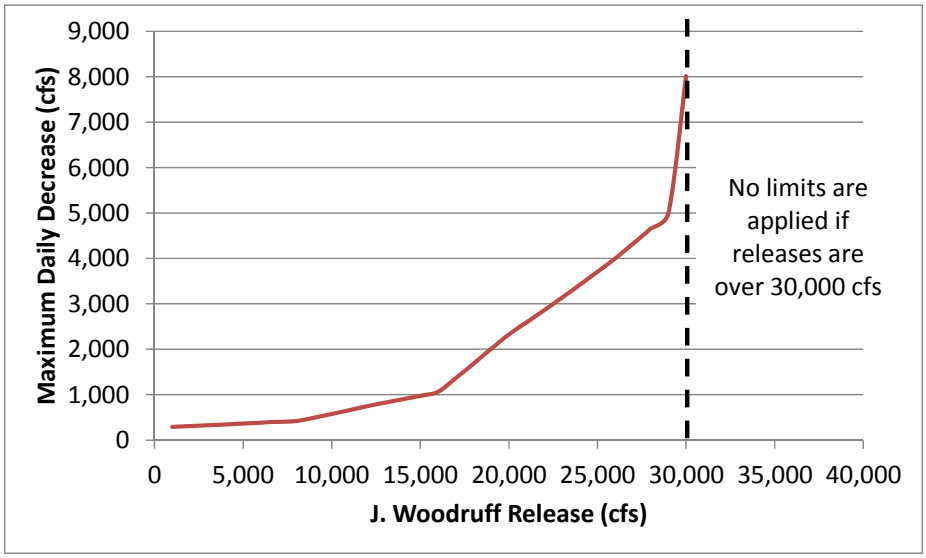

Figure B-6: RIOP Fall-Rate Limits Downstream of J. Woodruff: Baseline Operations. Elevation Change Limits Have Been Converted to Limits on the Change of Releases.

Validation of Oysters as Biomonitors of Pharmaceutical Pollution in Georgia

Basic Information

Title:	Validation of Oysters as Biomonitors of Pharmaceutical Pollution in Georgia
Project Number:	2014GA341B
Start Date:	3/1/2014
End Date:	2/29/2016
Funding Source:	104B
Congressional District:	Georgia 10th
Research Category:	Water Quality
Focus Category:	Water Quality, Non Point Pollution, Sediments
Descriptors:	None
Principal Investigators:	Marsha Carolyn Black

Publications

There are no publications.

Validation of Eastern Oysters as Biomonitors of Pharmaceutical Pollution in the Georgia Estuarine Environment

PI: Marsha C. Black; Co-PI: David Brew (PhD student)
Department of Environmental Health Science
University of Georgia, Athens GA 30602

Progress Report (May 15, 2015)

The objectives of the study are to:

(1) conduct chemical analysis of pharmaceuticals in oysters, suspended particles and sediments sampled bimonthly from estuarine environments of coastal Georgia that are susceptible to pharmaceutical pollution;

(2) determine age-related pharmaceutical deposition in oyster tissues to evaluate the use of native oysters as pharmaceutical biomonitors;

(3) develop a pharmaceutical pollution index and an oyster condition index for each of the sampling areas within each estuary as measures of environmental and biological (oyster) health in these areas related to pharmaceutical pollution;

(4) calculate a pharmaceutical risk quotient for each of the pharmaceuticals analyzed in the study,

(5) model environmental fate of pharmaceuticals in the estuarine environment, based on partitioning within oysters and environmental media (water, suspended particles and sediment)

Because of an invaluable partnership with Dr. Matthew Henderson (US EPA Region IV, Athens, GA) we have expanded our original analyte list from 8 pharmaceuticals to include 42 contaminants of emerging concern, including pharmaceuticals, personal care products and pesticides. With additional seed funding from various sources and in collaboration with Dr. Henderson we have also added metabolomics as an additional measure of biological effects in oysters during 4 sample events to strengthen the biological endpoints for calculation of the pharmaceutical and emerging contaminants risk quotient. In February 2015 we were granted a no-cost extension of this GA Water Resources Grant to extend our sampling dates through June 2015 and accommodate the additional analytical workload generated by these collaborations.

Progress to Date: Eastern oysters (*Crassostrea virginica*) have been sampled from natural oyster beds at Brunswick and Sapelo Island, Georgia bimonthly since October 2013, continuing through June 2015. Dispositional sediment samples, 1-liter water grab samples and filtered suspended sediment particles have been collected at each sample site since October 2014, also continuing through June 2015. The LC-MS/MS method validation for contaminants of emerging concern (CECs) in oyster tissue and water samples was completed in late August 2014 and method validation for sediments and suspended solids was recently completed in mid-May 2015. All analyses have been conducted at the US EPA ORD facility at Athens, GA.

Study Site Selection & Sample Regimen*:* Four study sites were chosen along the Brunswick River to coordinate with an ongoing UGA Marine Extension study examining the effects of land use and septic tank densities on water quality. These sites are affected by a medium-sized city (metropolitan area population ~100,000) and include sites with *C. virginica* beds subjected to

effluents from local wastewater treatment plants (WWTP) (due to tidal influences) and from septic fields in local housing areas (Figure 1). At Brunswick, Plantation Creek is the presumed reference site due to its location away from septic fields and WWTPs. Three sites are located on Sapelo Island, a small island with controlled (ferry) access and a small population (60-100 people, including island visitors) that is entirely serviced by septic tanks. The Sapelo Island sites (Figure 1) are located on small tidal creeks selected to include one site (Oak Dale Creek) where pharmaceuticals have been detected in oysters (Fuller 2012), a site adjacent to the UGA Marine Institute and a presumed reference site (Cabretta Creek).

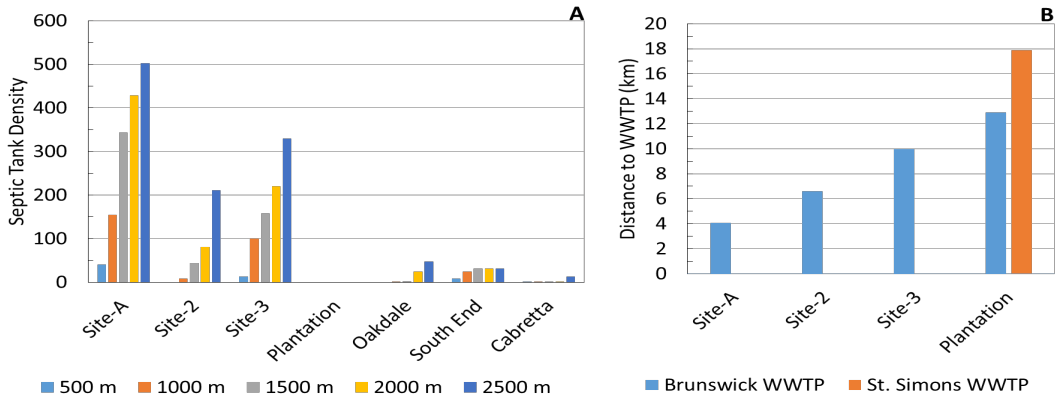

Figure 1: (A) Septic tank densities at specified distances (meters) from each sample site. (B) Distance (km) to local WWTPs from each sample site in Brunswick, Georgia. There is not a WWTP in McIntosh County that would impact Sapelo Island.

Analyte Concentration Results – Oyster tissues

Analyte extraction and LC/MS/MS analyses have been completed for oysters collected in October 2013, April 2014, June 2014 and August 2014. For ease of interpretation, individual analytes have been grouped by chemical class and reported as mean ± [95% confidence intervals (CI)]. Target CECs include: selective serotonin reuptake inhibitors (SSRIs: sertraline, fluoxetine), reproductive hormones (norethindrone, norgestrel, medoxyprogesterone, 17α-ethinylestradiol), anti-epileptics (carbamazepine), stimulants (caffeine, methylphenidate), antihistamines (diphenhydramine), analgesics (ibuprofen, naproxen, acetaminophen, diclofenac), heart/cholesterol medication (atenolol, propranolol, valsartan, gemfibrozil) personal care products (triclocarban, triclosan, DEET), herbicides (2,4-D, clofibric acid, atrazine), pesticides (imidacloprid, thiaclorpid), industrial pollutants (bisphenol-A) and illicit drugs (cocaine, benzoylmethylecgonine, tetrahydrocannabinol). Industrial pollutants and illicit drugs have not yet been analyzed.

October 2013: The SSRIs had the highest mean oyster tissue concentration at both Brunswick (BR) and Sapelo Island (SI) (Figures 2 and 3): BR, mean = 48.9 ng/g [38.5, 59.3]; SI, mean = 45.0 ng/g [0.0, 150.1]), followed by the analgesics (BR, mean = 45.0 ng/g [0.0, 121.3]; SI, mean = 28.1 ng/g [26.5, 29.5]), cholesterol medication (BR, mean = 19.7 ng/g [4.9, 34.4]; SI, mean = 34.9 ng/g [2.0,68.0]), personal care products (BR, mean = 14.0 ng/g [13.5, 14.4]; SI, mean = 21.3 ng/g [12.1, 30.4]), antihistamines (BR, mean = 7.0 ng/g [6.0, 8.0]; SI, mean = 3.5 ng/g [2.3, 4.6]),

and hormones (BR, mean = 7.8 ng/g [5.4, 10.2]; SI, mean = 6.0 ng/g [2.1, 9.9]). The remaining chemical classes were detected at mean concentrations <5 ng/g.

April 2014: Cholesterol medication had the highest mean oyster tissue concentration at both Brunswick and Sapelo Island (Figures 2 and 3): BR, mean = 25.1 ng/g [7.4, 42.8]; SI, mean = 16.0 ng/g [0.35, 31.6], followed by the analgesics (BR, mean = 8.2 ng/g [1.9, 14.6]; SI, mean = 22.7 ng/g [6.6, 38.8]), personal care products (BR, mean = 5.7 ng/g [4.2, 7.3]; SI, mean = 14.5 ng/g [11.3, 17.7]), hormones (BR, mean = 9.9 ng/g [3.7, 16.1]; SI, mean = 10.3 ng/g [1.6, 19.0]) and SSRIs (BR, mean = 4.1 ng/g [0.0, 14.5]; SI, mean = 2.3 ng/g [1.1, 3.5]). The remaining chemical classes were detected at mean concentrations <5 ng/g.

June 2014: The SSRIs had the highest mean oyster tissue concentration at Brunswick and Sapelo Island (Figures 2 and 3): BR, mean = 51.0 ng/g [0.0, 181.2]; SI, mean = 114.5 ng/g [±0.0, 341.6], followed by analgesics (BR, mean = 36.1 ng/g [0.0, 74.0]; SI, mean = 103.3 ng/g [0.0, 214.6]), cholesterol medication (BR, mean = 10.3 ng/g [6.1, 14.5]; SI, mean = 33.0 ng/g [23.3, 42.6]), personal care products (BR, mean = 14.0 ng/g [8.6, 19.4]; SI, mean = 30.1 ng/g [0.8, 59.3]), hormones (BR, mean = 7.4 ng/g [1.2, 16]; SI, mean = 7.3 ng/g [0.0, 8.2]), antihistamines (BR, mean = 8.2 ng/g [0.0, 17.6]; SI, mean = 12.3 ng/g [0.0, 26.5]) and blood pressure medication (BR, mean = 2.9 ng/g [1.4, 4.5]; SI, mean = 6.4 ng/g [0.0, 19.3]). The remaining chemical classes were detected at mean concentrations <5 ng/g.

August 2014: Personal care products had the highest mean oyster tissue concentrations at Brunswick and Sapelo Island (Figures 2 and 3): BR, mean = 9.5 ng/g CI [8.0, 11.0]; SI, mean = 18.1 ng/g CI [16.0, 20.2], followed by cholesterol medication (BR, mean = 10.6 ng/g CI [6.8, 14.4]; SI, mean = 14.9 ng/g CI [14.6, 15.2]) and analgesics (BR, mean = 3.7 ng/g CI [3.1, 4.3]; SI, mean = 5.2 ng/g CI [4.4, 5.9]). The remaining chemical classes were detected at mean concentrations <5 ng/g.

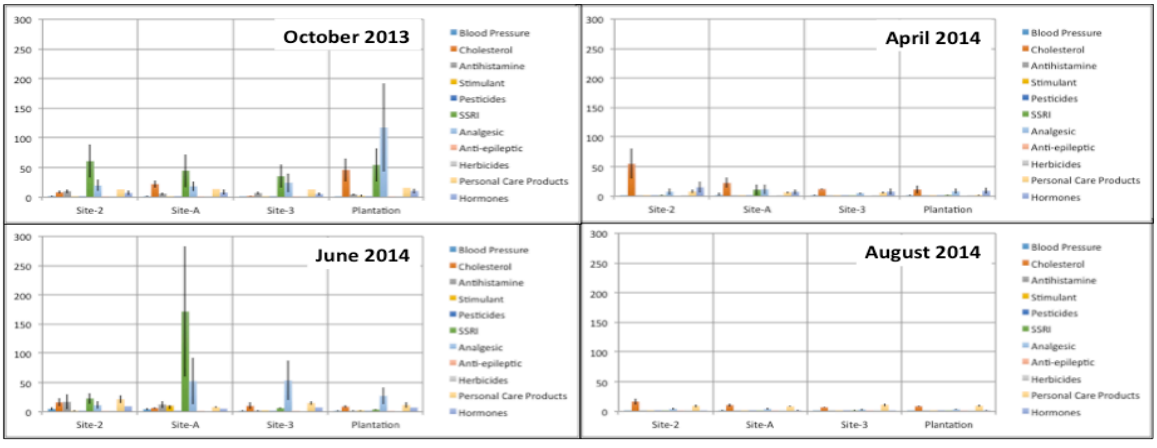

Figure 2: Mean oyster tissue concentrations (ng/g) at natural oyster beds in Brunswick, Georgia

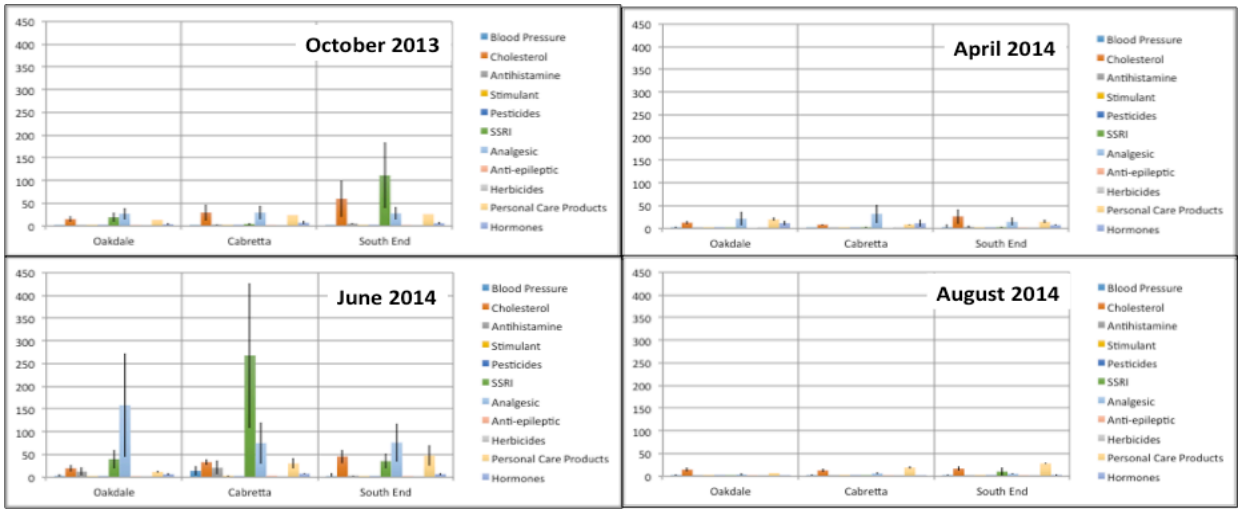

Figure 3: Mean oyster tissue concentrations (ng/g) at natural oyster beds on Sapelo Island, Georgia

Analyte Concentration Results – Water

October 2014: Analysis of 1-liter grab samples from each site detected caffeine, methylphenidate, diphenhydramine, DEET and atrazine ranging from <1 ng/L to 129 ng/L [CI]. Of the analytes detected at Brunswick (BR) and Sapelo (SI), DEET had the highest mean water concentration (BR, mean = 88.9 ng/L [61.7, 116.1]; SI, mean = 26.4 ng/L [9.6, 43.3]). Mean DEET concentrations at Brunswick were significantly higher (based upon 95% confidence intervals) compared to Sapelo Island. Caffeine had the second highest mean water concentration (BR, mean = 11.3 ng/L [11.3, 11.4]; SI, mean = 11.37 ng/L [11.35, 11.39]), followed by methylphenidate (BR, mean = 2.8 ng/L [2.79, 2.84]; SI, mean = 3.4 ng/L [1.8, 6.2]), diphenhydramine (BR, mean = 1.9 ng/L [1.4, 2.5]; SI, mean = 1.7 ng/L [1.1, 2.2]) and atrazine (BR, mean = 0.84 ng/L [0.66, 1.0]; SI, mean = 2.24 ng/L [0.0, 5.0]).

December 2014: Analysis of 1-liter grab samples from each site detected caffeine, methylphenidate, diphenhydramine, DEET and atrazine ranging from 1.7 ng/L to 95.5 ng/L [CI]. Again, DEET had the highest mean water concentration of the analytes detected at Brunswick and Sapelo (BR, mean = 75.4 ng/L [53.6, 97.2]; SI, mean = 37.9 ng/L [18.5, 57.2]). Caffeine had the second highest mean water concentration (BR, mean = 12.3 ng/L [112, 13.4]; SI, mean = 14.2 ng/L [11.5, 17.0]), followed by diphenhydramine (BR, mean = 6.7 ng/L [0.0, 14.2]; SI, mean = 1.8 ng/L [1.2, 2.5]), methylphenidate (BR, mean = 2.8 ng/L [2.76, 2.90]; SI, mean = 2.9 ng/L [2.8, 3.0]) and atrazine (BR, mean = 5.0 ng/L [4.1, 6.0]; SI, mean = 2.2 ng/L [1.6, 2.9]). Mean trazine concentrations were significantly higher compared to Sapelo (based upon 95% confidence intervals).

Only 5 of 30 analytes were detected in the water samples in October and December 2014 and there were only two statistically significant differences in mean analyte concentrations (DEET in October and atrazine in December, both higher mean concentrations at Brunswick). The similar mean concentrations at both locations is intriguing as Brunswick has a much larger population, with several WWTPs and >1000 septic fields, while Sapelo has fewer than 100 permanent residents and <100 septic fields. We hypothesize that the greater discharge of the Brunswick

River could be diluting contaminant concentrations, while the small tidal creeks on Sapelo Island could be concentrating contaminants.

Condition Index

The condition index is a measure of the overall fitness of the organisms. Mean [CI] values for all oysters collected on Sapelo Island (mean = 7.33 [6.89, 7.77]) and Brunswick (mean = 5.98 [5.62, 6.34]) suggest that overall the oyster populations on Sapelo Island are a significantly more robust population (based on 95% confidence intervals), despite the finding that oysters in Brunswick and Sapelo Island have similar body burdens of emerging contaminants. This result suggests that other factors (environmental, other contaminant classes) are adversely affecting the health of oysters at Brunswick, resulting in an overall reduced condition.

Work to be Completed

Field collection of samples will end in June 2015 and all of the samples will be extracted and analyzed by December 2015. Oyster tissue data combined with the condition indices and metabolomics data (from another related study) will be incorporated into calculation of a pharmaceutical risk quotient. Environmental data (analyte concentrations in water, sediment and suspended particles) will be used to model probable exposure pathways for the detected CECs. All data and metrics will be analyzed to detect any site or seasonal differences.

A subset of archived oyster shells will be sent to Dr. Aaron Shoults-Wilson (effective 8/15, at Illinois Wesleyan University) in September 2015. Over the past year Dr. Shoults-Wilson has developed a method to age oysters through microscopic analysis of thin sections of oyster shells. He will apply this method to our shells of different sizes to determine if size relates to age of oyster and consequently, exposure duration for analytes in our study.

We anticipate completing the final report for the project in spring of 2016.

The effect of salt marsh hydrodynamics on estuarine flow

Basic Information

Title:	The effect of salt marsh hydrodynamics on estuarine flow
Project Number:	2014GA344B
Start Date:	3/1/2014
End Date:	2/28/2015
Funding Source:	104B
Congressional District:	5
Research Category:	Engineering
Focus Category:	Wetlands, Surface Water, None
Descriptors:	None
Principal Investigators:	Kevin A Haas, Donald R. Webster

Publications

There are no publications.

The effect of salt marsh hydrodynamics on estuarine flow

Final Report

May 15, 2015

Kevin A. Haas
Donald R. Webster

School of Civil and Environmental Engineering
Georgia Institute of Technology
Atlanta, GA 30332-0355

Introduction

Georgia's salt marshes are one of the most valuable and productive ecosystems in the state. The extensive tidal flats and dense vegetation dampen wave and current energy, serving as an invaluable buffer between the developed and populated Georgia coastline and strong offshore storms, such as hurricanes. In addition, dampened currents allow for slow moving waters in estuaries, making excellent nursing habitats for numerous shellfish and fish species. Furthermore, vegetation and animals receive vital nutrients transported from the open ocean during floodward tidal currents and in return ebbward tidal currents bring food and nutrients from the salt marsh out to offshore fish species. By fostering environments for both in and offshore commercial fisheries, salt marshes are in part responsible for $224,956,000 of income and 7,390 jobs, adding $369,134,000 value for the State of Georgia (US Department of Commerce 2009).

Both the livelihood and benefits of salt marshes depend on the hydrodynamics in the estuaries and across the surrounding tidal marshes. It has been shown that the hydrodynamic exchange between the channels and marsh tidal flats dictate the tidal asymmetry of an estuary, or in other words the relative strengths and lengths of flood and ebb tide. Tidal asymmetry has direct effects on tidal currents, water levels, and residence times of any particulate tracer whether biological, chemical, sediment, or pollutant (Blanton et al., 2002; Dronkers, 1986). Thus, it has direct consequences for the export/import of vital nutrients and sediments for the sustenance of offshore fisheries and within the marshes themselves.

In 2002, Georgia's salt marshes were threatened with an extensive dieback over 800 ha, threatening the commercial fishing industry and increasing the state's vulnerability to destructive storms (Ogburn, 2004). A major restoration initiative has been the 'living shoreline' approach which utilizes natural materials and organisms for shoreline protection, and has been monitored through field measurements. The significance of such a dieback event is clear from the extensive private and public research dedicated. Much research has been invested in searching for the dieback cause and on developing restoration techniques, yet much of the hydrodynamic processes within the marshes still remain unknown.

In particular, flow into and out of the marsh is driven by pressure gradients resulting from water level differences between the marsh and main channel. These pressure gradients in turn directly depend upon the relative timing of the peak water levels within the marsh and the main channel. Any process which impedes the flow within the marsh, such as friction due to vegetation, will cause a lag in the water level elevation directly affecting the pressure gradients and induced fluxes. This alters the tidal asymmetry of the estuary, which has an effect on particulate exchange for the marshes and offshore waters. Thus, it is imperative to obtain the necessary field measurements to determine the specific relationship between the marsh and main channel.

The specific project objectives were as follows:

1) Obtain comprehensive synchronized water level and velocity field measurements in a Georgia salt marsh.

2) Analyze the data obtained in the field project to determine the relationship between the pressure gradient forcing and flows in the marsh and how this relates to the flow in the main channel.

Pilot Field Project

The experiment site (shown in Figure 1) was selected due to the researcher's prior field experience with the site and the availability of numerical model data of water levels (Bomminayuni et al., 2012; Bruder et al., 2014) and GPS survey of the marsh bathymetry. Because of the known difficulties with measuring accurate pressure gradients in a marsh environment, an initial pilot study was performed on August 10-11, 2014 to test the field techniques.

Figure 1: Map of Ogeechee Estuary. Red area marks are Rose Dhu Island. Inset image is map of southeastern United States for reference.

The pressure transducers used for this study are Onset HOBO Titanium Water Level Data Logger's, model U20-001-01-Ti. The device, pictured in Figure 2, provided temperature and absolute pressure measurements. The pressure measurements were converted to water level measurements through customized Matlab scripts using pressure readings from a nearby weather station (Skidaway Institute of Oceanography, Savannah, GA – see Figure 1). Three of these instruments were purchased and deployed in the marsh, programmed to record internally at 30 second intervals.

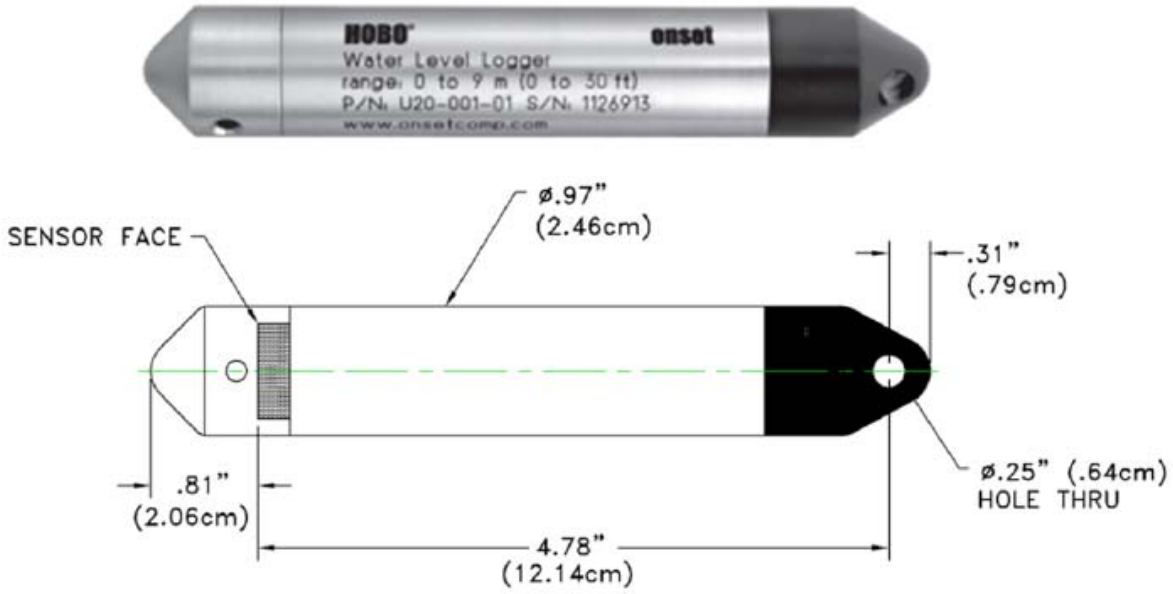

Figure 2: Photograph and Diagram of pressure transducer, HOBO Titanium Water Level Data Logger. Diagram courtesy of Onset.

Each instrument was housed in an Onset Water Logger Housing, which was a capped PVC pipe with a maximum diameter of 5.1 cm and length of 23.5 cm. As shown in Figure 3, the pressure transducer is inserted inside and secured in place using two zip ties. Additionally, all the instruments were placed in additional housing constructed by a researcher to secure the PT's at a fixed location and elevation above the bed and minimize wave interference. The 'wells,' diagrammed in Figure 4 were designed to secure the pressure transducers in-situ, dampen any wave motion or disturbance in water surface, keep sediment away from the instrument, and provide an attachment point for a GPS antenna.

Figure 3: Images of instrument housing from Onset instruction manual.

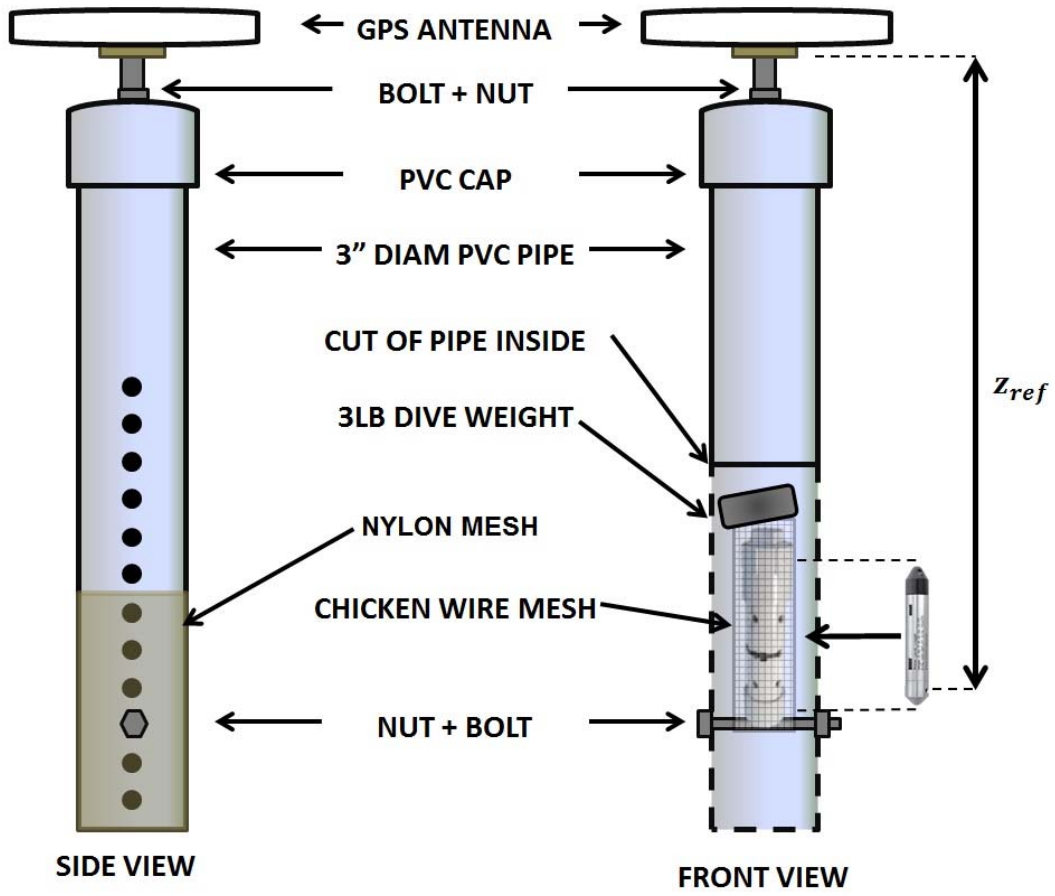

Figure 4: Diagram of constructed instrument assembly.

The general location of instrument deployment, pictured in Figure 5, was chosen due to proximity to both the island and the general marsh area that was to be measured in the larger study. In particular the wells were inserted into the mud at locations where a) the surrounding ground was not too soft, such that the researchers could stand and b) the elevation was low enough to capture all or the majority of the tidal cycle above MTL. The wells were placed relatively close to each other so that their water levels could be assumed constant. An atmospheric transducer was attached on the nearby dock in the open air.

The elevation of each well was measured daily using Ashtech ProFlex 500 GPS Receivers with Ashtech Duel Frequency Marine Antennae. Both receivers were programmed to record internally for two hours at 10 second intervals and were post processed as stationary based stations using the National Geodetic Survey Online Positioning User Service. A photograph of the deployed wells with the GPS antennae attached is shown in Figure 6.

Figure 5: Locations of Instrument Deployment for Pilot Study. Inset Image: general area relative to Rose Dhu Island, GA

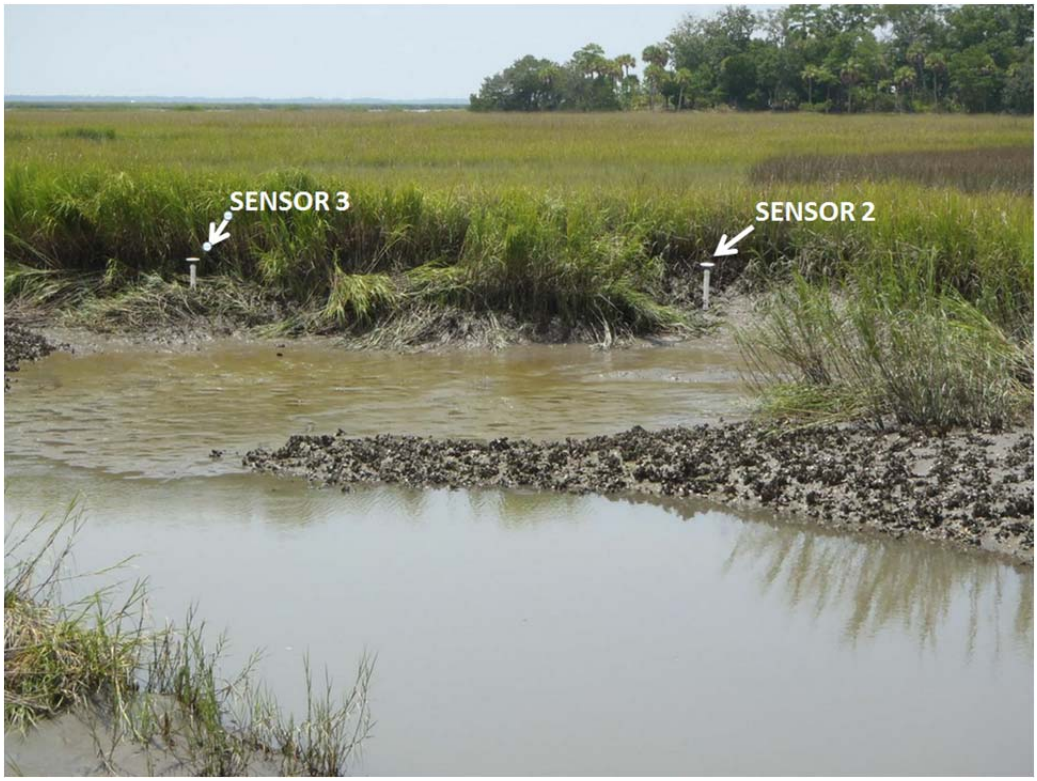

Figure 6: Deployed wells with GPS antennae attached.

After processing the data, it was determined that the pressure transducers in the marsh sank on the order of 2cm over approximately 1 day. In addition, the error of the GPS base station positioning were on the order of 7 cm. Because of the well movement and the uncertainty associated with the GPS processing, the water levels measured between the two wells differed by approximately 2 cm. Due to the proximity of the two wells, 9 m apart, this inaccuracy was unacceptable and changes to the measurement techniques were developed for the final field project. In particular, the design of the well was modified to incorporate a plate to prevent the well from sinking into the mud.

Full Field Project

The full field project occurred from November 2 to November 6, 2014. Three pressure transducers (PT's), two Nortek Vector ADV's and one Nortek Aquadopp were deployed along a transect in the marsh to measure the water levels at various points along the transect, and to correlate the resulting pressure gradients to the velocity in a nearby feeder tidal creek (Aquadopp) and two additional locations higher in the marsh (Nortek ADV's). The specific transect was selected to be easily accessible from the island, and ran perpendicular to the streamwise direction of the nearby main channel. A map showing the locations of the 3 pressure transducer wells, 2 ADV's and the Aquadopp is shown in Figure 7.

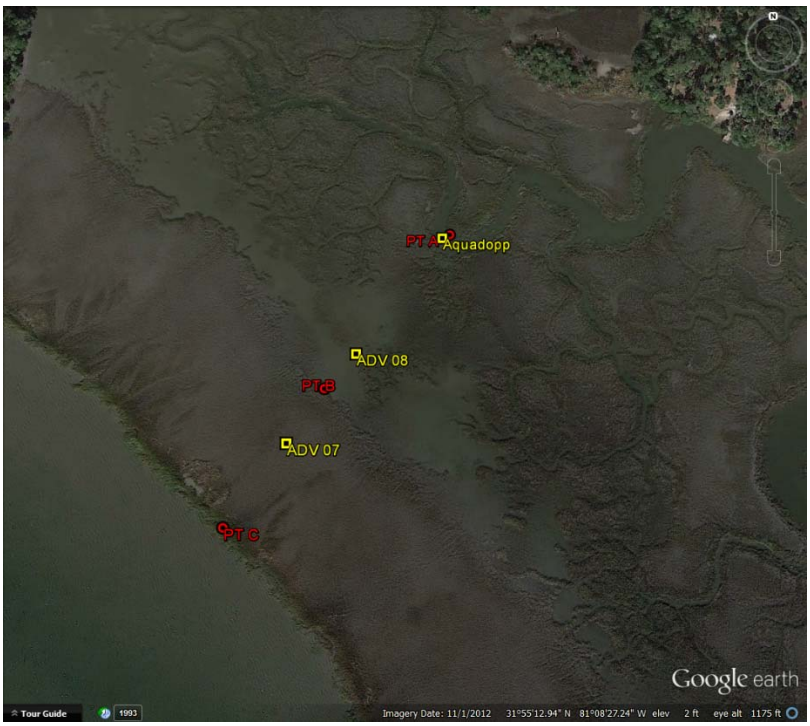

Figure 7: Map showing the locations of the six instruments deployed during this experiment. PT's are shown as red circles and velocity measurement instruments (Aquadopp, ADV's) as yellow squares.

Figure 8: Pressure transducer wells with new plate (left) and deployed well being surveyed with GPS (right).

Based on the experience from the pilot study, the pressure wells included an additional plate to help stabilize the well in the marsh mud. Figure 8 shows the 3 wells prior to the deployment as well as an example of a deployed well being measured with the GPS. The GPS processing was also modified by deploying an additional base station on site and using the GRAFNAV software for post processing. With these modifications, the movement of the wells was estimated to be a few millimeters and the GPS survey accuracy was under a centimeter.

The ADV's used in this experiment were Nortek Vector ADV's, deployed using a chemistry stand and clamp to hold the flexible ADV head in place at the appropriate elevation above the bed. The ADV and stand were attached to cinderblocks to prevent instrument shifts due to flow drag. Each ADV was set to record at 1 Hz for the duration of the experiment to maximize the amount of continuous deployment for four days using a long term deployment lithium battery. ADV's were useable in relatively shallow water, needing only approximately 26 cm of total water depth to sample a point 15 cm above the bed.

The upward looking Nortek Aquadopp was deployed in the center of the feeder tidal creek. As shown in Figure 9, the Aquadopp had a specialized low lying stand resulting in a nearly bottom mounted instrument. The ends of the stand were weighted with dive weights to avoid instrument shift. The Aquadopp measured continuously at 1 Hz with 10 cm vertical bins.

To process the velocity data, any taken during low tide (determined by instances of PT B having zero water depth) were discarded. Then, any data where the average correlation coefficient of the three beams was less than 70% for 45 consecutive samples, or where the average over 300 samples of the mean correlation coefficient

over the three beams dropped below 70% was discarded. Next the dominant flow direction (if one was present) was determined for each ADV by fitting an ellipse to all the east and north velocity measurements for each ADV. The major axis of the resulting ellipse was the new “streamwise" flow direction (correspondingly, the minor axis is the cross-stream direction). The horizontal velocity vector was rotated to correspond to the newly defined streamwise and cross-stream directions, then averaged over 30 sec. intervals.

Figure 9: A deployed ADV stand (left) and the Aquadopp stand (right) at low tide. Note that the high tide water level was nearly 0.65 m above the ADV and nearly 2 m above the Aquadopp.

Results

Over the span of the three days of measurements, 6 high tide cycles were measured. Figure 10 shows the water surface elevation (WL) measurements at the three PT's for the fourth high tide in the dataset. The fourth high tide was selected because it exhibits one of the largest tidal ranges of the six, but the general water surface elevation pattern was consistent across all tidal cycles. The results indicated that the water level at the two PT's in the marsh was quite similar. The water level in the tidal creek (PT A - blue line in Figure 10) did rise a bit faster and fell quicker than the water level higher in the marsh (PT B - red line in Figure 10), which was to be expected, but was essentially identical over the majority of the tidal cycle. In contrast, there was a clear differential water levels between the marsh and the main channel. The water level in the main channel (PT C - green line in Figure 10) began rising at the same rate as the tidal creek then started to rise more rapidly approximately halfway through the rising tide. However, the water level in the marsh caught up and exceeded the water level in the main channel just before high tide and remained higher than the main channel for the rest of the tidal cycle. At high tide, the water level difference between the main channel and the marsh was approximately 7-8 cm, but became as large as 15 cm during rising

and falling tide. Given that the distance between the central marsh (PT B) and the main channel (PT C) was less than 80 m, the observed differential water levels created a substantial transverse pressure gradient across the marsh.

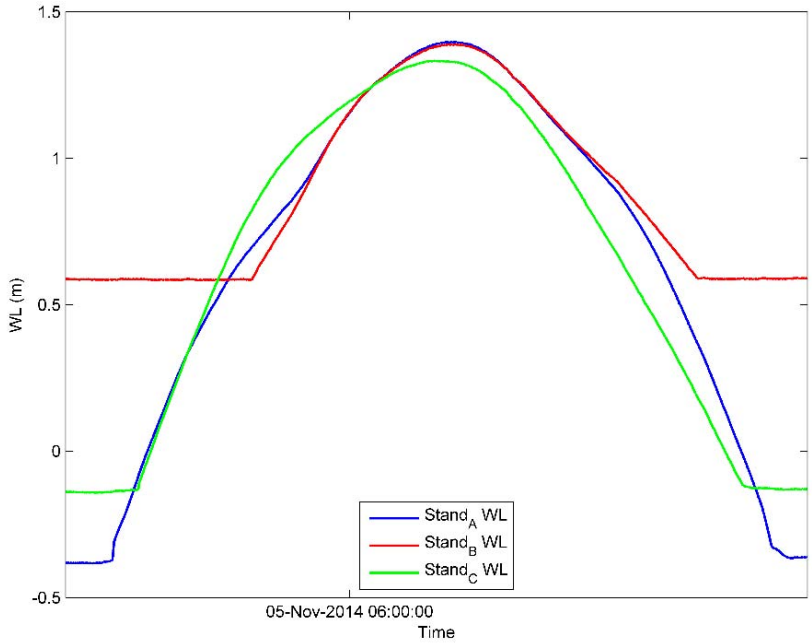

Figure 10: Water surface elevations (WL) at each of the three PT's for the fourth high tide in the dataset.

The results of the ellipse fitting technique to determine a primary flow direction for ADV07 north and east velocities along with the fitted ellipse are shown in the left panel of Figure 11. The velocity at this instrument was nearly entirely one-dimensional. Once the horizontal velocity vector was rotated to correspond to the major axis of this ellipse, the overwhelming majority of the velocity magnitude was confined to the streamwise direction, with comparatively little cross-stream flow. Furthermore, the difference between the angle of the newly defined streamwise direction and the angle of the PT transect (see Figure 7) was less than 9 degrees, indicating that the adjacent PT's were well placed to capture the pressure gradient driving the flow at this location.

The water level from the main channel (PT C) is plotted against the velocity from ADV07 in the right panel of Figure 11. As the tide rises (from right to left) during flood tide, the flow is initially directed from the main channel into the marsh as indicated by the positive velocities. However, as shown in Figure 10, the rise of the water level in the main channels slows down before the water level in the marsh and the pressure gradient flips and the flow is directed back towards the main channel prior to high tide. Interestingly, there is a kink in the velocity as the water level reaches close to high tide. This kink is most likely due to a small change in flow direction. As the tide continues to rise and finally begins to fall, the speed of the velocity towards the channel continuously increases.

The streamwise velocity at ADV07 for every tidal cycle is plotted against the corresponding pressure gradient in Figure 12. The relationship between the velocity and pressure gradient indicated a classical pressure gradient driven flow. The points at which the velocities switch direction identically coincided with the pressure gradient switching sign. Additionally, there appeared to be a transition in the dependence on the pressure gradient above 5 cm/s in which the slope of the plot shifted from the steeper region at lower velocity magnitudes to the milder slope region at higher velocity magnitudes. The change in slope appeared to occur for Reynolds numbers greater than approximately 15,000. Therefore, a two equation approach was used for evaluating the relationship between the velocity and pressure gradient for the low and high Reynolds number regimes.

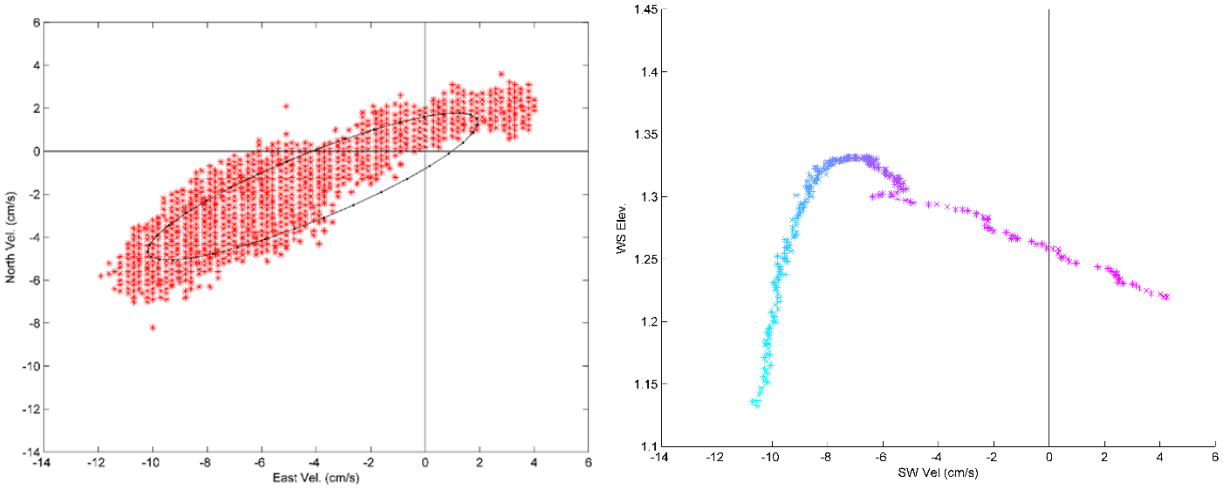

Figure 11: ADV07 north and east velocity measurements and the ellipse fit to the data (left). The WL at PT C plotted as a function of the streamwise velocity from ADV07 (right). Note that time evolves from right to left in the right panel.

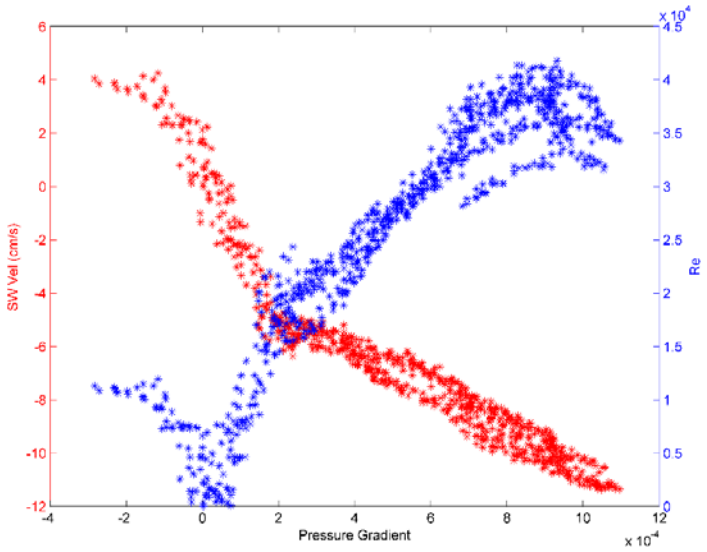

Figure 12: Streamwise velocity (red) and Reynolds number (blue) at ADV07 for each tidal cycle plotted against the corresponding pressure gradient.

Assuming a simple depth integrated momentum balance between the pressure gradient and the drag resulting from the seabed and vegetation, the relationship between the pressure gradient and velocity could be found as

$$\rho g h \frac{\partial \zeta}{\partial x} = -\frac{1}{2}\rho C_d V^2 \quad (1)$$

where the left-hand-side is the pressure gradient from the slope of the water surface, C_d is the drag coefficient and *V* is the measured velocity. For the low Reynolds numbers, a method by Tsihrintzis (2001) was applied to find the drag coefficient for the vegetation using

$$C_d = \gamma R_h^{-k} \quad (2)$$

where γ is a measure of the plant density, R_h is the Reynolds number based on the depth and *k* controls the functional dependence of the drag coefficient on the Reynolds number, governed by the type of vegetation. The parameter γ was found as

$$\gamma = 2K_o/s \quad (3)$$

where K_o is an empirically determined coefficient and *s* is the stem spacing. Using a least-squares best fit, the values of $K_o = 10^{2.01}$ and *k* = 0.72 was found. This agreed reasonably well with the range of values described by Lee et al. (2004).

For the larger Reynolds numbers, an approach using a Darcy-Weisbach type friction factor was used. Defining a shear velocity

$$u_* = \left(gh\frac{\partial \zeta}{\partial x}\right)^{\frac{1}{2}} \quad (4)$$

the velocity is given as

$$\frac{V}{u_*} = \left(\frac{8}{f}\right)^{\frac{1}{2}} \quad (5)$$

Using a modified version of the equation by Lindner (1983) to find the friction factor:

$$f = 4\alpha C_d \frac{dh}{s_x s_y} \quad (6)$$

where *d* is the stalk diameter, α is a free parameter and s_x and s_y are the lateral and longitudinal plant spacing, taken to be equal in this case. The value of C_d was taken to be 1.5 as recommended by Jarvelia (2002). Again using a least-squares fit for the data, α was found to be equal to 1.33.

Both the low and high Reynolds number data along with the velocities predicted by the two different models for each measured pressure gradient are shown in Figure 13. In general, both the low and high Reynolds number models performed well in predicting the velocity for given pressure gradients. They both captured the slope of the velocity dependence on the pressure gradient for the different regimes.

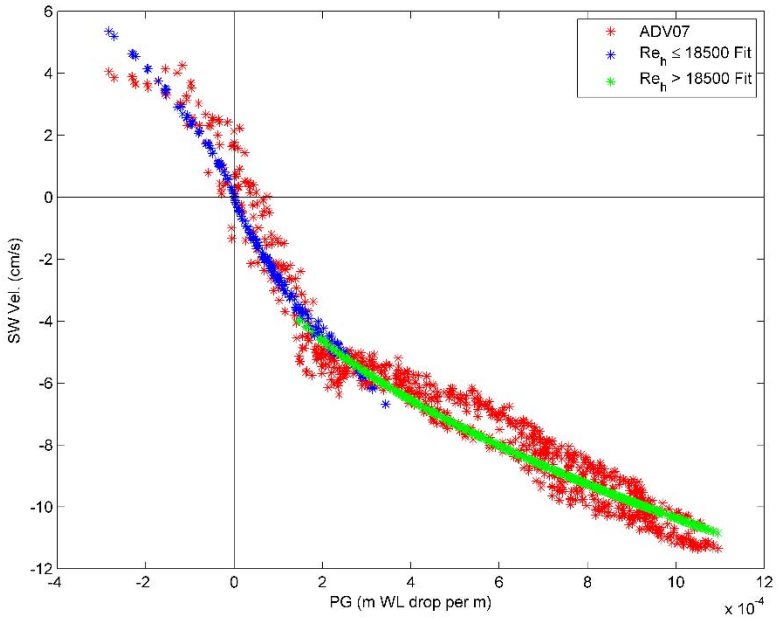

Figure 13: Predicted velocity for the low and high Reynolds number regimes. The streamwise data measured at ADV07 are plotted in red, the low Reynolds number predicted velocities are plotted in blue, and the high Reynolds number predicted velocities are plotted in green.

Conclusions

As a result of this project, the transverse pressure gradient in a tidal marsh system has been directly measured for the first time. These types of measurements have long eluded researchers due to the challenges of both deploying instruments in the marsh and for accurately recording a consistent vertical datum for multiple instrument locations. The unique measurement technique developed for recording this pressure gradient will be utilized in future field campaigns.

Analysis of the velocity and pressure gradient showed a clearly classical pressure gradient driven flow across the marsh. The heavy vegetative marsh induced significant drag on the flow, although this relationship had a critical dependence on the Reynolds number. Therefore, a two equation approach for low and high Reynolds number regimes demonstrated that existing models of flow through vegetation were capable of reproducing the measurements. Therefore, these types of models maybe used to estimate the friction coefficients in more advanced numerical models for estuary wide circulation.

Dissemination and Training

Two Ph.D. students (David Young and Brittany Bruder) have been partially supported by this project. The analysis of the data will be part of David Young's Ph.D. dissertation in Spring 2016. In addition, David will be presenting the work at the Young Coastal Scientists and Engineers Conference at the University of Delaware in July 2015.

References

Blanton, J.O., Lin, G.Q., Elston, S.A. 2002. Tidal current asymmetry in shallow estuaries and tidal creeks. Continental Shelf Research 22, 1731-1743.

Bomminayuni, S., Bruder, B., Stoesser, T. and Haas, K. (2012) Assessment of Hydrokinetic Energy near Rose Dhu Island, Georgia. Journal of Renewable and Sustainable Energy, 4(6), 063107.

Bruder, B., Bomminayuni, S., Haas, K and Stoesser, T. (2014) Modeling tidal distortion in the Ogeechee Estuary. Ocean Modelling, Vol 82, Pages 60-69.

Dronkers, J. 1986. Tidal asymmetry and estuarine morphology. Netherlands Journal of Sea Research 20, 117-131.

Jarvela, J. (2002) Flow resistance of flexible and stiff vegetation: a flume study with natural plants, Journal of Hydrology, vol. 269(1-2), pp. 44–54.

Lee, J., Roig, L., Jenter, H. and Visser, H (2004) Drag coefficients for modeling flow through emergent vegetation in the Florida Evergaldes, Ecological Engineering, vol. 22, pp. 237–278.

Lindner, K. (1982) The flow resistance of cultivated plants, Ph.D. dissertation, Leichtweiss Institute of Hydraulic Engineering - Technical University of Braunschweig, Germany.

Ogburn, M.B., 2004. Salt marsh dieback in Georgia. M.S. Thesis, University of Georgia.

Tsihrintzis, V., (2001) Discussion of Wu et al., 1999, Journal of Hydraulic Engineering, vol. 127(3), pp. 241–244.

U.S. Department of Commerce; National Oceanic and Atmospheric Administration, N.M.F.S., (2009). “Fisheries Economics of the United States 2009.”

Implications of eutrophication and climate change in promoting toxic cyanobacterial blooms in agricultural ponds across Georgia.

Basic Information

Title:	Implications of eutrophication and climate change in promoting toxic cyanobacterial blooms in agricultural ponds across Georgia.
Project Number:	2014GA345B
Start Date:	3/1/2014
End Date:	2/28/2015
Funding Source:	104B
Congressional District:	
Research Category:	Water Quality
Focus Category:	Water Quality, Toxic Substances, Management and Planning
Descriptors:	None
Principal Investigators:	Susan Bennett Wilde, Deepak Mishra

Publications

There are no publications.

Georgia Water Resources Institute Final Report

Susan B. Wilde, Warnell School of Forestry and Natural Resources and
Deepak Mishra, Geography Department, University of Georgia

Implications of eutrophication and climate change in promoting toxic cyanobacterial blooms in agricultural ponds across Georgia.

Excessive nutrient enrichment in watersheds has increased the prevalence of harmful algal blooms (HABs) in vital freshwater resources (Anderson, et al. 2002, Anderson, et al. 2008). Global climate change is predicted to enhance the frequency and spatial coverage of HABs that are typically composed of cyanobacteria species, which readily exploit excess nutrients and thrive in warm, low-flow systems (Heisler, et al. 2008, Moore, et al. 2008, Davis, et al 2009). While most HABs research has dealt with marine and estuarine systems, freshwater systems have historically been impacted as well (Glibert and Burkholder, 2006, Lewitus et al., 2003; Lewitus et al. 2008). The excess nutrient inputs resulting from agricultural and urban activities in the southeastern US promote these blooms. Hypereutrophic ponds and lakes used to water livestock and provide public water supply and recreation can develop HABs characterized by the exponential growth of planktonic cyanobacteria (commonly referred to as "blue green algae"). The cyanobacteria have many specialized adaptations that enable them to exist and flourish in environments that are inhospitable to most organisms. They are capable of nitrogen fixation and can regulate position within the water column to access nutrients and/or prevent photooxidative damage under extreme light conditions (Walsby and Booker, 1980). Excess phosphorous availability is the major factor driving cyanobacterial growth rates and has been shown to increase toxin production by these species (Sivonen and Jones, 1999). Nutrient loading, increased retention time, and moderate to high temperatures frequently co-occur in southeastern US ponds and lakes creating an ideal environment for these cyanobacteria to proliferate (Wicks and Thiel, 1990). Global climate change effects, such as drought and increased temperatures, exacerbate this major issue for the southeast; with an increase in temperatures and drought frequency, the effects of eutrophication are intensified in GA's watersheds. During hot periods with low rainfall we, we documented harmful cyanobacterial blooms in livestock drinking water ponds, golf course ponds, subdivision ponds and water supply reservoirs throughout Georgia.

Lakes and ponds are commonly constructed for agricultural and recreational purposes in GA and across the southeastern US, but they can reduce the quality and quantity of downstream water resources including rivers and streams already depleted by drought. In the case of GA, approximately 29% of the state is agricultural land, making over 9.8 billion dollars in revenue for the state (USDA: Economic Research Service, 2011). Ponds are commonly used to water livestock and for irrigation reserves. This practice is likely to become more common in light of recent well permit issue restrictions in drought-stricken southwest GA (Turner, 2012). These artificial farm ponds serve as a catch basin for allochthonous nutrient inputs from fertilization and animal waste. Over 87% of farms in GA are small, family owned operations with over 60% of those farms having only 1-99 acres; thus, their fertilization practices are not regulated (USDA: Economic Research Service, 2011). Because these small operations are not regulated, best management practices,

which include soil testing for determining the appropriate type and fertilization rate, may not be followed and fertilization regimes may only be based on past experience. This scenario, coupled with the availability of poultry litter (a common source of inexpensive fertilizer), can result in excess nutrients such as nitrogen and phosphorus. During rain events or direct input, these nutrients, are ultimately transported into watershed ponds or streams and rivers feeding larger reservoirs. High levels of phosphorus, preferentially support the growth of cyanobacterial and have been demonstrated to enhance toxin production (Sivonen and Jones, 1999). Eutrophication, and the danger of lethal cyanobacterial blooms, negatively impact overall water quality, which in turn affects the health of livestock, pets, wildlife, and humans utilizing the resource.

Cyanotoxins can cause mortality either by longterm subchronic doses or acutely during high density toxic algal blooms. The most common cyanotoxic species throughout the world and in GA is *Microcystis aeruginosa*, which produces the potent liver toxin microcystin. While no state or federal regulations currently exist for cyanotoxins in drinking water, the World Health organization recommends 1 ppb as a safe level level in drinking water. Empirical and experimental data have been used to propose risk levels for some important cyanotoxins in water. The level found in the Gwinnett, GA agricultural pond exceeded the subchronic danger level by 10-fold and was 2X the acute dose level. While conducting additional sampling during 2013-2015, we documented 28 additional locations from the mountain to coastal detention ponds where cyanobacterial species dominated and 19 sites had microcystin levels >5 ppt.

Our research is addressing fundamental questions regarding critical levels of limiting nutrients for initiating and sustaining cyanobacterial blooms. These aquatic systems cannot perform their ecological or agricultural function unless optimal watershed management strategies are implemented. This project combines chemical analysis, ecotoxicology, watershed assessment, identification and toxic potential of harmful algal species, and animal health effects to enable farmers and reservoir managers to make changes to improve both the health of their domestic animals or wildlife and downstream water quality.

While agriculture comprises a large percentage of land use in Georgia, habitation in general, including suburban development, adds to nutrient loading of ponds and other freshwater resources. In residential subdivisions, ponds are commonly constructed to detain storm water or as mitigation for development. The runoff captured in these ponds concentrates nutrients from lawn fertilizers, pet wastes, and even poorly functioning septic systems; therefore, cultural eutrophication can promote HABs as well (Lewitus et al. 2003; Lewitus et al. 2008). Besides serving as a sink for nutrient and stormwater runoff, these ponds are used by wildlife and recreationally by humans. These interactions increase the likelihood of human and pet exposure to algal toxins directly or indirectly through trophic transfer (Lewitus et al. 2008). Mortality events due to acute HABs exposure are routinely documented in pets (Van de Mere et al., 2012).

Our overarching objective was to better understand the critical driving forces promoting harmful cyanotoxins in inland waters and determine the best management solutions. In

cooperation with the University of Georgia's Agricultural and Environmental Services Laboratories, we investigated the relationship among watershed management practices, the presence of harmful cyanotoxins, and livestock mortality in Georgia. Analysis was in inland waters ranging from mountains to sea, investigating the potential impact of lethal algal blooms in waters across diverse physiographic and biogeochemical regimes. We have a network of county extension offices in place throughout the state to assist in conducting a landscape level survey of aquatic sites within agricultural production watersheds and evaluate current ecological conditions relative to existing management practices.

Objectives:
Monitor and map sites cyanoHABs sites throughout the state of Georgia. Document animal health conditions and/or mortality events related to cyanotoxin exposure in ponds. Examine the factors that promote harmful cyanotoxin production in pond systems by measuring multiple abiotic and biotic factors. Assess BMPs lacking in cyanoHAB ponds to promote specific management practices effective in prevention of cyanoHABs. Test and refine an existing laboratory-based algorithm developed by Mishra et al. (2009) to detect and quantify the cyanobacterial concentrations in Georgia sites using remote sensing data from hyperspectral radiometers.

We aimed to develop both multispectral Landsat based as well as proximal hyperspectral models. As such, several models of phycocyanin (PC) estimation have been developed using various approaches such as empirical (Vincent et al, 2004, Mishra et al, 2009), semi-analytical (Simis et al., 2005), and Quasi analytical (Mishra et al, 2013). Vincent's model applied an empirical approach for multispectral data using Landsat ETM, while the rest employed hyperspectral proximal sensing data. In this study, the first data sets collected (June 16th, 2014) was used for model calibration and the second set of field data (July 2nd, 2014) was used for model validation. Based on the models developed by Vincent et al (2004), two other models were developed based on the stepwise regression approach, using Landsat 8 spectral bands instead of Landsat 7 used in the original study. In addition, we also tested a multiple linear regression and slope difference models using combinations of visible and NIR bands. The best model was selected based on statistical parameters such as coefficient of determination (R^2) and Percent Normalized Root Mean Square Error (%RMSE) as detailed in Lee et al. (2002). The selected model was applied to the Landsat 8 subsets to produce time series composites of PC concentrations and distributions.

Methods
Pond locations with harmful algal blooms (HABs) were identified using University of Georgia's (UGA) Agriculture and Environmental Service laboratory (AESL) and previous HAB site data collected by Wilde lab at Warnell School of Forestry and Natural Resources. Additional pond locations were added in locations within counties where cyanoHAB's were documented. Sites from piedmont Georgia were monitored more frequently to track seasonality of cyanoHABs. At each site, duplicate 50mL water samples were collected for algal enumeration, toxin analysis, and nutrient analysis. Samples were collected during mid-day, representing the peak of bloom formation. In addition to water samples pH,

dissolved oxygen, turbidity, and water temperature were measured using a hand-held multimeter.

Phytoplankton identifications and cell counts, using a hemacytometer, were performed using light microscopy. Samples with relatively high (>10,000 cells/mL) of toxigenic species were analyzed for microcystin using the commercially available ELISA (Abraxis Bioscience, www.abraxiskits.com). We conducted water chemistry on a subset of samples including: pH, Hardness, Phosphorus and Nitrogen (total and dissolved).

Sites were evaluated to assess whether BMPs were followed or if additional safeguards should be put in place to in prevent further eutrophication. The BMPs utilized will be based upon pond usage (i.e. agricultural vs. urban pond). Considering the potential variability among ponds, pond management will follow BMP recommendations from both the U.S. EPA for urban ponds and USDA – NRCS for agricultural ponds.

Hyperspectral remote sensing reflectance data was acquired from selected water sample collection sites using a dual sensor-system with two inter-calibrated Ocean Optics spectroradiometers (Ocean Optics Inc., Dunedin, FL, USA) as described in DallO'lmo, et al. (2005). The hyperspectral remote sensing reflectance data is in the range 400-900 nm with a sampling interval of 0.3 nm. Radiometer 1, equipped with a 25° field-of-view optical fiber will measure the upwelling radiance just below the air-water interface, expressed in digital numbers as $DN_{Lu}(\lambda)$; whereas, radiometer 2, equipped with an optical fiber and cosine diffuser (yielding a hemispherical field of view) acquired above surface down welling irradiance, expressed in digital numbers as $DN_{Ed}(\lambda)$. To match their transfer functions, inter-calibration of the radiometers was accomplished by measuring the upwelling radiance of a white Spectralon reflectance standard (Labsphere, Inc., North Sutton, NH, USA) simultaneously with incident irradiance. The two radiometers were inter-calibrated immediately before and after measurements in each field site. After the data acquisition, *remote sensing reflectance (*R_{rs} expressed in sr^{-1}) was calculated as follows:

$$R_{rs}(\lambda) = \frac{t}{n^2}\frac{DN_{Lu}(\lambda)}{DN_{Ed}(\lambda)}\frac{DN_{Ed,ref}(\lambda)}{DN_{Lu,ref}(\lambda)}\frac{\rho_{ref}(\lambda)}{\pi}F_i(\lambda) \qquad (1)$$

where, t is the transmittance at the air-water interface (0.98); n is the refractive index of water (1.34); $DN_{Lu,ref}$ and $DN_{Ed,ref}$ are digital numbers representing upwelling radiance and downwelling irradiance over the white Spectralon panel; ρ_{ref} is the irradiance reflectance of the Spectralon panel; F_i (λ) is the spectral immersion factor (Ohde and Siegel, 2003). For each sampling location, consecutive scans were recorded and further averaged to calculate a representative $R_{rs}(\lambda)$ spectrum using a handheld USB 4000 hyperspectral radiometer (Ocean optics Inc., FL). The primary goal of this part of the project was to test, fine-tune, and transform an existing laboratory-based algorithm developed by Mishra et al. (2009) to detect and quantify the cyanobacterial concentrations in GA waters using remote sensing data from hyperspectral radiometers.

Cloud and shadow masking:

To get rid of the residual clouds and shadows, we compared 3 methods to detect cloud and cloud shadows in Landsat 8 images, including an object based cloud and cloud shadow

algorithm Fmask (Zhu and Woodcock, 2012), pixel-based supervised classification method using Maximum Likelihood Classification (MLC), as well as object-based supervised classification using K Nearest Neighbors (KNN) method. Involving Landsat Top of Atmosphere (TOA) reflectance and Brightness Temperature (BT) data as inputs, the Fmask algorithm computes a cloud mask from a probability mask and a scene-based threshold based on the spectral variability, brightness, and temperature information extracted from inputs, as well as cloud physical properties. Both pixel-based and object-based supervised classifications were conducted using five layers including blue, green, red, infrared bands and Normalized Difference Vegetation Index (NDVI) layer. Mixed pixels of water and vegetation areas were excluded first according to NDVI values. Then MLC was applied to identify water, cloud and cloud shadow classes within the five layers. Multiresolution image segmentation was utilized first to segment images into different objects before classification. Then the sample space were chosen based on the mean and standard deviation of each layers and object samples were selected for water, cloud and cloud shadow classes. Then KNN classification method was applied to classify objects into different classes. Finally, the performances of all three methods were assessed based on visual interpretation and the object-based classification was chosen.

Algorithm development and application:

We aimed to develop both multispectral Landsat based as well as proximal hyperspectral models. As such, several models of phycocyanin (PC) estimation have been developed using various approaches such as empirical (Vincent et al, 2004, Mishra et al, 2009), semi-analytical (Simis et al., 2005), and Quasi analytical (Mishra et al, 2013). Vincent's model applied an empirical approach for multispectral data using Landsat ETM, while the rest employed hyperspectral proximal sensing data. In this study, the first data sets collected (June 16th, 2014) was used for model calibration and the second set of field data (July 2nd, 2014) was used for model validation. Based on the models developed by Vincent et al (2004), two other models were developed based on the stepwise regression approach, using Landsat 8 spectral bands instead of Landsat 7 used in the original study. In addition, we also tested a multiple linear regression and slope difference models using combinations of visible and NIR bands. The best model was selected based on statistical parameters such as coefficient of determination (R^2) and Percent Normalized Root Mean Square Error (%RMSE) as detailed in Lee et al. (2002). The selected model was applied to the Landsat 8 subsets to produce time series composites of PC concentrations and distributions.

Results:

Mapping HAB sites, documenting toxicity and effects on livestock

Sample were collected from sites within all of the Level III Ecoregions of Georgia (Ridge and Valley, Blue Ridge, Piedmont, Southeastern Plains, and Southern Coastal Plain) (Figure 1). While samples were collected from March-December, the cyanoHABs were most prevalent during June-September when water temperatures exceeded 30°C in surface waters of ponds and lakes were thermally stratified. Dissolved oxygen levels were limiting for fish and other aquatic biota (<2ppt) below the thermocline in all of the lakes with cyanoHAB's.

Phosphorus, chlorophyll, and secchi disk transparency ranged oligotrophic in some locations within the large Georgia Power Reservoirs to hyper-eutrophic within many of the small farm ponds with ongoing cyanoHABs. Carlson (1996) used index values for chlorophyll, Phosphorus, secchi disk to categorize trophic classes.

Trophic Index	Chl (μL^{-1})	P (μL^{-1})	SD (m)	Trophic Class
<30—40	0—2.6	0—12	>8—4	Oligotrophic
40—50	2.6—20	12—24	4—2	Mesotrophic
50—70	20—56	24—96	2—0.5	Eutrophic
70—100+	56—155+	96—384+	0.5—<0.25	Hypereutrophic

Watersheds represented combinations of agricultural (cattle, chicken houses, and crop production), subdivisions, and golf courses. Water collected in all ecoregions from farm ponds, fishing ponds and a recreational swimming lakes had frequent detections of harmful algal blooms (>10,000 cells/ml) of toxigenic species. The most common species was *Microcystis aeruginosa*, additional cyanoHAB species included Aphanizomenon flos-aquae, Lyngbya wollei, and Oscillatoria sp. Microcystin concentrations >5ppb were detected in 19/33 sites. Sick or dead cattle were noted at 7 of the sites evaluated.

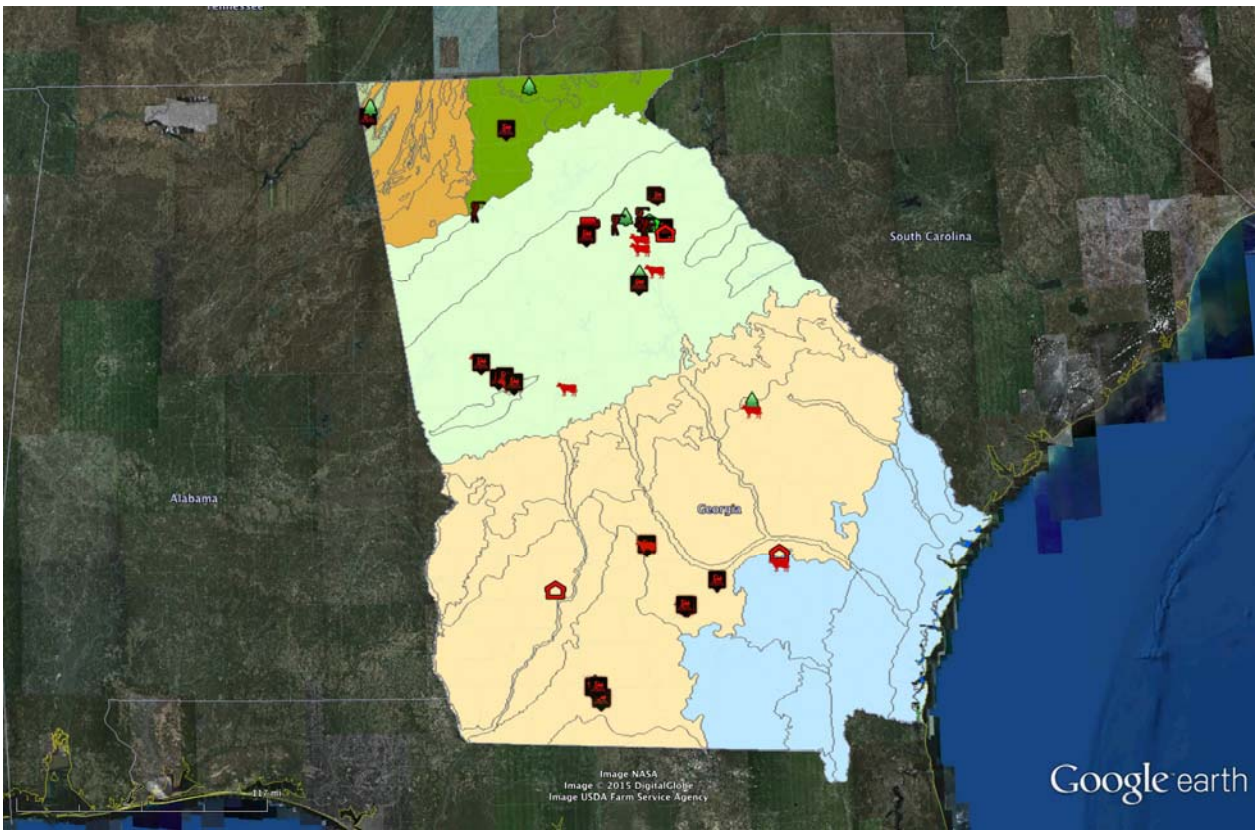

Figure 1. CyanoHABs were detected in all ecoregions throughout Georgia in agricultural watersheds. Red icons represent ponds with bloom densities (>10,000/ml) toxigenic cyanoHAB species in agricultural (cattle, chickens, crops) golf courses and subdivisions. No cyanoHABs were documented in the forested watersheds.

Table 1. Water samples from various counties throughout Georgia evaluated for cyanoHAB's and cyanotoxins were initiated following the observance of discolored pond water or sickened/dead cattle.

County	**Watershed**	**Primary use**	***Toxigenic species***	**Toxin (microcytin)**	**Cattle**
Appling	Agriculture/ suburban	Recreational swimming	*M.aeruginosa*	>10 ppb	
Dade	Agriculture	Cattle watering	*M.aeruginosa*	nd	2 dead*
Dade	Agriculture	Cattle watering	*M.aeruginosa*	>5 ppt	
Elbert	Agriculture	Cattle watering	*M.aeruginosa*	>5 ppt	
Elijay	Agriculture	Cattle watering	*M.aeruginosa*	nd	
Emanuel	Agriculture	Recreational fishing	*M.aeruginosa*	>10 ppb	
Grady	Agriculture	Cattle watering	*nd*	nd	8 dead*
Greene	Agriculture	Cattle watering	*nd*	nd	
Gwinnett	Agriculture	Cattle watering	*M.aeruginosa*	>10 ppb	4 dead
Gwinnett	Agriculture/ suburban	Cattle watering	*M.aeruginosa*	>10 ppb	
Gwinnett	Agriculture	Cattle watering	*M.aeruginosa*	>10 ppb	
Gwinnett	Agriculture/ suburban	Cattle watering	*M.aeruginosa*	>10 ppb	
Gwinnett	Agriculture	Cattle watering	*nd*	nd	
Gwinnett	Agriculture/ suburban	Cattle/fishing	*M.aeruginosa*	>10 ppb	
Gwinnett	Agriculture/ suburban	Recreational fishing	*M.aeruginosa*	nd	
Habersham	Agriculture	Cattle watering	*nd*	nd	
Irwin	Agriculture	Cattle watering	*M.aeruginosa*	>10 ppb	
Johnson	Agriculture	Cattle watering	*nd*	nd	4 dead*
Johnson	Agriculture	Cattle watering	*M.aeruginosa*	>5 ppt	
Madison	Agriculture	Cattle watering	*M.aeruginosa*	>5 ppt	
Madison	Agriculture	Cattle watering	*M.aeruginosa*	>10 ppb	2 sick
McDuffie	Agriculture/ suburban	Recreational fishing	*Lyngbya wollei, M.aeruginosa*	>5 ppt	
Meriweather	Agriculture	Cattle watering	*M.aeruginosa*	nd	
Meriweather	Agriculture	Cattle watering	*M.aeruginosa*	nd	
Monroe	Agriculture/ suburban	Recreational fishing	*M.aeruginosa*	>5 ppt	
Morgan	Agriculture/ suburban	Cattle/fishing	*M.aeruginosa*	nd	
Morgan	Agriculture/ suburban	Recreational fishing	*Oscillatoria*	nd	

Oconee	Agriculture	Cattle watering	*Aphanizomenon flos-aquae*		
Spaulding	Agriculture	Cattle watering	*M. aeruginosa, Aphanizomenon flos-aquae*	nd	2 sick
Thomas	Agriculture/ suburban	Recreational fishing	*M.aeruginosa*	>5 ppt	
Thomas	Agriculture	Cattle/fishing	*M.aeruginosa*	>5 ppt	
Troup	Agriculture/ suburban	Cattle/fishing	*M.aeruginosa*	>5 ppt	
Wilcox	Agriculture	Cattle watering	*M.aeruginosa*	>10 ppt	
Wilcox	Agriculture/ suburban	Recreational fishing	*M.aeruginosa*	nd	

**Suspected* cattle poisonings: Dead and sick cattle were reported by owners.

This cattle watering pond in Oconee County (Figure 2) provides an example of a cultivated watershed for a small cattle-watering pond without vegetated pond buffers. An Irwin County cattle watering pond and Troup County recreational fishing ponds have obvious cyanoHAB's visible in the Google Earth image from August 2014 (Figure 3, 4).

Figure 2. Cattle watering pond in Oconee County with dense bloom of *Aphanizomenon flos-aquae*.

Figure 3. Cattle watering pond in Irwin County is surrounding by cultivated watershed and lacks vegetated pond buffers.

Figure 4. These cattle watering pond and adjacent recreational fishing ponds in Troup County also demonstrated the consequences of a lack of BMP's in this agricultural landscape. 2/5 ponds had cyanoHABs during July-August 2014.

Harmful algal blooms are monitored worldwide using various techniques, including remote sensing. Freshwater blooms typically consist of cyanobacteria species; a clade of organisms with a unique pigment known as phycocyanin. Current remote sensing efforts targeting cyanobacteria (HABs) have been able to exploit the organisms' phycocyanin spectral signature evident around 620 nm. Many researchers have received viable signals for this pigment (Ruiz-Verdu et al. 2008; Song et al. 2013). Cyano-HABs can be remotely sensed using spectral bands available in the Medium Resolution Imaging Spectrometer (MERIS), onboard ENVISAT, based upon the pigment phycocyanin (Simis et al. 2007). Their results were ultimately limited in conditions where low phycocyanin concentrations were evident, but high chlorophyll concentrations were present. One of the main problems in remote sensing cyanobacterial blooms is the presence of chlorophyll. High chlorophyll concentrations tend to inflate phycocyanin concentrations based upon remote sensing data (Mishra et al. 2009, Simis et al. 2005). Studies by Mishra et al. (2009) compared various algorithms for properly predicting phycocyanin concentrations and concluded that a 700 and 600 spectral band ratio was much less sensitive to chlorophyll.

Our research built upon these studies while incorporating high resolution Landsat 8 data. A combination of satellite imagery and in-situ ancillary data will be used to validate and calibrate four proposed spectral band ratio models: 1) Vincent's single band and band ratio models (2004); 2) Schalles and Yacobi's model (2000); 3) stepwise band ratios, and 4) multiple linear regression slope model. These models will help to develop a spatiotemporal cyanobacterial detection tool and the production of cyanobacterial distribution maps. Ultimately, these products will help configure reservoir management strategies to promote optimal aquatic ecosystem health.

Using NASA's newest Landsat-8 satellite data, we can frequently detect and predict water bodies at highest risk over wide landscapes. Four inland reservoirs located in the Georgia Piedmont were identified for analysis and include: 1) Lake Oconee, GA (33.45°, -83.26°); 2) Lake Sinclair, GA (33.19°, -83.28°); 3) Lake Juliette, GA (33.05°, -83.79°); 4) Jackson Lake, GA (33.37°, -83.86°) (Figure 5). These Georgia Power Reservoirs are multi-use and provide various services such as electricity and drinking water. Lake Oconee was created in 1979 after Georgia Power constructed the Wallace Dam on the Oconee River. It is the second largest reservoir in Georgia and covers a 7710 ha area. Lake Oconee drains into Lake Sinclair, a 6200 hectare lake, made in 1953 after the construction of the Sinclair Dam. Jackson Lake, one of the oldest reservoirs in Georgia, was made after the construction of the Lloyd Shoals Dam in 1910. Despite being relatively small (1922 hectares and less than half the size of Lake Sinclair), it can provide up to 21,000 kilowatts of electricity. Lake Juliette, a 1456 ha reservoir near Macon, GA, is primarily used as a source of cooling for a coal-fired power plant. The lake also provides recreational opportunities to the surrounding community. All sites are in the Piedmont region of Georgia with trophic status ranging from oligotrophic to mesotrophic.

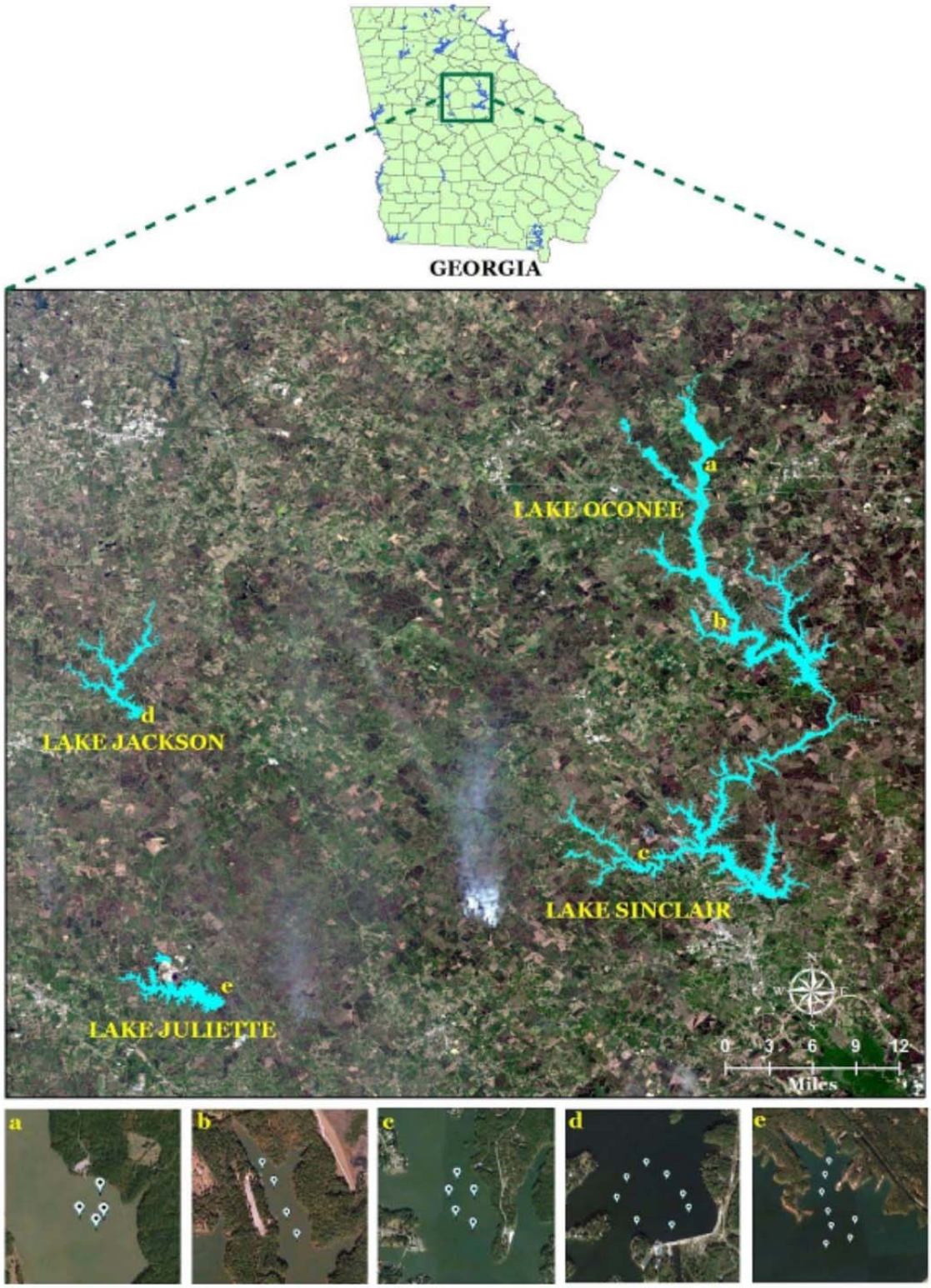

Figure 5: Four Georgia Power Reservoir evaluated in the remote sensing study of cyanopigments as a predicted tool for cyanoHABs were; Lake Oconee (a, b), Lake Sinclair (c), Lake Jackson (d), and Lake Juliette (e).

Mapping Results

Atmospheric Correction:

After comparison between spectral profiles post-FLAASH and DOS correction, it was evident that FLAASH was able to remove atmospheric noise in the visible range of the spectrum, particularly in the lower wavelengths. DOS on the other hand was unable to correct for atmospheric noise in the blue region of the spectrum, as evident from the absence of chlorophyll absorption in wavelengths between 400 to 500 nm (Band 2, Blue) (Figure 3a and b). The FLAASH corrected spectra showed a prominent chlorophyll absorption feature between 450 - 500 nm ranges (Blue Band). Further, GER spectral bandwidths showed spectral response patterns similar to FLAASH corrected spectra than DOS. Therefore, FLAASH was the chosen method of atmospheric noise removal, and applied to entire set of images downloaded for the study period (Figure 4)

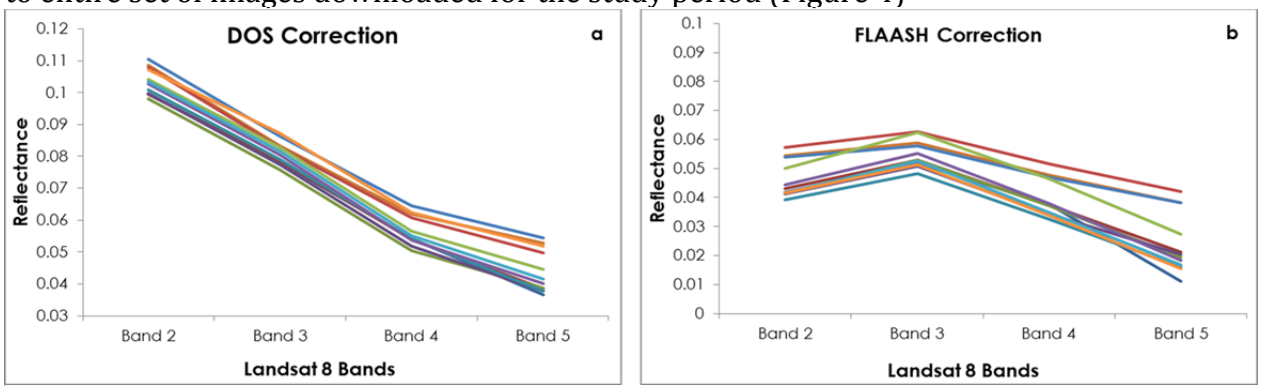

Figure 3: Comparison between spectral profiles extracted from DOS and FLAASH atmospheric correction of Landsat 8 images (May 12, 2014)

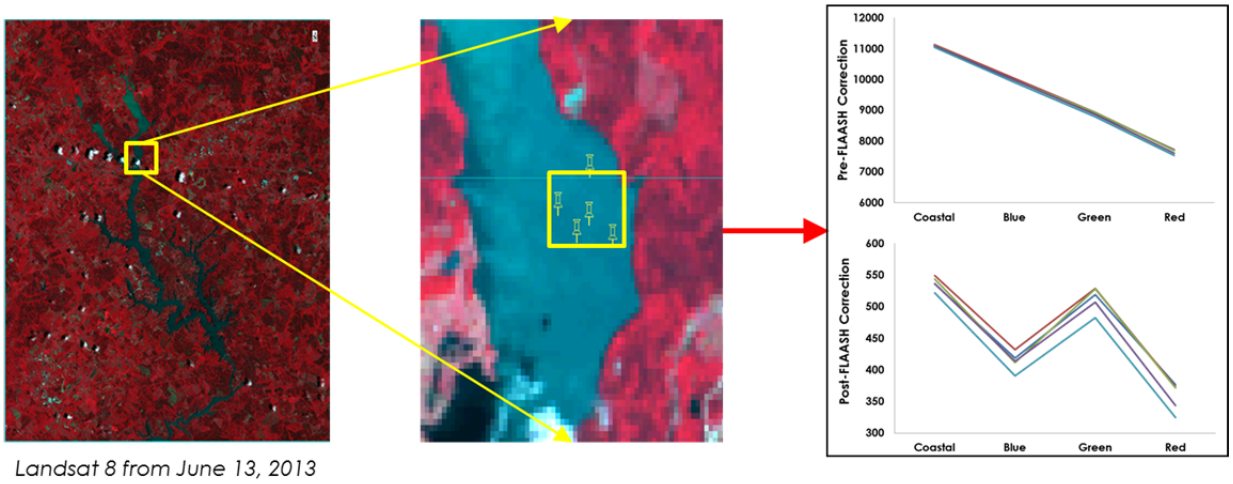

Figure 4: Comparison between spectral profiles extracted from Pre and Post atmospheric correction of Landsat 8 images (May 12, 2014)

Cloud and Shadow Masking:

Regarding the performances of all three methods, though F_{mask} can identify the clouds and shadows as a pair, it cannot direct accurate boundaries. As water bodies may have similar digital number (DN) values to shadows, it is difficult to distinguish water bodies and shadows simply using pixel-based classification. As a result, cloud and cloud shadow

boundaries were created using object-based image classification results. Example of cloud and shadow masking is illustrated in Figure 5, using Landsat 8 image on May 12, 2014; with the yellow areas masking out the clouds and the green areas masking out the shadows. Final water boundaries were applied to create time series maps for PC concentrations.

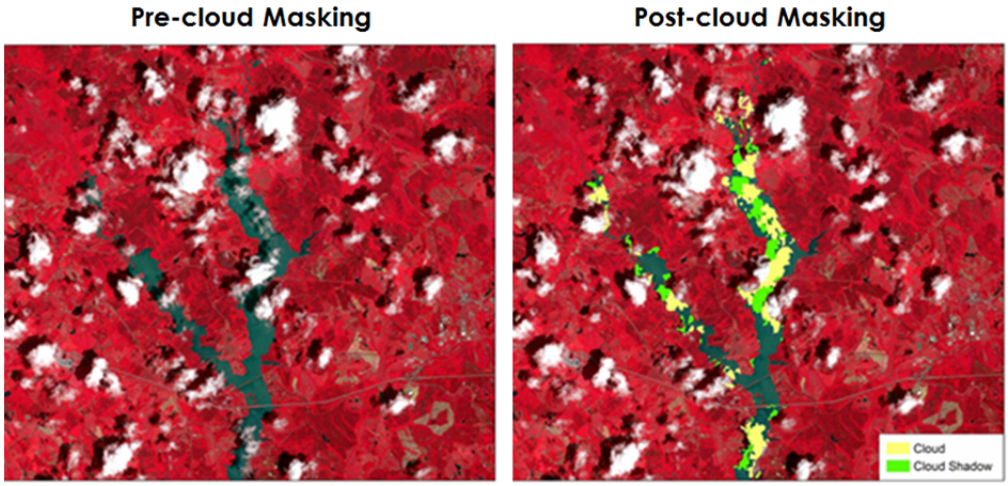

Figure 5: Pre and post cloud and cloud-shadow masking of Landsat 8 images (May 12, 2014)

Model Calibration and Validation:

Independent datasets were used for both calibration and validation (first field trip data used for calibration; second for validation). Several existing models for PC remote estimation were applied in this study. Empirical models solely on statistical relationship between remote sensing reflectance and phycocyanin concentrations; and as such are much simpler in nature as compared to semi-empirical and analytical models, however, with limited applicability. Vincent's (2004) single bands and band ratio empirical models derived from stepwise regression were tested using the field data, however, the performance of these models were not satisfactory when tested for our study area, with model errors exceeding 79%.

Vincent (2004) used stepwise regression for estimating the phycocyanin concentrations. Stepwise regression has ability to include only significant variables into the model, when there are too many variables involved. On the other hand, multi-linear regression is often considered when there are few variables to be included. The single band model was used with the consideration to highlight important bands that are correlated to phycocyanin concentrations. Some studies have used band ratios as independent variables in the stepwise model. Using the band ratio has several advantages for estimating water constituents. First, it can be used to represent the most sensitive as well as the least sensitive bands to a certain water quality parameter. This combination helps retrieve good predictors for estimating water constituents. Secondly, band ratios can be used to cancel out the unknown parameters related to a variable.

For our study, stepwise regressions using both single bands as well as band ratios were used as model inputs. In addition, a multi-linear regression model for slope between two

bands as independent variables was also developed. Here, two slope variables, which are slope between green and red bands (slope_GR), and slope between red and NIR (slope_NIR), were included. The basis for using slope as a variable is because of variations in green, red, and NIR that might be attributed to variations in phycocyanin concentrations. To extend the possibility of finding the best model, additional stepwise regression models were developed using combinations of single bands, band ratio, and slope variables. Figure 6 summarizes the performances of models tested in this study. After comparisons of co-efficient of determination (R^2), and percent normalized RMSE, we chose the model developed from stepwise regression using single band variables, for mapping phycocyanin concentrations. The residuals using this model showed no trends of over or under-estimation (Fig. 7)

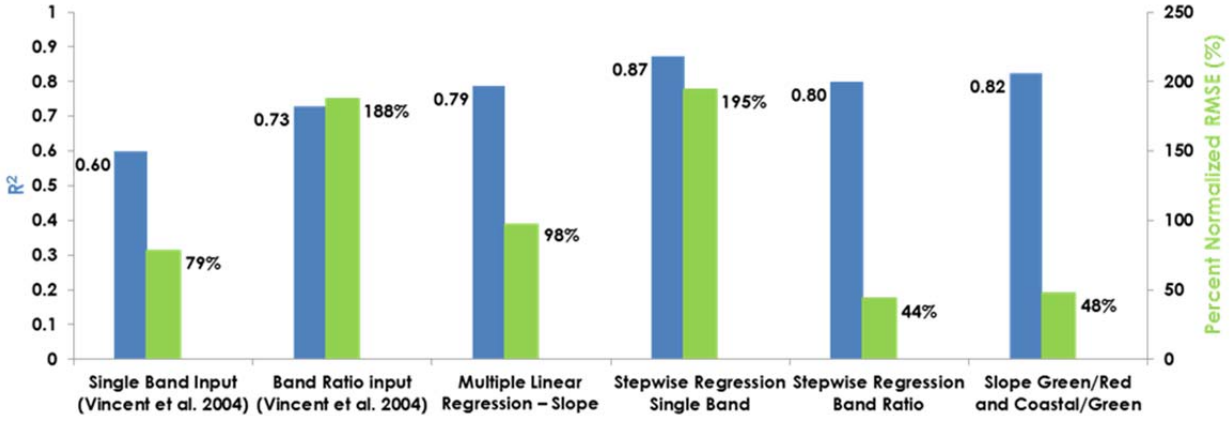

Figure 6: Phycocyanin models tested using Landsat 8 data. Blue bars represent coefficients of determination (R^2); green bars represent percent normalized root mean squared error (%RMSE).

Various factors might have contributed to errors and uncertainties associated with the results. Considering that our field data had to correspond with Landsat 8 overpass events, all data collection had to be weather dependent. As such, field trips could not be conducted under unfavorable weather conditions. In addition, unavoidable data collection and processing errors and sampling biases cannot be ruled out. However, the results obtained so far provides enough confidence that the models can be refined and made more robust using additional field data.

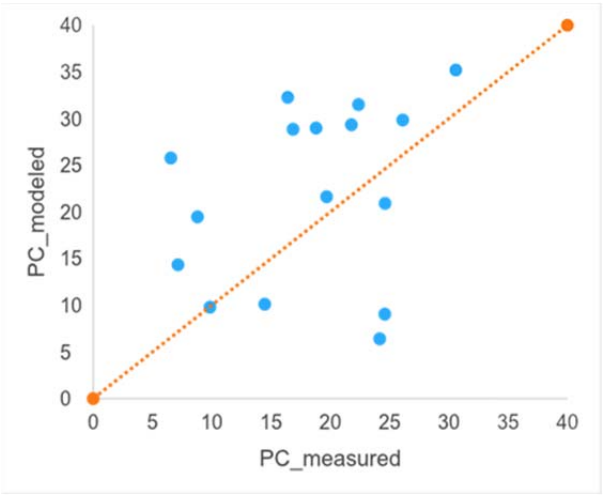

Figure 7: Residuals for theStepwise regression band ratio for phycocyanin.

Time Series Composites:
Sample time series composites were prepared using stepwise regression with band ratio input. The time series composites were utilized to investigate the spatio-temporal variations of CyanoHABs in the four lakes chosen for this study (Figure 6).

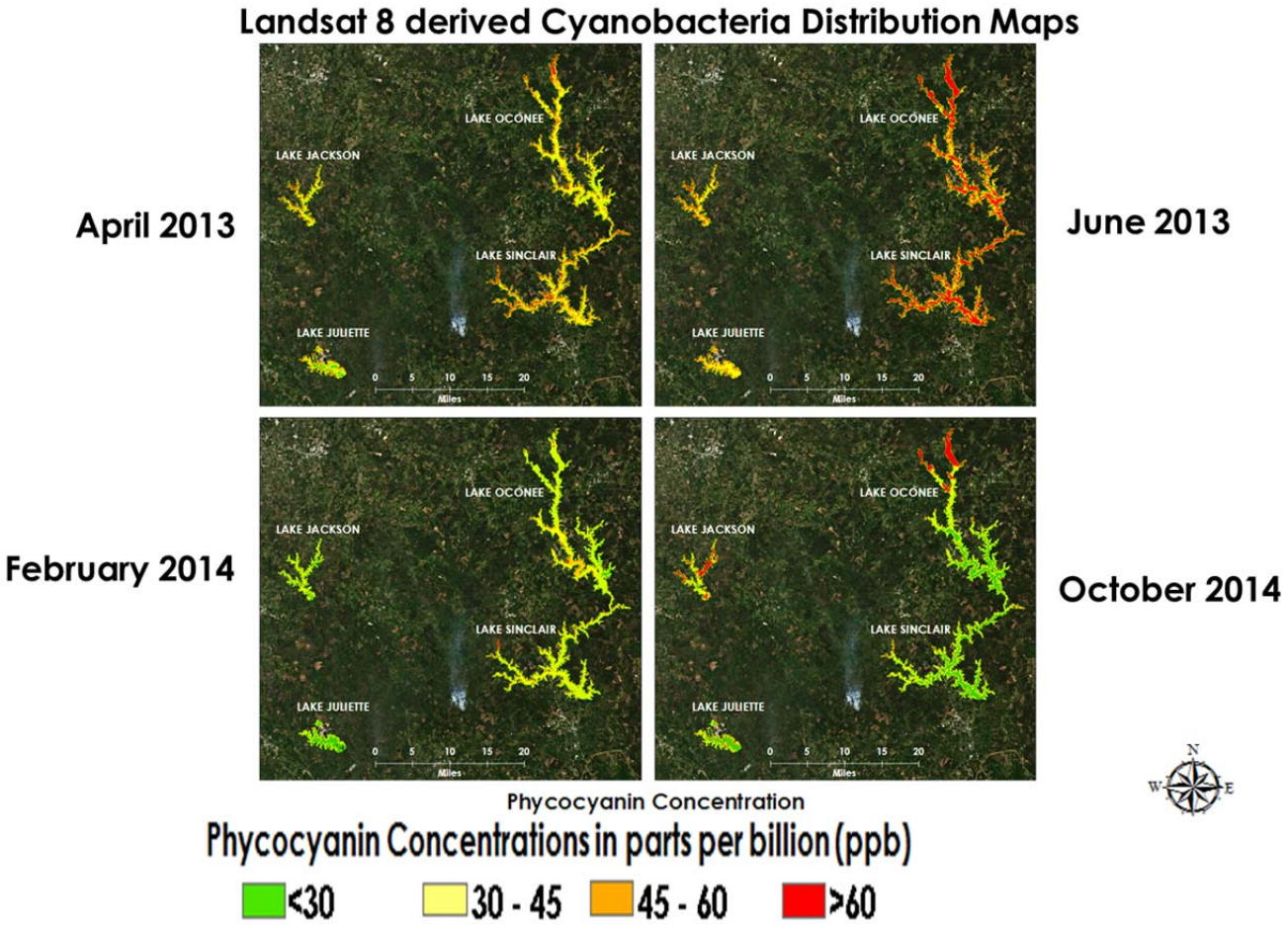

Figure 6: Time series composites showing phycocyanin concentrations (ppb) throughout study sites using a stepwise regression band

Once a model is selected thereafter, time-series maps, and further quantitative analysis of the spatio-temporal trends of CyanoHABs can be performed. These composites, additional tools and products will assist state wide environmental agencies in Georgia when making efficient water management decisions to prevent public exposure to these harmful algal blooms occurrences through periodic monitoring, detection and prediction. Furthermore, the models developed can also be tested on other inland water bodies facing similar problems from CyanoHABs.

Conclusion
In Georgia watersheds experiencing the effects of nutrient loading from both agriculture and storm-water runoff paired with increased temperature and drought due to climate change, HABs have the potential to affect 9.8 million people with health risks and impart

economic losses to livestock producers. Previous reports by Hoagland et al. (2002) and Anderson et al. (2000) have estimated economic impacts from HABs on public health, commercial fisheries, recreation/tourism, and management ranging from $34 to $82 million dollars annually. Considering the economic losses, statewide sampling and monitoring is needed in order to get an accurate representation of HAB effects and to determine a means to restore impaired watersheds.

Understanding the dynamics of the microbiota in agricultural ponds used for livestock drinking water will enable us to improve water quality, minimize cyanobacterial blooms, and protect animal health. Toxicities associated with HABs will be determined in laboratory assessments using fish and aquatic invertebrates to provide information concerning risk. By incorporating evidence of potential toxicity, HABs can be predicted and appropriate management practices can decrease the frequency of dangerous toxin levels in agricultural, subdivision, and drinking water impoundments.

This research addressed fundamental questions regarding critical biotic and abiotic factors necessary to initiate and sustain a HAB. Identifying these factors will inform management decisions. Furthermore, development of a remote sensing method to detect and quantify bloom-forming species will greatly improve the speed and accuracy of monitoring efforts that are currently confined to laboratories with skilled algal taxonomists and expensive microscopes.

References:

Anderson, D.M., P. Hoagland, Y. Kaoru, and A.W. White. 2000. Estimated annual economic impacts from Harmful Algal Blooms (HABs) in the United States. *Woods Hole Oceanog. Inst. Tech. Rept*. 1-100.

Anderson, D.M., P.M. Glibert, and J.M. Burkholder. 2002. Harmful algal blooms and eutrophication: nutrient sources, composition, and consequences. *Estuaries* 25: 704-726.

Anderson, D.M., J.M. Burkholder, W.P. Cohlan, P.M. Glibert, C.J. Gobler, C.A. Heil, R. Kudela, M.L. Parsons, J.E.J. Rensel, D.W. Towsend, V.L. Trianer and G.A. Vargo. 2008. Harmful algal blooms and eutrophication: examining linkages from selected coastal regions of the United States. *Harmful Algae* 8: 39-53.

Davis, T.W., D.L. Berry, G.L. Boyer and C.J. Gobler. 2009. Harmful algal blooms and eutrophication: nutrient sources, composition, and consequences. *Harmful Algae* 8: 715-725.

Glibert, P.M. and J.M. Burkholder. 2006. The complex relationships between increases in fertilization of the Earth, coastal eutrophication, and proliferation of Harmful Algal Blooms. *Ecological Studies* 189: 341-354.

Heisler, J., P.M. Glibert, J.M. Burkholder, D.M. Anderson, W. Cochlan, W.C. Dennison, Q. Dortch, C.J. Gobler, C.A. Heil, E. Humphries, A. Lewitus, R. Magnien, H.G. Marshall, K. Sellner, D.A. Stockwell, D.K. Stoecker, and M. Suddleson. 2008. Eutrophication and harmful algal blooms: a scientific consensus. *Harmful Algae*. 8: 3-13.

Hoagland, P., D.M. Anderson, Y. Kaoru, and A.W. White. 2002. The economic effects of Harmful Algal Blooms in the United States: estimates, assessment, issues, and information needs. *Estuaries*. 25: 819-837.

Kissel, D.E. and L. Sonon. 2008. Soil Test Handbook for Georgia. Special Bulletin 62.

Moore, S.K., V.L. Trainer, N.J. Mantua, M.S. Parker, E.A. Laws, L.C. Backer, and L.E. Fleming. 2008. Impacts of climate variability and future climate change on harmful algal blooms and human health. *Environmental Health* 7: 1-12.

Lee, Z., Carder, K.L and Arnone, R.A. (2002). Deriving inherent optical properties from water color: a multiband quasi-analytical algorithm for optically deep waters. *Applied Optics* 41 (27):5755-5772.

Lewitus, A.J., L.B. Schmidt, L.J. Mason, J.W. Kempton, S.B. Wilde, J.L. Wolny, B.J. Williams, K.C. Hayes, S.N. Hymel, C.J. Keppler, and A.H. Ringwood. 2003. Harmful algal blooms in South Carolina residential and golf course ponds. *Population and Environment* 24: 387-413.

Lewitus, A.J., L.M. Brock, M.K. Burke, K.A. DeMattio, and S.B. Wilde. 2008. Lagoonal stormwater detention ponds as promoters of harmful algal blooms and eutrophicaton along the South Carolina coast. *Harmful Algae* 8: 60-65.

Mez, K., K.A. Beattie, G.A. Codd, K. Hanselmann, B. Hauser, H. Naegeli, and H.R. Preisig. 1997. Identification of a microcystin in benthic cyanobacteria linked to cattle deaths on alpine pastures in Switzerland. *European Journal of Phycology*. 32: 111-117.

Mishra, S., D.R. Mishra and W.M. Schluchter. 2009. A novel algorithm for predicting phycocyanin concentrations in cyanobacteria: a proximal hyperspectral remote sensing approach. *Remote Sensing*. 1: 758-775.

Mishra, S., Mishra, D. R., & Lee, Z. (2013). Bio-Optical Inversion in Highly Turbid and Cyanobacteria-Dominated Waters. *IEEE Transactions on Geoscience and Remote Sensing*, 52(1), 375-388.

Simis, S.G.H., Peters, S.W.M. & Gons, H.J. (2005). Remote sensing of the cyanobacterial pigment phycocyanin in turbid inland water. *Limnology and Oceanography*. 50: 237-245.

Sivonen, K. and G. Jones. 1999. Cyanobacterial toxins. *Toxic Cyanobacteria in Water: A Guide to Public Health Consequences, Monitoring, and Management*. I. Chorus and J. Bartram, eds. London, E & FN Spon (on behalf of WHO):41-111.

Turner, J.H. 2012. Georgia to suspend consideration of some new farm water permit applications. Georgia Department of Natural Resources: Environmental Protection Division.
URL:http://www.gaepd.org/Files_PDF/news/GeorgiaEPD_Newsrelease_AgPermitting Suspens ion_073012.pdf

USDA Drought Monitor. 2012. URL: http://droughtmonitor.unl.edu/

USDA Economic Research Services. 2011. State Fact Sheets: Georgia. URL: http://www.ers.usda.gov/data-products/state-fact-sheets/state-data.aspx?StateFIPS=13&StateName=Georgia

van der Merwe, D., L. Sebbag, J.C. Neitfeld, M.T. Aubel, A. Foss, and E. Carney. 2012. Investigation of a *Microcystis aeruginosa* cyanobacterial freshwater harmful algal bloom associated with acute microcystin toxicosis in a dog. *Journal of Veterinary Diagnostic Investigation* 24 (4): 679-687.

Vincent, R. K., Qin, X., McKay, R. M. L., Miner, J., Czajkowski, K., Savino, J., & Bridgeman, T. (2004). Phycocyanin detection from LANDSAT TM data for mapping cyanobacterial blooms in Lake Erie. *Remote Sensing of Environment*, 89(3), 381-392.

Baseline Conservation Analysis for Agricultural Irrigation in Priority Watersheds of the Lower Flint River Basin

Basic Information

Title:	Baseline Conservation Analysis for Agricultural Irrigation in Priority Watersheds of the Lower Flint River Basin
Project Number:	2014GA346B
Start Date:	3/1/2014
End Date:	2/28/2016
Funding Source:	104B
Congressional District:	2
Research Category:	Ground-water Flow and Transport
Focus Category:	Conservation, Irrigation, Management and Planning
Descriptors:	None
Principal Investigators:	Mark Masters

Publications

There are no publications.

The deadline of this project was extended into Fiscal Year 2015. As a result, the final report will be filed during that Fiscal Year.

Information Transfer Program Introduction

None.

USGS Summer Intern Program

None.

Student Support					
Category	**Section 104 Base Grant**	**Section 104 NCGP Award**	**NIWR-USGS Internship**	**Supplemental Awards**	**Total**
Undergraduate	0	0	0	0	0
Masters	3	0	0	0	3
Ph.D.	5	0	0	0	5
Post-Doc.	1	0	0	0	1
Total	9	0	0	0	9

Notable Awards and Achievements

NATIONAL CLIMATE ASSESSMENT

The National Climate Assessment (NCA) is carried out under the auspices of the U.S. Global Change Research Program and aims to assess the science of climate change and its impacts across the United States, now and throughout this century. It documents climate change related impacts and responses for various sectors and regions, with the goal of better informing public and private decision-making at all levels.

A team of more than 300 experts, guided by a 60-member National Climate Assessment and Development Advisory Committee produced the 3rd Climate Assessment Report with input from public and private sector stakeholders, resource and environmental managers, researchers, representatives from businesses and non-governmental organizations, and the general public.

The assessment draws from a large body of scientific peer-reviewed research, technical input reports, and other publicly available sources; all sources meet the standards of the Information Quality Act. The report was extensively reviewed by the public and experts, including a panel of the National Academy of Sciences, the 13 Federal agencies of the U.S. Global Change Research Program, and the Federal Committee on Environment, Natural Resources, and Sustainability.

The 3rd NCA Report summarizes recent advances and findings in climate change science; assesses the climate change impacts within and across key societal and environmental sectors (i.e., human health, water, energy, transportation, agriculture, forests, and ecosystems and biodiversity) and U.S. regions (i.e., Northeast, Southeast and Caribbean, Midwest, Great Plains, Southwest, Northwest, Alaska, and Hawai‘i and the U.S. affiliated Pacific Islands, as well as coastal areas, oceans, and marine resources); assesses the current state of responses to climate change, including adaptation, mitigation, and decision support activities; highlights major gaps in science and research to improve future assessments; and describes a vision for and components of an ongoing, long-term assessment process.

GWRI's Director, Dr. Aris Georgakakos, led the development of the NCA Water Resources chapter and contributed to the southeast impact assessment.

The NCA report and associated materials are available at http://nca2014.globalchange.gov.

SUSTAINABLE WATER MANAGEMENT IN THE APALCHICOLA-CHATTAHOOCHEE FLINT(ACF) RIVER BASIN

The development of an equitable ACF water sharing compact has challenged Alabama, Florida, and Georgia for more than two decades. Among the outstanding critical needs are (i) inclusive and effective stakeholder participation in planning and management processes; and (ii) development of comprehensive and reliable information and knowledge pertaining to the interdependencies of the basin water uses and their local and basinwide impacts.

The ACF Stakeholders (ACFS; http://acfstakeholders.org/) was established in 2010 to address the need for effective stakeholder participation and the development of a sustainable water management plan. ACFS is an inclusive 503(c) nonprofit organization with membership from 56 river basin stakeholders and is open to any group with interest in the ACF water management--cities, lake associations, farmers, industries, environmental citizen groups, power companies, fishermen, NGO's, and many others.

Under this project, GWRI is developing the technical information and knowledge base necessary to inform the stakeholder discussions toward a consensus and sustainable ACF water management plan. The main project tasks include:

-Comprehensive assessment of the historical ACF basin unimpaired inflows;

-Development of modeling tools for (1) river and reservoir simulation, (2) reservoir optimization, and (3) estuary hydrodynamic flow and salinity assessments;

-Systematic and integrated use of the modeling tools to quantify the benefits, impacts, and tradeoffs of various water management alternatives formulated by the ACF stakeholder caucuses;

-Communication of assessment findings to ACF stakeholder through several interactive workshops;

-Development of reservoir regulation policies and other management strategies reflecting and realizing the stakeholder shared vision for sustainable water management.

In May 2015, ACF Stakeholders, Inc. (ACFS) completed and unanimously approved a Sustainable Water Management Plan (SWMP) for equitably managing water in the Apalachicola, Chattahoochee and Flint River Basin, including its impact on the Apalachicola Bay.

The official ACF press release is available at
http://acfstakeholders.org/wp-content/uploads/2015/05/ACF-Stakeholders-May-13-2015-Press-Release.pdf.

The Draft Executive Summary of the plan is available at
http://gwri.gatech.edu/sites/default/files/files/announcements/acfs_sustainable_water_management_plan_draft_executi